IEEE Power & Energy Society

TECHNICAL REPORT

December 2024

PES-TR127

Synchro-Waveform Measurements and Data Analytics in Power Systems

PREPARED BY THE IEEE PES TASK FORCE ON BIG DATA ANALYTICS FOR SYNCHRO-WAVEFORM MEASUREMENTS

Subcommittee: Big Data and Analytics (BDA)

Committee: Analytic Methods for Power Systems (AMPS)

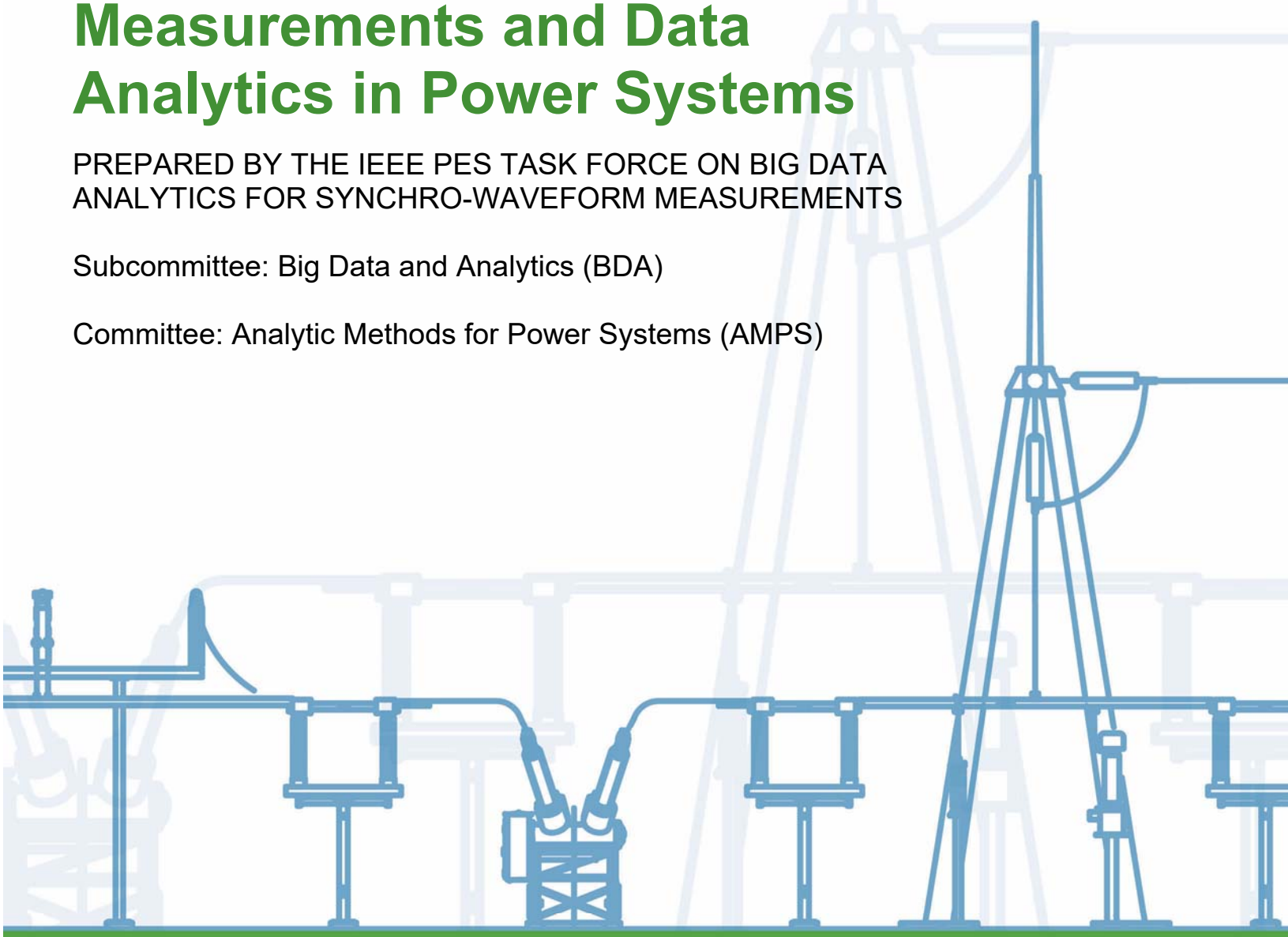

THIS PAGE LEFT BLANK INTENTIONALLY

TASK FORCE ON
Big Data Analytics for Synchro-Waveform Measurements

Chairs: Hamed Mohsenian-Rad and Jhi-Young Joo
Contributors: The following individuals contributed content to this technical report.

Hamed Mohsenian-Rad	University of California, Riverside
Jhi-Young Joo	Lawrence Livermore National Laboratory
Michael Balestrieri	Southern California Edison
Lakshan Piyasinghe	Hubbell
Shuchismita Biswas	Pacific Northwest National Laboratory
Kaustav Chatterjee	Pacific Northwest National Laboratory
Hamed Valizadeh-Haghi	Southern California Edison
Kyle Chang	Southern California Edison
Joseph Grappe	Sentient Energy
Theo Laughner	Lifescale Analytics
Steven Blair	Synaptec
Chris Mullins	Power Monitors
Yilu Liu	University of Tennessee
Yuru Wu	University of Tennessee
Biao Sun	University of Tennessee
Vincent Choinière	Hydro Québec
Hossein Mohsenzadeh-Yazdi	University of California, Riverside
Fatemeh Ahmadi-Gorjayi	University of California, Riverside
Lei Chen	Peking University
Jim Follum	Pacific Northwest National Laboratory
Younes Seyedi	Hubbell
Alexadra Karpilow	École Polytechnique Fédérale de Lausanne
Mario Paolone	École Polytechnique Fédérale de Lausanne
Mirrasoul J. Mousavi	Sentient Energy
Subhransu Ranjan Samantaray	Indian Institute of Technology, Bhubaneswar
Jeffery Dagle	Pacific Northwest National Laboratory
Aaron Wilson	Oak Ridge National Laboratory
Chester Li	Hydro One
Alireza Shahsavari	San Diego Gas and Electric
Masoud Mohseni Bonab	Hydro Québec
Antonella Ragusa	De Montfort University
Mohamed Ramadan Younis	University of Toronto
Bassam Moussa	Hydro Québec
Hassan Ghoudjehbaklou	San Diego Gas and Electric
Deepjyoti Deka	Massachusetts Institute of Technology
Mostafa Farrokhabadi	University of Calgary
Farrokh Aminifar	Quanta Technology
Christoph Lackner	Grid Protection Alliance
Farnoosh Rahmatian	NuGrid
Ralph Brown	Brown Wolf Consulting
Richard Kirby	Schweitzer Engineering Laboratories

KEYWORDS

Synchro-waveforms

Synchronized waveform measurements

Point-on-wave measurements

Continuous streaming of waveform measurements

Event-triggered waveform capture

Waveform measurement unit

Big data in power systems

Big data analytics

Power system monitoring

Inverter-based resources

Event signatures

Incipient fault

Data-driven applications

CONTENTS

THIS PAGE LEFT BLANK INTENTIONALLY

Abstract

The concept of synchro-waveforms has recently emerged as a promising frontier in power system monitoring and data-driven applications. By providing access to raw waveform samples, synchro-waveforms can capture not only the typical major disturbances but also the seemingly minor, yet sometimes highly informative, disturbances in voltage and current that are missed by other time-synchronized measurements, such as synchrophasors. As a result, synchro-waveforms can support a wide range of existing and new measurement-based applications in power system monitoring, control, and protection.

However, several open issues remain in this field. The true value of synchro-waveforms has yet to be fully realized. At the same time, their much higher data volume and faster reporting rate compared to synchrophasors introduce new challenges in power system data analytics that must be addressed.

This technical report identifies and addresses some of these challenges through a collaborative effort. It explores currently available technologies and case studies in this rapidly evolving area, while also examining future needs in data handling, standardization, and real-time processing capabilities.

Specifically, the chapters in this report cover the following core subjects: synchro-waveform technology and infrastructure; data collection, storage, and communication; different forms of synchro-waveform data representation; basic methods for working with synchro-waveform data; case studies and future applications; and synchro-waveform standardization needs.

This report was prepared with contributions from a diverse group of individuals with varying expertise. While some sections reflect on well-understood concepts, many sections seek to explore preliminary ideas. Together, these contributions provide valuable insights and suggestions for future directions in this field.

This report serves as a resource for industry, academia, and all stakeholders interested in leveraging synchro-waveform data for enhanced situational awareness and other power system applications. Its ultimate goal is to raise awareness within the power systems community and related disciplines about the growing field of synchro-waveforms and the diverse range of emerging topics in this domain.

1. Introduction

1.1. Background and Needs

Waveforms are the most authentic representation of voltage and current in power systems. With the latest advancements in power system sensor technologies, it is now possible to obtain time-synchronized waveform measurements, namely synchro-waveforms, across the power system geographical area [1], [2], [3], [4], [5]. Synchro-waveforms can capture the most inconspicuous disturbances that are overlooked by other types of time-synchronized sensors, such as synchro-phasors. They also monitor system dynamics at much higher frequencies as well as much lower frequencies than the fundamental components of voltage and current that are commonly monitored by synchro-phasor data analytics tools. Therefore, synchro-waveforms introduce a new frontier to advance power system situational awareness, system dynamics tracking, incipient fault detection and identification, condition monitoring, and so on.

Synchro-waveforms can also play a critical role in monitoring, protection, and stability of inverter-based resources (IBR) due to the high-frequency switching characteristics of IBRs. Other potential applications of synchro-waveforms are in location-based problems such as oscillation source detection; analysis of sub-synchronous and super-synchronous oscillations; analysis of direct current (DC) circuits, where phasor data is not applicable; wildfire monitoring, to characterize the signatures of the events that can lead to ignition, or to correlate the outcome of synchro-waveform analytics with external factors, e.g., weather conditions; differential protection, relay coordination, distributed protection; as well as transient and dynamic state estimation in power systems.

In spite of the unprecedented advantageous of synchro-waveform measurements, collecting data at a much higher reporting rate than synchro-phasors creates a wide range of challenges in data transportation, management, and archiving as well as Big Data Analytics (BDA) in power systems.

The IEEE Task Force (TF) on Big Data Analytics for Synchro-Waveform Measurements was established in May 2023 to promote big data analytics methodologies and applications of high-resolution waveform and synchro-waveform measurements in power systems. This technical report summarizes the basic concepts and potential applications of synchro-waveforms. This report seeks to help facilitate industry acceptance of this new data-intensive technology, identify challenges and opportunities, and encourage collaboration in academia and industry.

1.2. Objective of the Report

The objective of this report is to provide the first comprehensive overview of the recent advancements, applications, and challenges associated with the emerging field of synchro-waveform measurements in power systems. A wide range of topics are discussed throughout this report, ranging from relevant sensor technologies, data representations and handling frameworks, and case studies. This report aims to encourage the adoption and integration of synchro-waveforms into grid monitoring and control systems. By gathering input from various experts from academia, industry, and national laboratories, this report presents the latest efforts and results in this growing field. This technical report serves as a resource for industry experts and academic researchers interested in leveraging synchro-waveform data for enhanced situational awareness, event detection, root cause analysis, and various other power system applications.

1.3. Scope and Limitations

Although this technical report is comprehensive and covers a wide range of relevant topics, it is inevitably limited to the currently available technologies and case studies, while also considering future needs in data handling, standardization, and real-time processing capabilities.

This report was prepared based on contributions from a large group of individuals with varying types and levels of expertise. Some content is well-understood and has already undergone peer review in journals and conferences. Several other sections are on concepts that are still preliminary. Nevertheless, they provide valuable insights and suggestions for future directions in this field.

Depending on their background, readers may be more familiar with certain aspects of this report and less familiar with other aspects. Our goal here is to raise awareness about the growing field of synchro-waveforms and the wide range of topics that are expected to emerge in this field.

The field of synchro-waveforms is still evolving. A lot can change in this field in the near future. Additional methods and use case may emerge in the future that are not covered in this report. There will likely be a need to revisit and update this report after a few years to include new advancements.

2. Synchro-Waveform Technology and Infrastructure

2.1. Sensor technology

The sensor device to record synchro-waveforms may be referred to as waveform measurement unit (WMU) [6]. WMUs record time-synchronized waveform measurements of voltage and current at different locations of a power system. In some literature, synchro-waveforms are also referred to as time-synchronized point-on-wave (POW) measurements or time-synchronized sampled values (TSSVs) [7]. WMUs are also in some literature referred to as POW sensors or synchro-waveform measurement units (SMUs) [2]. On the other hand, it is possible to use waveform measurements from conventional sensor technologies that are *not* time-synchronized, such as from conventional power quality meters, and use data-driven methods to align the waveforms to practically serve as synchro-waveforms, e.g. see the technologies and experimental results in [8] [9]. Other technologies for time-synchronized high-resolution grid monitoring are also discussed in [3].

When synchro-waveforms are compared with synchro-phasors, and WMUs are compared with phasor measurement units (PMUs), several similarities and differences may be observed. Similar to PMUs, time-synchronization is done in WMUs by using the global positioning system (GPS) or the precision time protocol (PTP). In this regard, WMUs can be seen as an extension of the conventional PMUs. The difference is that a WMU reports the time-synchronized raw samples of the voltage and current waveform measurements. On the contrary, a PMU uses the raw samples to calculate phasor representations of the fundamental voltage and current waveforms. Accordingly, WMUs provide the most authentic representation of voltage and current signals, including transients, in power systems. Since PMUs report calculated values of sampled voltage and current, the sampling rate and reporting rate may be different. However, WMUs usually report every raw sampled measurement without down-sampling the measurements. Depending on the application, the reporting rate of a WMU may vary from kilohertz to megahertz; which is much higher than a PMU reporting rates, since the reported samples are intended to represent the waveforms.

Figure 1 provides a comparison between the conventional phasor measurements versus the raw waveform measurements. The three-phase voltage phasor measurements (magnitude and phase angle) are shown in Figure 1(a). While the phasors can indicate the presence of a major voltage sag between cycle 25 and cycle 30, the details of such an event cannot be perceived based on phasor measurements. However, such details can be observed in the raw waveform measurements in Figure 1(b), where the exact shape of the waveforms reveals that not only Phase C, which is impacted most severely, but also Phases A and B have also experienced slight distortions.

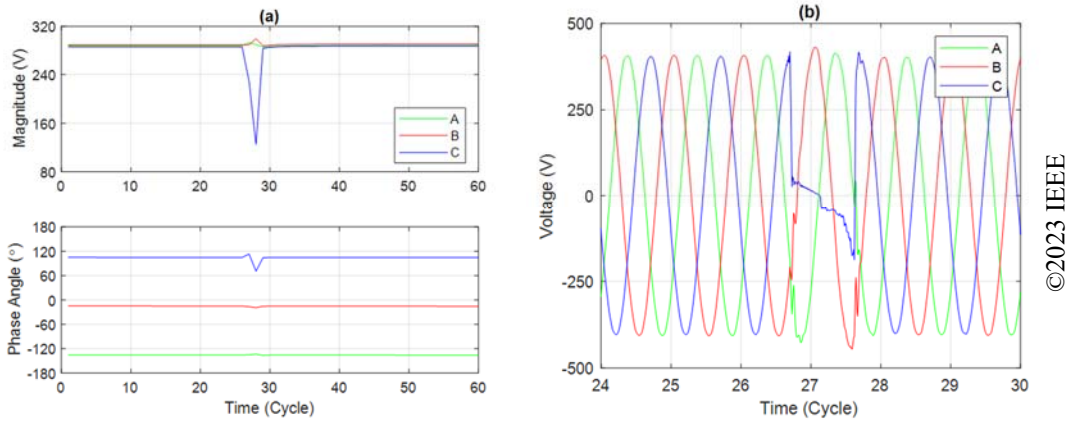

Figure 1. Comparing phasor representation in (a) with raw voltage waveforms in (b) [1].

As shown in Figure 2, WMUs may report synchro-waveforms as a continuous (gapless) series of the measurement samples; or they may operate on an event-triggered basis, where the waveform data is not reported unless a certain event detection criterion is met. The latter scenario overlaps with some other existing sensor technologies, such as digital fault recorders (DFRs) and power quality (PQ) meters. If a DFR or a PQ meter is capable of time-synchronization, then they too can serve as WMUs to provide synchro-waveforms (albeit in an event-triggered basis). The event-triggered waveform captured in Figure 2 is from a PQ meter.

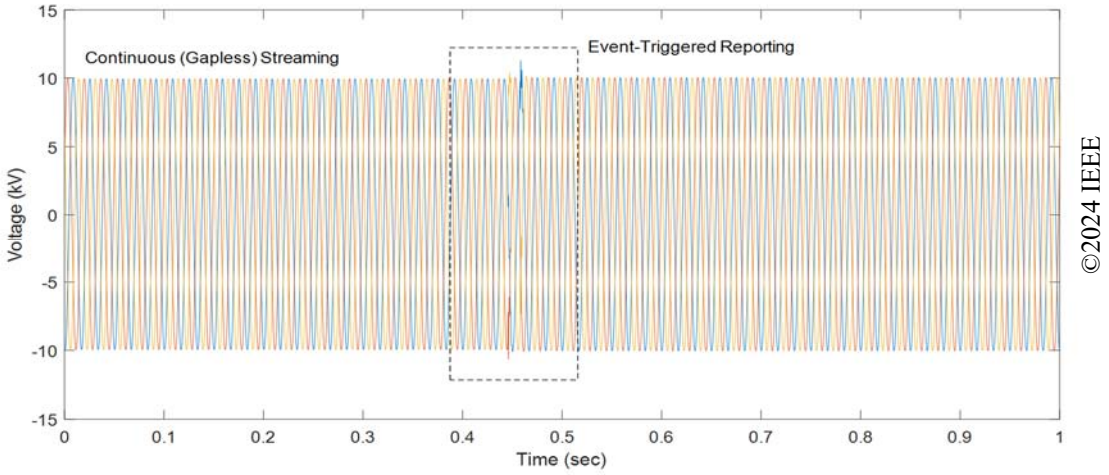

Figure 2 . Continuous versus event-triggered reporting of synchro-waveforms [10].

Figure 3 shows different examples for the real-world installation of WMUs. These installations include three-phase medium-voltage installations at a substation, three-phase low-voltage installations at grid assets, such as IBRs, and single-phase low-voltage installations at power outlets. The basic principles are similar.

Figure 3. Examples of real-world WMU installations in Riverside, California: (top and bottom left): three-phase 12.47 kV installation at a substation; (top-right): three-phase 480 V installation at a PV inverter; (bottom-right): single-phase 120 V installation at a power outlet [1].

Regardless of the sensor devices being used and the locations of sensors, the key in obtaining synchro-waveform data is that the data sampled from different locations are precisely time-synchronized, providing simultaneous view to various physical phenomena in power systems in the most granular temporal resolution.

The value of synchro-waveforms is simply demonstrated in Figure 4 by three illustrative examples. In all cases, WMU 1 and WMU 2 are located at two nearby power distribution feeders. In Case 1, WMU 1 and WMU 2 capture similar signatures on all phases. In Case 2, WMU 1 captures a voltage sag on Phase A; as marked inside the dashed red oval. WMU 2 simultaneously captures a much more severe signature of a momentary fault on Phase A. The difference between Cases 1 and 2 is due to the different nature and different location of the event in these two cases. In Case 3, WMU 1 captures a high-frequency resonance on all three phases, which is not seen by WMU 2. This suggests that the resonance is local. Other similar instances of system-wide resonance, i.e., observing resonance by both WMU 1 and WMU 2, have been captured as well.

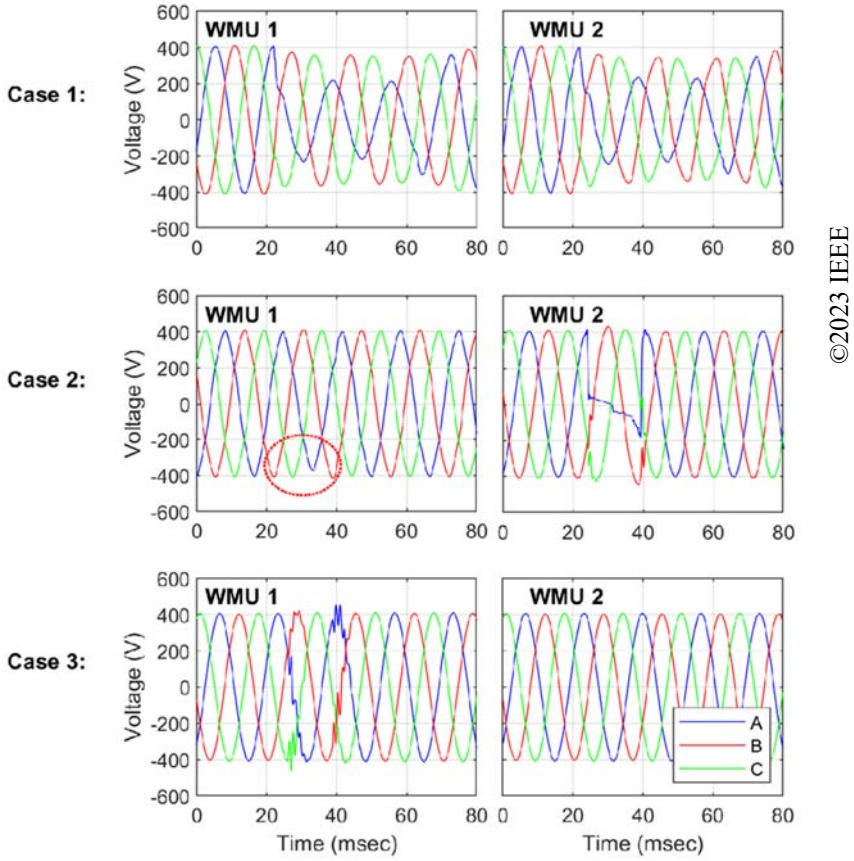

Figure 4. Examples of voltage synchro-waveforms from two WMUs [1].

The key feature of synchro-waveforms is ultimately their ability to make the raw waveform measurement samples available, instead of providing phasors or other forms of approximated representations. Every data-driven power system application may of course use some form of waveform data filtering or processing. However, having access to raw time-synchronized waveform samples assures that such filtering and processing is customized for each application to maintain the intended information in the data to meet the specifications of that application.

WMUs can be installed at different segments and components of the power system, at both transmission level and distribution level. At transmission level, installing WMUs can enhance wide-area monitoring [10]. At distribution level, WMUs can significantly enhance observability across distribution feeders to address the growing complexity of grid edge technologies. Figure 5 shows examples of many locations where WMUs can be installed on distribution networks [11].

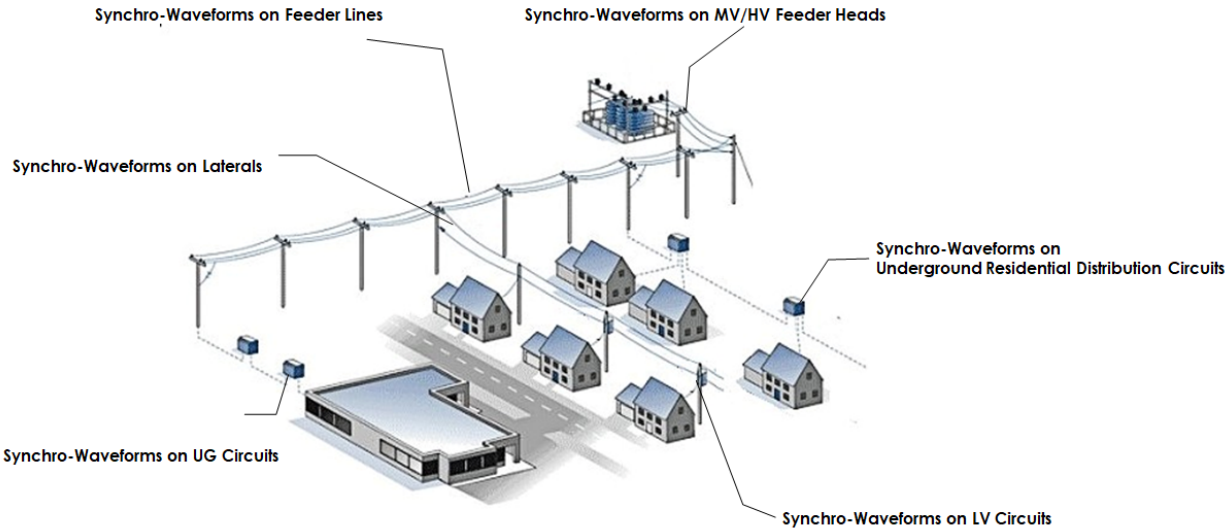

Figure 5. Examples of various locations and segments to install WMUs to provide synchro-waveforms at distribution networks [11].

Before we end this section, it is worth adding that some WMUs may rather measure the waveforms of the *electric field* (instead of voltage) and *magnetic field* (instead of current). An example is shown in Figure 6, where the waveform electric field waveforms are captured during a fault, at 14.4 kHz waveform sampling rate. See the example analysis in [10] about how synchronized electric field waveform measurements are used in monitoring power transmission lines.

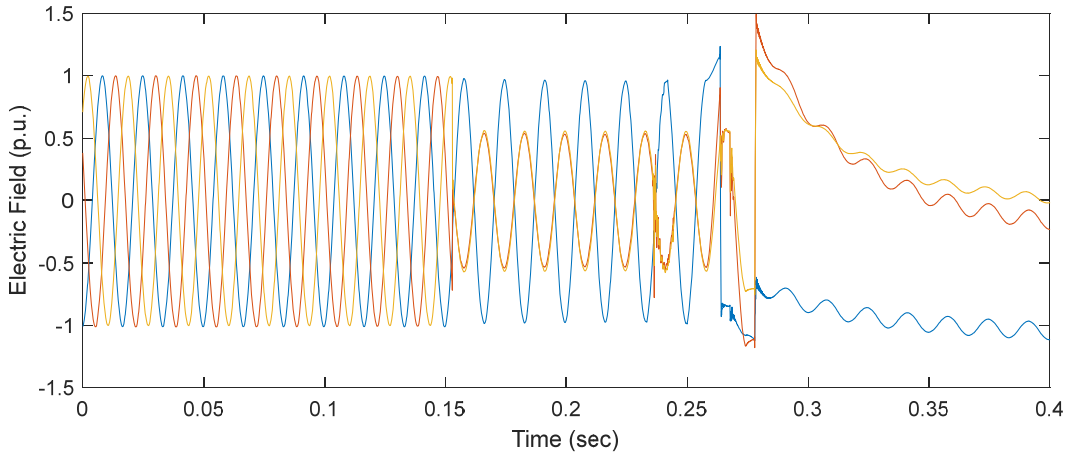

Figure 6. Electric field waveform measurements at a transmission line during a fault.

2.2. Instrumentation, Measurement, and Data Quality

2.2.1. Bandwidth

Power electronics associated with distributed energy resources (DER) have increased harmonics in the power system. However, many in-situ measurement systems do not have the sufficient bandwidth to faithfully reproduce waveform data with frequencies over 600 Hz. The measurement

system includes both the instrumentation transformers (potential and current transformers) and the sampling rate of the sensor device itself.

A Nyquist sampling rate of double the frequency of the phenomenon is the minimum rate required to observe such a phenomenon. For example, to measure a 5 kHz phenomenon, the frequency response of the system must be at least 10 kHz. Figure 7 shows the frequency response of a variety of voltage transducers (VTs) [12]. As can be seen, the frequency response is very non-linear for a variety of VTs even below the 3 kHz range. The IEEE Standard for Harmonic Control in Electric Power Systems (IEEE 519-2022) requires measurement of up to the 3 kHz range, which makes many of the current commercial sensors inadequate for measuring harmonics.

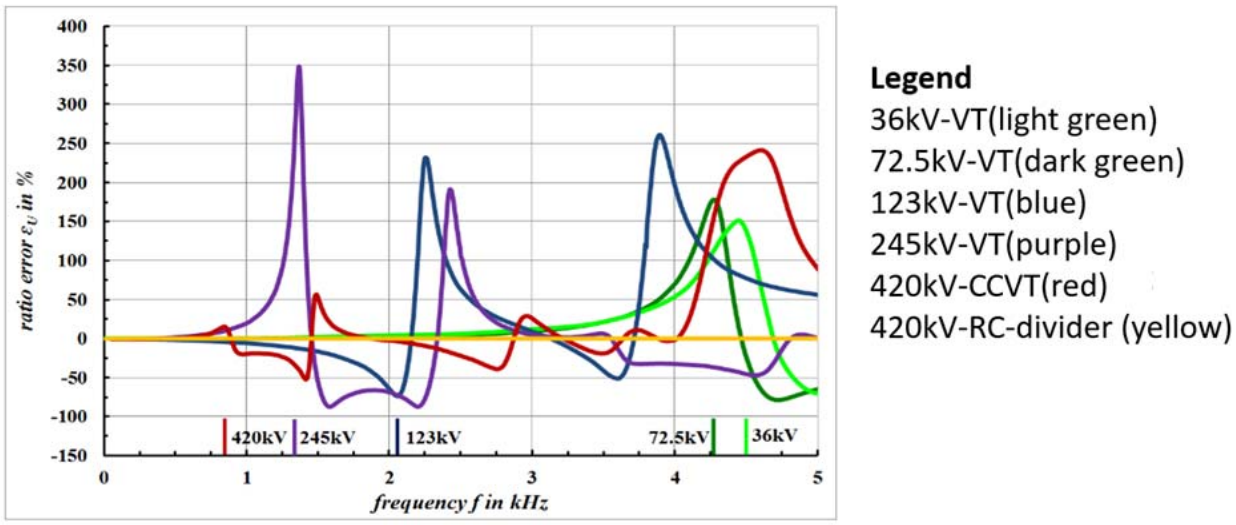

Figure 7. Voltage transducer frequency response

In Figure 8, the performance of a traditional current transducer (CT) is compared to an alternative sensor with an improved bandwidth [13]. Clearly, the alternative sensor more faithfully reproduces the waveform compared to the traditional CT. If the waveforms being measured have significant noise, then the traditional CT will not be able to adequately assess the extent of the harmonics.

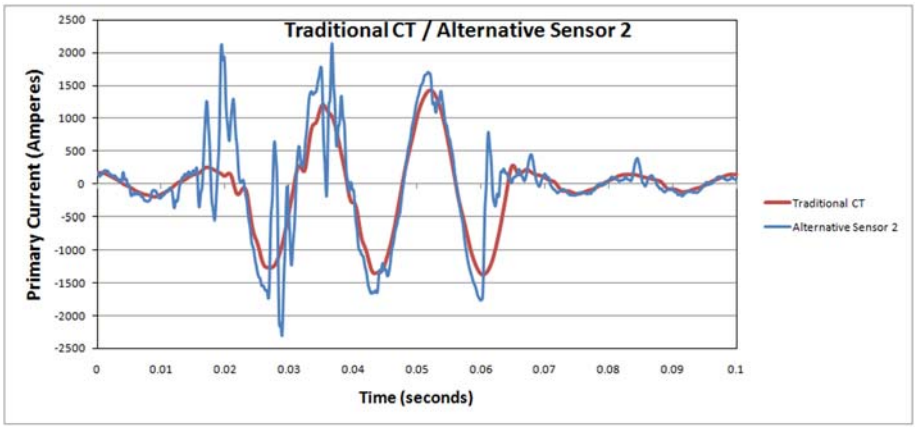

Figure 8. Comparing CTs in terms of Harmonic Details Passed Through

2.2.2. Delay

Some data applications require very precise time stamping, such as in traveling wave (TW) fault location which uses time stamps to locate the position of a fault in the grid. Since the speed of electromagnetic waves in a vacuum is 299,792,458 m/s, approximately 3x108 m/s, the time stamping for traveling wave fault location must be extremely precise [14]. The fault location and the time of the fault are estimated by measuring arrival times of the traveling waves caused and propagated by the fault. Error in the estimated fault location on an overhead transmission line is typically within one tower span (300 m; 1,000 ft) on average. Error in the estimated fault location in a cable transmission line is typically within 150 m (500 ft) on average. When the propagation time through instrument transformer secondary cables is significantly different at each line terminal, the accuracy can be affected. To increase accuracy, the traveling wave fault locator can be configured to compensate for the time delay associated with the secondary cables by backdating the time stamp of the initial TW through use of a compensation time setting.

It can be important to characterize and correct for the group delay introduced by PTs and transformers that may separate different measurement locations. For example, consider an event on a distribution circuit that is captured by one WMU at a substation and one WMU on the secondary of a distribution transformer. Each WMU will have a certain group delay through the PT or distribution transformer. These delays must be accounted for if precise synchronization is needed. If the magnitude and phase frequency response of the transformer and associated cabling is known, the group delay becomes a constant over the frequency, equivalent to a simple time delay.

2.2.3. Sampling timing methods

There are three primary clocking methods in use for WMU sampling: i) power line synchronous, ii) free running sampling, and iii) GPS-disciplined. Each method has strengths and weaknesses, especially when combining datasets from different sources. The method determining the precise timing of the A/D clock, which actually triggers the sample/hold or A/D conversion itself, can be independent of the timestamping process.

2.2.3.1. Powerline Synchronous Sampling

Powerline synchronous sampling involves continuously adjusting the A/D sampling clock to remain synchronized with the powerline frequency using a phase locked loop (PLL) algorithm, ensuring an exact integer number of samples per powerline cycle. This method simplifies the processing of power metrics like RMS values and harmonics, as it allows for consistent data analysis across cycles. However, while it provides advantages for power quality and revenue meters, it has significant drawbacks in wide-area monitoring applications. The sampling rate varies with changes in powerline frequency, leading to non-constant time intervals between samples and complicating long-term data analysis. Additionally, this method can obscure important frequency data, such as the rate of change of frequency (ROCOF), unless precise timestamps are maintained for each sample. Consequently, artifacts may arise during phase shifts or voltage sags as the PLL adjusts, integrating the PLL's behavior into the data itself.

2.2.3.2. Free Running Sampling

Free running sampling utilizes an A/D clock that operates independently of the powerline frequency or GPS-derived time, typically set at a fixed sampling rate determined by a crystal oscillator. While this method is straightforward to implement and provides regularly spaced samples, it introduces drift over time, which can complicate data accuracy. Unlike powerline synchronous sampling, free running sampling allows for direct computation of rate of change of frequency (ROCOF) and PMU information without PLL artifacts. However, it poses challenges for calculating cycle-based metrics like RMS voltage and harmonics due to variable samples per cycle, leading to issues such as ripple in RMS values and spectral leakage. These challenges can be mitigated by applying a software PLL to the raw data offline, allowing for digital resampling to achieve results similar to powerline-synchronized data, albeit at a higher computational cost.

2.2.3.3. GPS-disciplined Sampling

GPS-disciplined sampling involves continuously adjusting the A/D clock using a hardware or software PLL to synchronize with a reference clock from a GPS receiver or other precision time sources like IEEE 1588 or IRIG-B. This method ensures a fixed, integer number of samples per second, maintaining a constant sampling rate and time between samples, which reduces the need for frequent absolute timestamps. If the GPS signal is lost, the system typically defaults to free-running sampling, and sophisticated systems may track oscillator drift to maintain accuracy. While this method offers both sampling rate and absolute time accuracy, facilitating easier data comparison across devices, it is complex and costly, requiring precise timing hardware. The challenges of asynchronous sampling to the powerline frequency remain, but offline software PLL algorithms can be applied to create a powerline-synchronized time series and compute ROCOF and PMU data.

2.2.4 Sampling Resolution

WMU data is a digital representation of continuous time series waveforms; see Figure 9. These original signals are quantized in both amplitude and time, with a possible loss of information.

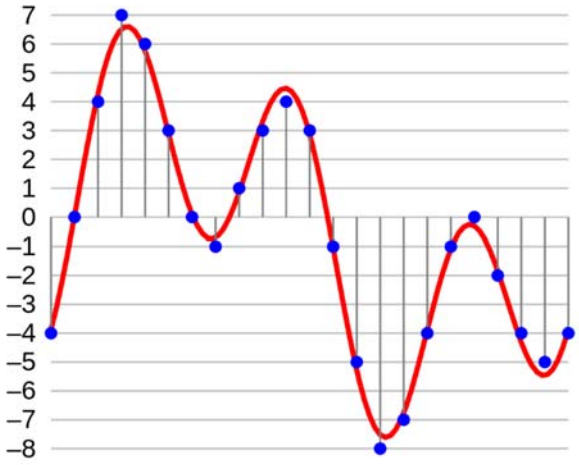

Figure 9. WMU data is a digital representation of continuous time series waveforms. The mismatch between the red waveform and blue samples is due to quantization.

2.2.4.1. Time Resolution

Quantization in time is due to a finite sampling rate. The faster the sampling rate, the finer the time resolution and greater the frequency bandwidth. The time resolution will limit the travelling wave analysis. For example, a 512 samples/cycle (30.72 ksps (killo-samples-per-second) at 60 Hz or 25.6 ksps at 50 Hz) rate gives 32.6 µs between samples. Traveling wave propagation speed depends on the medium, such as free space, air, or solid insulation of cable. Consider an overhead transmission line with a traveling wave propagation speed of 0.98c, where c = 299,792,458 m/s [14] [15], roughly 984 ft/µs (300 m/µs) for an overhead disturbance line. At 512 samples/cycle, 1 sample would represent a 5.94-mile (9.56 km) resolution for travelling wave analysis, regardless of the absolute timing accuracy. Whereas for an underground or subsea cable with traveling wave propagation speed of 0.55c [14] [15], roughly 541 ft/µs (165 m/µs) for a cable disturbance, 1 sample would represent a 3.34-mile (5.37 km) resolution for travelling wave analysis. A higher sampling rate can improve time resolution until the bandwidth of the transducer, instrumentation transformer or sensor, etc. are reached. Increasing the sampling rate beyond the bandwidth of the sensor system will not increase time resolution, but may be used to increase amplitude resolution.

2.2.4.2 Amplitude Resolution

Amplitude resolution in WMU data quantization is defined by the number of A/D bits, with the number of discrete amplitude levels being 2^{bits} (e.g., a 16-bit converter allows for 65,536 distinct amplitudes). This resolution impacts the minimum detectable signal after quantization, which is crucial for applications like monitoring feeder current in substations, where nominal currents range from 50-200 amps, but fault currents can reach 10,000 amps. A 16-bit system may have a resolution of 0.43 amps ($= 10{,}000\sqrt{2} \times 2/2^{16}$), insufficient for detecting small high-impedance faults. While reducing the maximum input can enhance resolution for small currents, it risks clipping during faults. Techniques exist to trade time resolution for amplitude resolution, such as downsampling a high-speed data stream to improve amplitude resolution while sacrificing the time resolution. However, the reverse is not possible; high amplitude resolution cannot enhance the time resolution. Therefore, dynamic range requirements must be carefully considered when selecting sampling rates and A/D resolution to ensure effective data capture, particularly since current applications typically demand a higher dynamic range than voltage.

2.2.5. Data Quality

Data quality issues can take shape in a variety of ways: missing data, latched (duplicate) data, inaccurate data, or erroneous (incorrect) data. Missing data occurs when the instrument fails to record or transmit the data collected. Latched data occurs when the instrument records the exact same value for multiple measurement periods. Inaccurate data occurs when the value recorded is different from the value expected which is often the result of instrument misconfiguration. An example of inaccurate data often occurs with clock drift or clock misconfiguration, such as losing sync with the GPS system or misconfigured time zones. Finally, erroneous data typically appears as an outlier in a stream of data. Erroneous data can be characterized as something that is not physically possible for the quantity being measured. For example, if the system being measured is only 120 volts, then it would be highly unlikely for the value to be 300 volts. Examples of each are shown in Figure 10 [16].

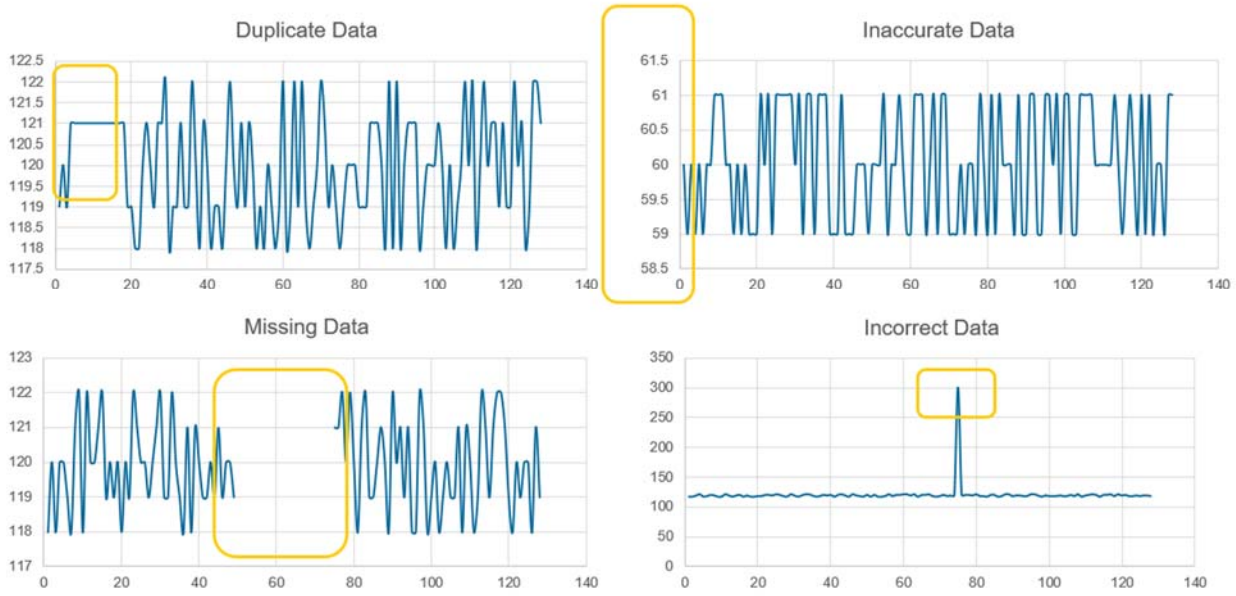

Figure 10 – Conceptual (not real-world) examples of different types of bad data. The x-axis indicates each reading from a sensor. These concepts can be similarly imagined for waveform data.

2.3. Data Collection and Communications Infrastructure

Modern data collection systems leverage a variety of architectures that rely on ubiquitous communications infrastructure and storage systems. Some of the most common network and communication architectures in use for data collection are described in Appendix A as a background. This section will discuss information specific to synchro-waveform data and WMUs – such as requirements for communications bandwidth, data storage, data compression, and data management and processing architectures and platforms.

2.3.1. Data Communications Requirements

Communications are nearly ubiquitous, but not all communication paths provide the same level of security or bandwidth. These considerations must be made when choosing a communications path. For example, control system related data generally must be kept separate from other types of data that leave the substation due to the sensitive nature of the control data. Similarly, a control system generally sends status points every 2-4 seconds. This may be done on a connection with limited bandwidth like a microwave for frame relay communications path.

Waveform data, especially at higher sampling rates, creates a significantly greater network burden than event-trigger data that should be considered when planning a sensor installation. Conversely, a PMU requires a minimum of 15 kilobits per second (kbps) bandwidth for a 30 frames per second (fps) reporting rate. This can be achieved with a variety of communication technologies like cellular or fiber optic networks. If multiple PMUs are reporting to a single point of aggregation, then that single point may require a network connection with 3 Mbps bandwidth.

An alternative technology option to utilize the existing broadband communication networks to deliver time-synchronized waveform measurements will be discussed in Section 2.5.

2.3.2. Integrating WMUs into an IEC 61850 infrastructure

PMUs, DFRs, and PQ meters traditionally function within distinct systems, separate from those based on the IEC 61850 standard. Typically, PMUs, DFRs, and PQ meters utilize a centralized architecture, which contrasts with the decentralized nature of IEC 61850 systems. The communication protocols for these devices often vary and may be proprietary, necessitating specific protocols to fully leverage their features.

When "Synchro-Waveform" data is employed exclusively for post-event analysis, the system architecture can adopt a flexible stance—be it centralized, decentralized, or a hybrid form, either integrated with or independent of IEC 61850. This adaptability grants a measure of independence from the IEC 61850-based control and protection systems, while effectively managing bandwidth and protocol limitations through various strategies. However, for real-time applications or optimizing Centralized Protection and Control (CPC) systems [17], considerations such as bandwidth, storage capacity, and integration with the IEC 61850 standard become essential.

To reduce data transmission across the Wide Area Network (WAN), one viable solution is to incorporate WMUs into a centralized platform at the substation level. This could include systems like CPC or Distributed Dynamic State Estimation (D-DSE), which operate using values sampled in line with IEC 61869-9 standards. To fully harness the potential of waveform analysis, new standard sampling rates may be necessary. The current rate of 14,400 Hz might not suffice for in-depth waveform studies, which could require sampling rates of 30 kHz, 60 kHz, or even the use of 10 Gbps Ethernet. While IEC 61869-9 also suggests a preferred sampling rate of 96,000 Hz, this frequency may be excessively high for certain applications.

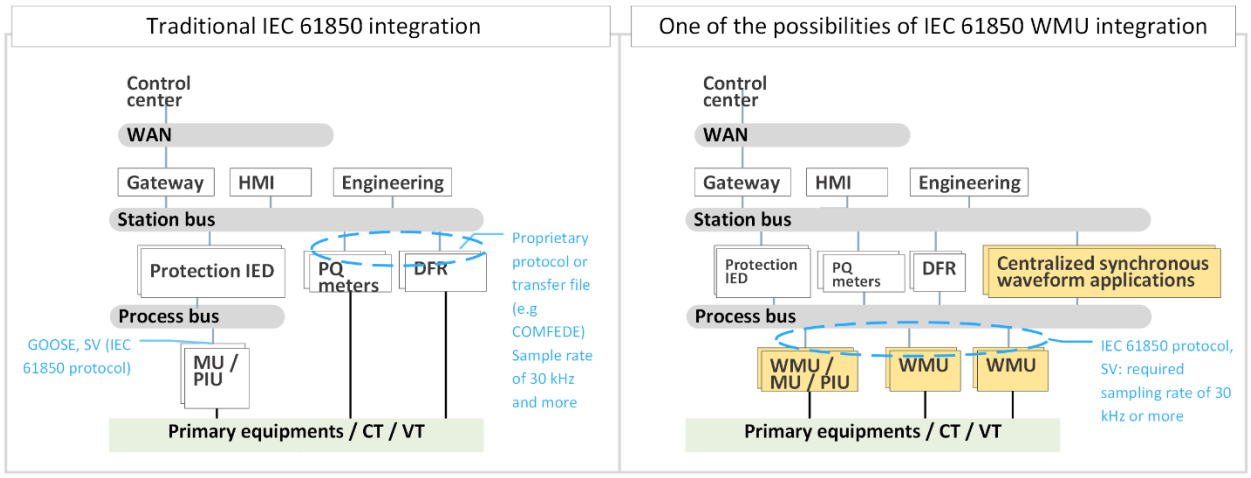

Figure 11. Integrating WMUs into an IEC 61850 infrastructure

2.3.3. Data Storage Requirements

Data volume is a principal concern for storing the data from the devices. This is influenced by at least three different factors: how long the data will be stored, the size of the individual files, and the number of instruments being deployed. In Table 1, if a single DFR produces one record per day that is roughly 3 MB in size, then a fleet of 250 DFRs will record nearly 750 MB/day. Therefore, to keep event files for a year from the entire fleet would require an estimated 273 GB of storage. Meanwhile, storing a single channel worth of data from a PMU will require nearly 60 GB of storage for the year.

Table 1. Data Volume Example

Description	DFR	PMU	PQ Monitor
Number of Devices	250	1	1500
Channels/Device	80	1	300
File / Data Size	3 MB / Event	164 MB / Day	3 MB / Day
Events / Day	1	10.3 M Points/Channel	144 Points / Channel
Total Storage for All Devices / Day	750 MB / Day	165 MB / Day	4.5 GB / Day
Number of Channels for All Devices	20,000	1	450,000

2.3.4. Synchro-Waveform Data Compression

Clearly, the use of waveform data has a disadvantage in terms of managing the high density of data, and the communications bandwidth required for streaming or bulk transfer of data between locations. The quantity of raw data which is generated and potentially transferred over a wide-area network (WAN) is much greater than typical synchro-phasor or SCADA data streams.

This inherent barrier means that system operators need to manage transmitting data over a WAN and long-term storage, and therefore the benefits from new applications must outweigh the operational burden from deploying infrastructure to support synchronized waveform monitoring.

However, there are promising approaches for lossless, or near-lossless, compression of waveform data for streaming and storage [18], [19], [20], [21], which can greatly reduce the burden on data communications and data archiving. Some compression techniques can operate in real-time and, counter-intuitively, have the benefit of reducing overall latency. This is because there is less data to transfer over the communications network leading to greatly reduced transfer time, so the computation time for compression and decompression is compensated (or becomes negligible [19]).

For high-density synchro-waveform data characterized by a sampling rate of 6,000 Hz and a 16-bit resolution, data storage can be decreased by 70% [22], with further compression up to 77.6% [23]. Additionally, by utilizing event-driven data compression, the data storage can be decreased by more than 95% [24].

2.3.5. Data Architecture (Centralized, Decentralized, or Hybrid)

The architecture for applying analytics to WMU data can be deployed as a centralized, decentralized, or hybrid system largely depending on whether the data is serving offline analytic development, real-time alerting or a combination of both use-cases. Applying advanced algorithms to WMU data, especially continuous waveforms, presents new "big data" challenges for utilities and vendors. Architecture and data engineering lie at the core of what makes big data analytics feasible to serve the needs of the analytics developers. Before diving into a big data architecture, it is necessary to discuss what a traditional event-based WMU data repository might look like, and why it is lacking in terms of big data analytics.

A traditional utility repository for WMUs is commonly a network attached storage server, where the individual data files are centrally stored from the WMU sensor fleet in their original file format, and sorted out in directories by substation, circuit, device, or date, for example. Or in a non-networked case, the data files are stored locally in the WMUs, and the user manually extracts them when needed for analysis. Metadata on the event, such as device, event date, event type, etc., is often concatenated into the filename where querying a set of events would involve some crafty scripts to parse the file names and extract the text, while much of the details about the event such as event triggers, remain unpacked. The waveform data will likely be stored in a standard waveform event format like COMTRADE or PQDIF where performing the analytics requires the user to know the standard to parse the file.

This sets up many challenges that make the analytics more complicated and unapproachable without domain knowledge of the file format standards. Furthermore, storing continuous waveform data is even more cumbersome due to its volume and lack of a standardized structure. Another challenge is the computation power required to process continuous waveform data, where traditionally analytics performed on standard desktop computers are ill equipped for the volume and scale of a fleet of WMU devices.

A big data approach addresses these challenges by pursuing the objectives below:

- Eliminate manual data retrieval from source devices
- Create a flexible access point to the data, eliminating the need for device-specific design
- Extract all data and metadata into a standardized database as a master repository
- Create a scalable system that can accommodate growing amounts of datasets, and a data management procedure that purges or compresses/archives data as needed
- Leverage an open-platform approach for cross-system compatibility and adaptability built in at the initial design stage

The following section proposes a generalized architecture intended to help guide organizations when selecting the specific technology components/vendors to meet their needs.

2.4. Data Processing Architecture for Waveform Analytics

2.4.1. Big Data Analytics Platform

There are significant opportunities in speculative analysis and visualization of historical data, collected from system-wide sources. However, this requires infrastructure for data warehousing

(for long-term data storage) and computation (such as for training and testing machine learning models) [18]. It also requires expertise in data science and cybersecurity. Depending on the size of the network managed by a system operator, this could be achieved in multiple ways:

- Ad-hoc analysis campaigns with temporary deployment of monitoring equipment, perhaps partnering with third-party specialists for data analysis.
- In-house data centers forming a private cloud, with dedicated teams for data analysis and cybersecurity. This requires maintaining significant resources and specialists.
- Public and commercial cloud infrastructure. This approach does require some caution for securing connections from the utility's systems to the cloud. However, being able to leverage existing, proven patterns and experts from the cloud provider can enable smaller utilities to avoid the need for employing specialized in-house teams to manage cybersecurity. It therefore only requires a low capex commitment and offers flexibility.

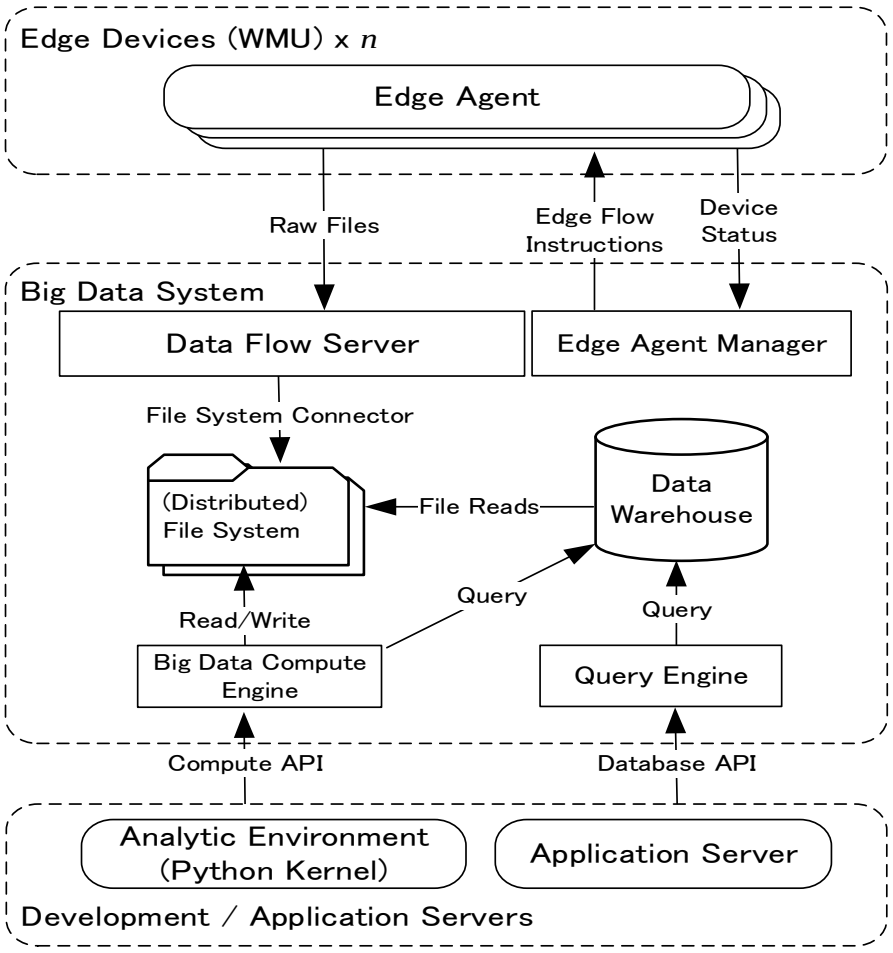

Figure 12. A generalized big data architecture for WMU data and other edge sensors alike.

2.4.1.1. Data Ingestion: Edge Agent and Agent Manager

There are multiple methods of obtaining data from WMU edge devices, where the nature of doing so largely depends on the specific device being used. The simplest method would be manually retrieving the storage drive from the field device and offloading its data. As rudimentary as it may seem, it might be the only option if existing communication networks cannot support the file transfer bandwidth. Ideally though, an automated data pipeline will bring in the data to a centralized system, enabling near real-time processing.

To address automating this file transfer, a background service running on a device can be used to orchestrate shipping the files off to a data collection server. This service is often referred to as an edge agent. Some WMUs will natively include this agent. For those that do not include this natively or maybe some customization of file transfer/processing is needed, an open-source option is Apache MiNiFi, which can run on both Linux and Windows systems with both Java and C++ versions. MiNiFi, for example, includes many commonly used connectors such FTP and HTTP, and the major cloud storage buckets. The agent can even handle some more advanced processing of files through scripts before the files leave the device. If there is a large fleet of WMU devices, an edge agent manager can be used to deploy data flow instructions at scale to all the edge WMU without needing to make modifications at the individual device level.

Another consideration is the frequency of data transfer. For event data, closest to real-time may be desired depending on the application. For continuous data, that may depend on the nature of how the device creates the data and network availability. For example, this could be processed in batches or streamed continuously if the device and network support streaming.

2.4.1.2. Data Flow

In some cases, an interface will be needed between the WMU endpoints and the central repository that acts as a single collection point for the fleet of WMU. This step can address these needs:

- File routing to storage system without modifying the data/file format
- Perform various type of data processing or transformation
- Provide data throughput regulation for the case of variable data input rates
- Run some analytics on the data as it is being received that maybe is not capable of being deployed on the WMU.

The nature and usage of the data flow will largely depend on the use-case and where it makes the most sense to deploy the analysis processes.

2.4.1.3. File System / Data Warehouse / Engines

The file system used for a central repository, data warehouse, and query/compute engine all work together where the file system serves as the backbone. In an open-source Hadoop ecosystem, the Hadoop Distributed File System (HDFS) serves that role, such that the query engines use HDFS as the backend for data access, while the query engines maintain metadata about the file structure. In most big data systems, writing data is slow, but once written, they support fast data access, key for dealing with large amounts of events and continuous waveform records from a WMU fleet.

Also noted here is the term “data warehouse” which is used to encapsulate the way most enterprises operate with many different types of data being stored together in one system. WMU data will likely be operationalized with other enterprise data which benefits having all the required data for a use-case in one location. Proper data engineering, such as table partitioning, will play a large role in the performance of the database.

To efficiently perform big data analytics, the data should be stored in a database that enables fast access, bulk query of data, i.e., using standard query language (SQL), and should not require the analytic users to parse the waveform files from their raw format. Since Python has somewhat been adopted as an unwritten standard for analytics, the database should support a Python API. This allows the most flexible usage of the data.

2.4.1.4. Analytics Environment / Applications

As mentioned above, most analytics are developed in Python, so if the database supports a Python API, the environment can be flexible with a vast number of algorithms readily available. To enhance usability of the data, wrapping frequently used database queries for the WMU data into a python library will help developers. Special cases of processing continuous waveform data in bulk quantities will require more robust compute needs to accomplish development and testing algorithms in a timely manner. Fitting in with the open-source Hadoop ecosystem is Apache Spark, a distributed computer engine designed to run on data stored in HDFS, while parallelization speeds up operations on huge amounts of data. Major cloud providers will either use Spark or have their own version of it. A Python-Spark API (PySpark) also exists to simplify code development.

At the end of the data pipeline, visual applications are the final step in achieving value from WMU data. Applications support both operational end-users and developers. Being able to visualize waveforms quickly and in one system aids in an overall greater user experience. When troubleshooting grid issues, having an application that can visualize data from other grid systems, such as circuit connectivity models, SCADA devices, and AMI meters plays into the need for a data warehouse and strong integration between systems that need to share data.

2.4.2. Data Processing and Real-Time Processing Architecture

To deliver a variety of real-time applications, suitable infrastructure for robust time synchronization, computation, and communications must be deployed. The infrastructure needs to be scalable in terms of the number of waveform measurement devices supported and the geographic area addressed.

A strategy for avoiding high bandwidth data transfers is to perform initial processing of waveform data streams locally within substations. Data only needs to leave the substation by exception, such as when local processing has characterized an event. Data compression schemes already exist to significantly reduce data transfers during steady-state conditions, with somewhat increased data bandwidth requirements during system events. Furthermore, processed outputs, such as a frequency spectrum, can be transferred instead of the raw waveform data – so that computation is inherently distributed over multiple substations.

However, some applications, such as robust wildfire prevention, may require continuous data streaming of waveform data between multiple locations over a wide area. This can be challenging and costly to achieve, particularly for complex distribution networks.

Table 2 proposes a suitable architecture for various waveform monitoring applications, using the following categories:

- **Local substation**: "edge" processing within the substation can perform the function, perhaps with non-real time reporting to a central location.
- **Wide-area, some substations**: wide-area coordination is required, but sparse deployment of waveform monitoring devices is acceptable.
- **Wide-area, every substation**: full deployment of waveform monitoring at every substation/node is required for optimal results.
- **Grid-wide**: coordination of data over a large synchronous AC region is required.

Table 2 illustrates that significant value can be delivered using local waveform-based computation within substations, involving minimal additional infrastructure. Expanding the deployment of waveform measurements across multiple substations further increases the opportunities, such as for locating transients and oscillations.

Table 2. Waveform monitoring applications and associated infrastructure requirements

	Monitoring locations required			
Application	**Local substation**	**Wide-area, some substations**	**Wide-area, every substation**	**Grid-wide**
Capacitor switching monitoring	✓			
Circuit breaker condition monitoring	✓			
Cable condition monitoring (e.g. tracking incipient faults)	✓			
Locating transients		✓		
Fault or other event classification	✓	✓ (ideally)		
Wildfire detection/prevention		✓	✓ (ideally)	
Oscillation detection and location	✓ (detection only)	✓	✓ (preferred)	✓ (ideally)
Power quality monitoring	✓ (for some applications)	✓	✓ (ideally)	
Converter dynamics	✓			
Inertia monitoring	✓	✓	✓	✓

■ Edge Processing

Throughout this section, edge processing has lightly been discussed since there are so many ways it can be approached. In general, edge processing takes a burden off the central storage, computation and network requirements by reducing the amount of data backhauled. Most WMUs come out of the box with edge processing in the form of event triggering. Today, the industry is

working to develop more advanced forms of event triggers, looking for specific grid phenomena such as arcing. To develop these triggers, it often requires first looking at continuous waveform data or a vast amount of historic event data, justifying a need for a big data architecture first. As this industry evolves, it may become more common for these advanced event triggering algorithms to reside on the WMU devices, rather than transferring vast amounts of data to a central repository.

2.5 Synchro-waveform Measurements from Adjacent Infrastructure

The existing broadband communication networks run parallel to the existing distribution grid, draws power from it, and deploy hundreds of thousands of industrial Uninterruptable Power Supplies (UPS) that already monitor the grid for power outages to provide backup power to the broadband network; see Figure 13(a). Therefore, broadband communication networks can be utilized for the purpose of transmitting WMU measurements, especially from locations outside of the substation, where the utility may not have access to high-speed communication. This removes the constraint of limited communication capacity in solving the grid visibility problem.

In this regard, there is an opportunity to co-locate low-cost WMUs on the secondary feeds, within the existing UPS enclosures that deliver power to the broadband network and leverage the cable modems they already contain for telemetry data. The direct availability of high-bandwidth, low latency wired communications allows a design approach of high frequency sampling of the power waveform (12-bit samples at 10kHz, synchronized via GPS timestamp), with continuous streaming of that data to centralized monitoring/analytics server infrastructure.

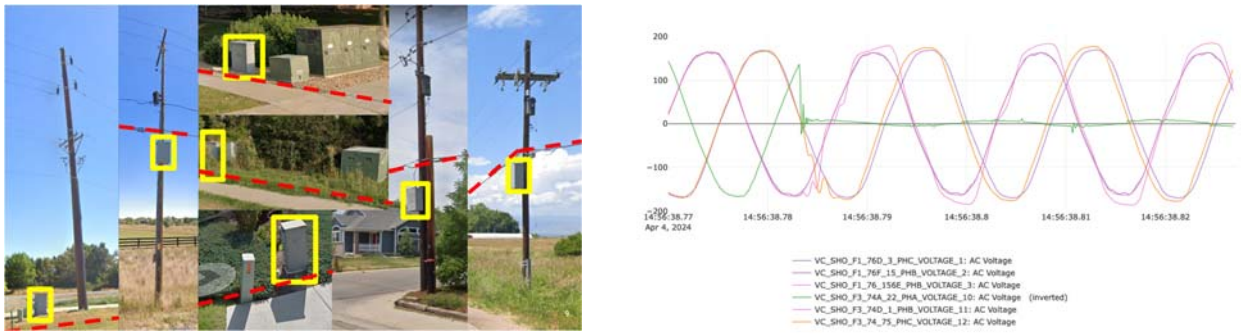

(a) **(b)**

Figure 13. (a) Broadband network parallels distribution grid; and (b) Example waveform data [25].

Figure 13 (b) shows an example of waveform measurements that are simultaneously recorded at UPS enclosures at existing broadband communication networks during a fault.

A project by CableLabs® [26] recently developed and demonstrated a sensor package and system to provide this kind of high-fidelity grid monitoring; leveraging the existing cable broadband networks by placing a sensor package within the broadband UPS hosting sites. Several pilot projects are underway demonstrating the value of this approach; see [25] for more details.

3. Synchro-Waveform Data Representation

Raw synchro-waveform measurements are time-stamped waveform samples. However, synchro-waveform data can be represented also in other forms, as we will discuss next.

3.1. Event Signature Extraction

Waveform data is particularly useful when it contains disturbances or abrupt changes. As a result, it is beneficial to conduct event-based data analytics. To use this strategy, one needs to address the following tasks: event detection (using techniques in time-domain, frequency domain, and hybrid wavelet concepts), event classification (by feature extraction, such as transient oscillation modes, impulses, graphical features, number of affected phases, firing angle, magnitude, and duration of events), and event location identification (using data-driven and model-based methods to pinpoint the source location of the event, including sub-cycle and transient events). Many of these techniques may require extracting the "event waveform" from the raw waveform data, such as by using the concept of differential waveforms [1] [27]. An example is shown in Figure 14. Here, the differential waveform is obtained by subtracting the waveform cycle that is before the event cycle from the event cycle. The extracted event waveform can be used in various studies, such as modal analysis to examine the frequency and the damping rate of the high-frequency oscillations in the system. The frequency of the damping oscillations in Figure 14(b) is about 1 kHz.

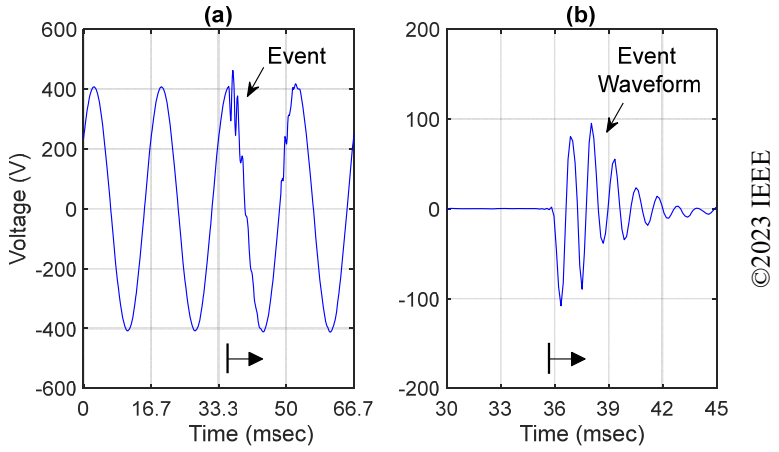

Figure 14. Real-world voltage waveform during an event, as in (a), and its extracted event waveform, as in (b) [1] [28].

3.2. Harmonic Phasor Representation

Synchro-waveforms can also expand our ability to conduct analysis in the phasor domain. While PMUs are traditionally focused on reporting synchro-phasors at the fundamental frequency of the power system (such as 60 Hz in North America), synchro-waveforms can provide synchro-phasors also at harmonics or other frequencies. In other words, synchro-waveforms can provide us with harmonic synchro-phasors, i.e., the measurements provided by Harmonic Phasor Measurement

Unit (H-PMU). The H-PMU is a technological evolution of the conventional PMU. Unlike a conventional PMU that solely captures fundamental phasors, an H-PMU encompasses the measurements of both fundamental and harmonic phasors. H-PMUs provide the complete representation of a signal in each harmonic, including both magnitude and phase angle [29], [30].

An example is shown in Figure 15. The phasor measurements in Figure 15(a), which include magnitude and phase angle over 800 milliseconds, correspond to the signature of an event as it is captured at the fundamental frequency. Such measurements are those that are commonly provided by PMUs. As for the phasor measurements in Figure 15(b) and Figure 15 (c), they correspond to the signatures of the same event during the same period, but they are captured at the 3rd harmonic frequency and at the 5th harmonic frequency, respectively. The additional information provided by the harmonic synchro-phasors can complement and enhance the analysis one can do with the synchro-phasors in the fundamental frequency. Therefore, even in a frequency-domain analysis, the use of synchro-waveforms can be potentially advantageous due to their ability to provide both fundamental and harmonic synchro-phasors. Of course, whether at the fundamental frequency or at harmonic frequencies or at any other arbitrary frequency bin, synchro-phasors are inherently meant for steady-state analysis. On the contrary, synchro-waveforms can capture the raw transient event in the time domain.

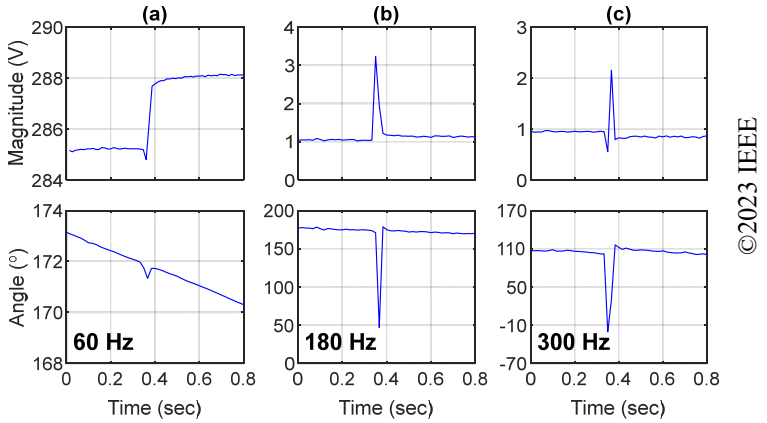

Figure 15. Signatures of an event at different frequencies: (a) fundamental frequency; (b) 3rd harmonic; and (c) 5th harmonic [1] [31].

The enhanced detail provided by harmonic phasor measurements allows for more accurate and insightful analysis of power system events. For example, the information from harmonic phasors can be used to improve event clustering, enabling better identification and categorization of events based on their unique signatures across different harmonics. To see this, consider the feature spaces in Figure 16, which are based on the fundamental phasor and third harmonic phasor measurements, respectively. The colors represent the same clusters identified in Figure 16 using fundamental phasor measurements. Comparing these figures reveals that the clusters based on fundamental phasor features do not hold for higher harmonic feature spaces. This discrepancy indicates that clustering based solely on fundamental phasors may miss characteristics existing in higher harmonic phasor features [29].

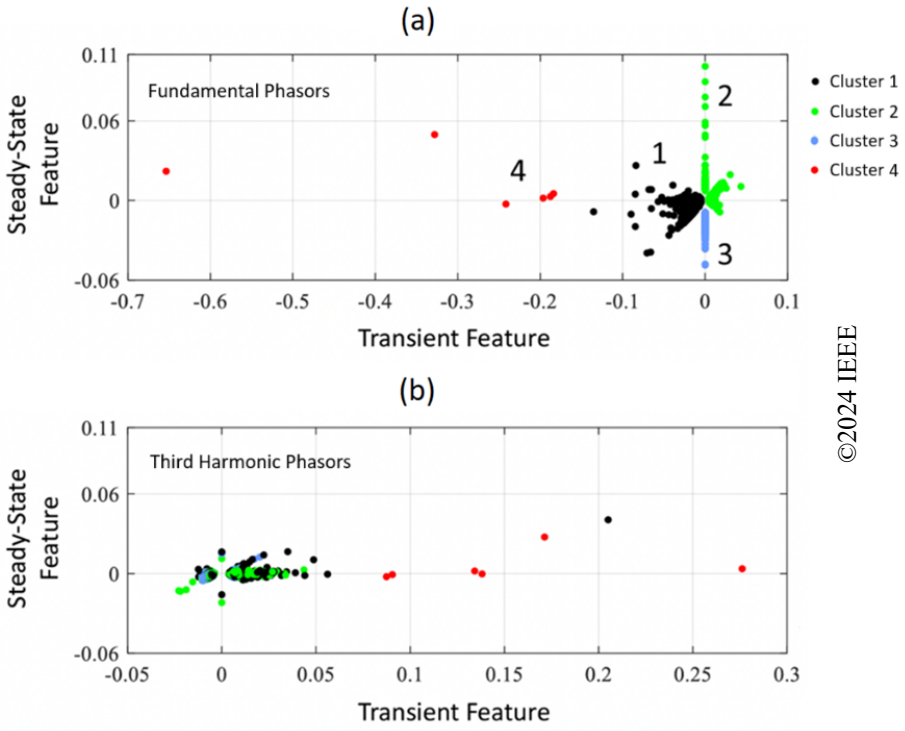

Figure 16. (a) Event clustering based on *fundamental* phasor signature feature space; (b) Same clusters based on their third harmonic phasor signature feature space. It is clear that considering the features in the third harmonic phasor would significantly change the outcome of clustering [29].

Harmonic synchro-phasors can also be used in topology and phase identification and harmonic state estimation; e.g., see the recent studies in this area in [32] [33] [34] [35].

3.3. Wideband Phasor Representation

Due to the interactions between the power electronic devices and the power grids, wideband oscillation events have occurred frequently in renewable power systems with frequencies from several Hz to several kHz. For example, in 2017, a high-frequency oscillation event has occurred in China's Southern Grid due to the interaction between a Modular Multilevel Converter (MMC) and the AC networks [36]. Wideband phasor measurement (WB-PMU) can be used to monitor the wideband oscillation online and alarm the operator to cope with such an issue in real time [36].

There is only a definition for the fundamental synchro-phasor in the IEEE/IEC standard [37]. A harmonic synchro-phasor can be a phasor referring to the frequency of the harmonic order multiplying the nominal frequency. Accordingly, an inter-harmonic synchro-phasor can be a phasor referring to the nominal frequency or the closest harmonic frequency.

One typical application for the WB-PMU and H-PMU measurements is their use in the adaptive mitigation of the high-frequency oscillation in MMC-HVDC systems [38]. Due to the variation of the power system operating conditions, the frequency of the wideband oscillation can be time-varying. Traditional oscillation mitigation methods with determined parameters are difficult to

suppress high-frequency oscillation with time-varying frequency, and the wideband phasor measurements can be used for wideband oscillation adaptive mitigation.

To do so, oscillation source identification should be done based on the WB-PMUs [39]. Several WB-PMUs can be deployed at MMC conversion stations and substations. Moreover, a centralized oscillation source identifier can be installed at the main station. Wideband state estimation can be conducted based on the WB-PMUs, and wideband power flows at the oscillation frequency can be calculated. The oscillation source can be identified by checking that it outputs wideband power.

Next, oscillation mitigation controls can be done at the oscillation source. To deal with the problem of traditional mitigation methods, an adaptive wideband oscillation mitigation scheme based on the wideband phasor measurements is proposed. Specifically, the wideband frequency measurements are used to adaptively change the center frequency of the notch filter embedded in the MMC control loop.

The test results have been shown in Figure 17. The WB-PMUs can successfully capture an oscillation mode with a frequency of about 1273 Hz at 3.14 s. Then the center frequency of the notch filter is adaptively adjusted, and the oscillation components quickly disappear. As seen, the WB-PMUs are useful in high-frequency oscillation mitigation.

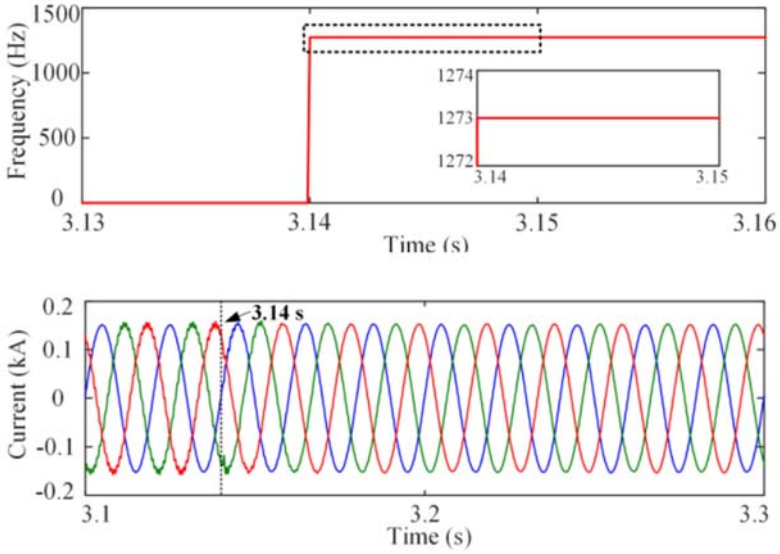

Figure 17. Schematic diagram of the ANF-based HFR mitigation method.

3.4. Graphical Representations

Graphical concepts, combined with tools from image processing, can also be used, such as by expressing the waveform measurements as a Lissajous graph [40], by plotting the current waveform versus the voltage waveform, as shown in Figure 18, either in a raw waveform or in a differential waveform. Different features of the Lissajous graph can be analyzed accordingly to extract graphical features. For example, the shape of the Lissajous graph itself can help identify

the type of event. The rotational angle of the Lissajous graph can sometimes help identify the location of the event. Further, similar events may result in different Lissajous graphs that in fact become similar after rotating them. This fact too can be used in identifying the type of event. The area of the Lissajous graph can also be used to detect an event or disturbance.

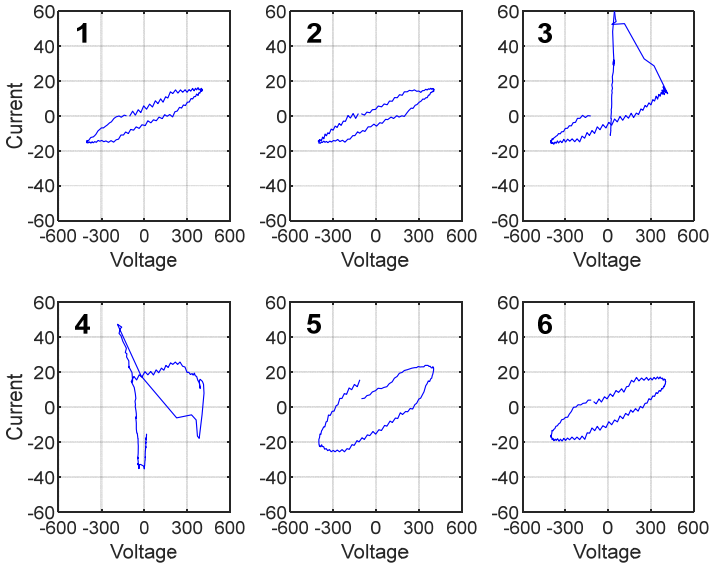

Figure 18. An example of a graphical representation of waveform data. Per-cycle Lissajous graphs for voltage and current during six cycles, where a transient event occurs at cycle 3 [1] [40] [41].

3.5. Other Per-Cycle Representations

When raw waveform samples are available, various per-cycle metrics can be obtained from the raw data. Some concepts from power quality analysis can be particularly used in the analysis of synchro-waveforms, albeit after some modifications. For example, consider the concept of THD. In power quality analysis, THD is often examined over a long period of time, and via statistical metrics. However, in the analysis of synchro-waveforms, we can obtain THD on a per-cycle basis (or other forms of short-term THD) and compare the results across different WMUs in a synchronized fashion. An example is shown in Figure 19. Here, the synchro-waveforms are measured continuously over two hours. Accordingly, a total of 432,000 per-cycle THD values are obtained in this period. There are two instances in this figure, i.e., in two cycles, when the THD is unusually higher than the rest of the cycles. These two instances indicate the occurrence of two separate sub-cycle events, as marked with arrows. The first sub-cycle event occurs at a moment when there is also a sudden change in the long term THD. The THD suddenly drops when we compare the cycles before the first sub-cycle event versus the cycles after the first sub-cycle event. As for the second sub-cycle event, it is an isolated incident since it does not cause a change in the rest of the per-cycle THD values before and after this sub-cycle event occurs. We can similarly plot the per-cycle THD profile for every WMU. By comparing similar graphs from multiple WMUs we can identify the source region of the sub-cycle events for further investigation.

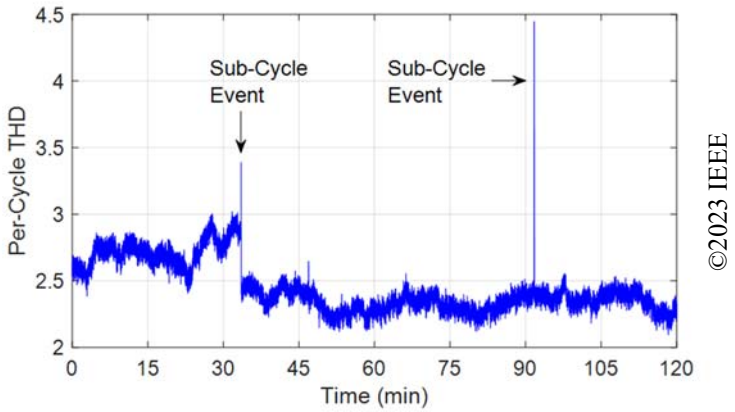

Figure 19. Per-cycle THD in a continuous stream of synchro-waveforms. Two sub-cycle events are marked [42].

Recently, synchro-waveforms have been used in an empirical study to address voltage harmonic distortion under incipient faults in distribution systems [43] . Basically, data-driven algorithms can be developed to extract short-time total harmonic distortion using waveform data reported by sensors at different nodes (locations) along the feeder. These sensors are equipped with synchronous waveform capturing capabilities and perform as essential measurement devices at the grid edge. By analyzing their data, one can obtain comprehensive insights into the voltage distortions during various fault conditions. Experiments conducted in a real-world distribution system indicate that the voltage distortions during the fault interval can be remarkably different depending on the sensor location. Furthermore, the numerical results revealed that some temporary/permanent faults exhibit a voltage distortion similar to the distortions observed under incipient faults [43].

3.6. Joint Analysis of Synchro-waveforms with Other Data (PMU/AMI/SCADA)

Event reports from North American Electric Reliability Corporation (NERC) highlight the need for both phasor and synchro-waveform measurements for analysis of inverter-related disturbance events [44] [45] [46]. High-resolution synchro-waveform measurements from the points of interconnection (POIs) of the IBRs offer deeper insights into the signatures of the disturbance events and the response of IBRs which may otherwise be missed by phasor measurements [47]. Synchro-waveform measurements can complement the existing phasor-based analyses and enhance the capabilities of the disturbance monitoring applications. For instance, in root-cause analysis of an IBR-related event like a trip, a voltage deviation, or a momentary cessation, the synchro-waveform recordings jointly with the phasor measurements from the POI can accurately pinpoint the protection setting violations which led to the event. The analysis can also demonstrate the trip or the momentary cessation complied with the ride-through requirements stipulated in the NERC and IEEE reliability standards [48] [49]. The reliability guidelines specify the frequency and voltage ranges, both in instantaneous and root-mean-square (RMS) values (see Table 3), the inverter is expected to ride through without tripping or going into momentary cessation. Detailed analysis of IBR events, therefore, requires analyzing both the PMU and synchro-waveform disturbance data. To illustrate this, a case study with two examples is presented next.

Table 3. Frequency and Voltage Ride-Through Requirements (Source: Southern Power [49])

Frequency, f (Hz)	Minimum Ride-Through Time (s)
$f > 61.8$	No ride-through requirement
$61.6 < f \leq 61.8$	299
$61.2 < f \leq 61.6$	540
$58.8 \leq f \leq 61.2$	Continuous
$58.4 \leq f < 58.8$	540
$57.0 \leq f < 58.4$	299
$f < 57.0$	No ride-through requirement

Root-Mean-Square Voltage (p.u.)	Minimum Ride-Through Time (s)
$V \geq 1.2$	No ride-through requirement
$1.1 < V \leq 1.2$	1
$0.9 \leq V \leq 1.1$	Continuous
$0.7 \leq V < 0.9$	3
$0.5 \leq V < 0.7$	2.5
$0.25 \leq V < 0.5$	1.2
$V < 0.25$	0.16

Instantaneous Voltage (p.u.)	Minimum Ride-Through Time (s)
$V \geq 1.8$	No ride-through requirement
$1.7 < V \leq 1.8$	1
$1.6 \leq V \leq 1.7$	Continuous
$1.4 \leq V < 1.6$	3
$1.2 \leq V < 1.4$	15

The examples consider a disturbance monitoring application that detects and analyzes IBR-related events like trips and momentary cessation. The application is designed to have two layers. At the top layer, the PMU data detects and informs the user with high-level information on the occurrence of an event. Analyzing the PMU data, the application at this layer also checks if the event complied with the ride-through requirements with respect to the RMS voltage and frequency at the POI. At the next layer, the synchro-waveform data offers detailed analysis of the disturbance waveform. Similar to the top layer, the analysis at this layer checks if the event complied with the ride-through requirements prescribed for the instantaneous quantities. The waveform data for this study are obtained from the electromagnetic transient (EMT) simulation of PV trip events. Two example cases are presented. In each case, the PVs tripped due to a disturbance in the power network. However, the protection setting violations and the ride-through compliance behavior for each case are different. These example cases demonstrate the utility of using both PMU and WMU data to detect and distinguish between different trip scenarios.

For the trip scenario in example 1, the voltage and current phasor magnitudes and the event-triggered synchro-waveform records are shown in Figure 20. The trip is detected from the

magnitude of the current phasor dropping to zero and remaining at that value for successive reporting windows. For the root cause analysis, the frequency and the voltage phasors and their waveforms are compared against the requirements in Figure 20. The RMS voltages for all three phases and the frequency are within the ride-through limits. Therefore, with only PMU data observation, one may erroneously infer that the IBR was supposed to stay online and not trip. However, as seen from Figure 20, there is an instantaneous overvoltage (OV) in phase A. The voltage in this case exceeded 1.2 p.u. for over 1.5 ms, which is outside the requirements for instantaneous OV ride-through. Therefore, the IBR trip was permissible and legitimate. Note that this detail is seen only with the synchro-waveform data and not captured by the RMS quantities reported by the PMU.

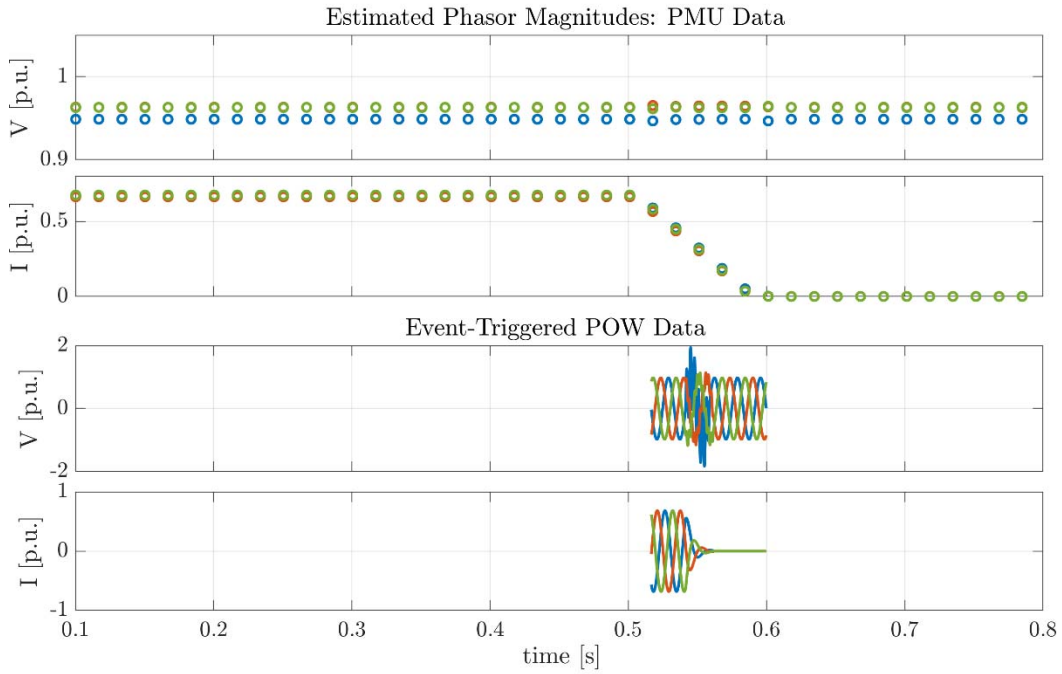

Figure 20. PMU and WMU data for the disturbance in example 1.

Next, for the trip scenario in example 2, the PMU data and the event-triggered synchro-waveform disturbance record are shown in Figure 21. The PV trip in this case is due to a fault in a nearby bus, which led to instantaneous overcurrent (OC) in one of the phases. In this case, both the RMS voltages and the instantaneous voltages during the disturbance are within the ride-through limits. This implies that the IBR should have withstood the disturbance and remained online. Still, the IBR tripped due to an inappropriate instantaneous OC protection setting. Event analysis, therefore, flags this as a nuisance trip.

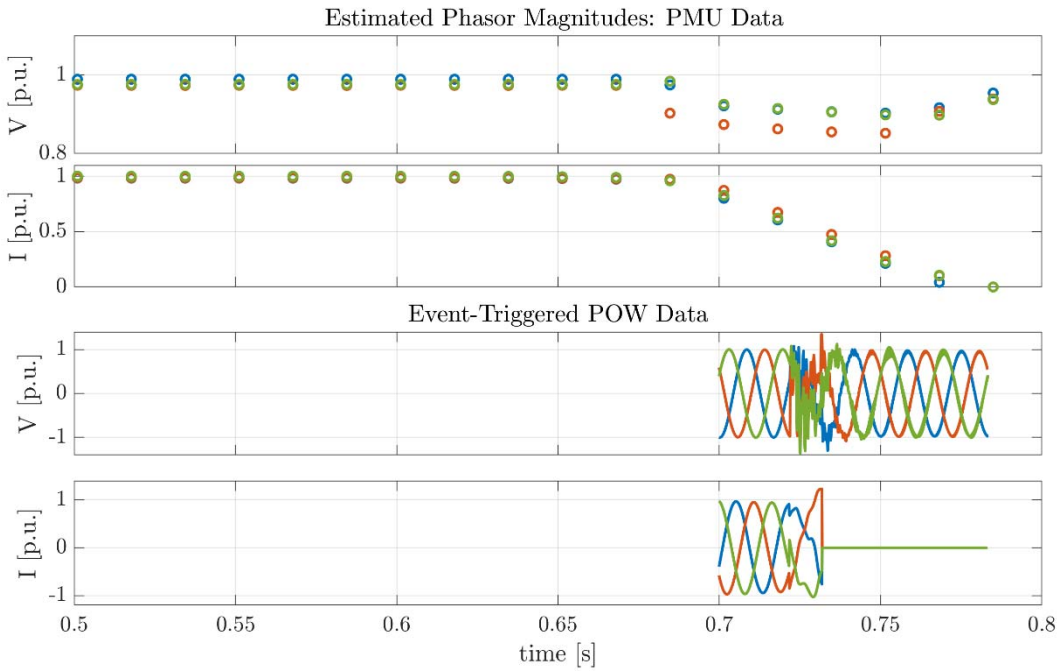

Figure 21. PMU and WMU data for the disturbance in example 2.

4. Basic Methods to Work with Synchro-Waveform Data

As the integration of IBRs increases in power systems, the need for synchronized waveform measurements to address limitations of existing synchro-phasor-based monitoring approaches becomes apparent. Several events from the recent past, like that of the Blue Cut Fire, Canyon Fire, and others [44] [45] [44] [50] have underscored this requirement and prompted analysis by regulatory bodies like NERC [46] [51]. The NERC draft Standard PRC-028-1 for "Disturbance Monitoring and Reporting Requirements for Inverter-Based Resources" [52] requires fault and dynamic disturbance recordings at $\geq$ 128 samples-per-cycle at IBR facilities, to be retrievable for at least 30 calendar days [52]. The standard further requires the data recordings to be synchronized to UTC, with the synchronized clock accuracy being within $\pm 100\mu s$ of UTC. The synchronization accuracy required by the IEEE 2800-2022 is more stringent, requiring all IBR plant-level monitoring devices to be synchronized to UTC with $\pm 1\mu s$ accuracy [48]. Therefore, as synchronized waveform recordings will play a key role in analyzing grid disturbances going forward, understanding methods for acquiring, transporting, storing, and analyzing said measurements is required.

This chapter presents a high-level overview of the methods enabling the streaming, acquisition, and analysis of waveform measurements for a variety of end-use applications. Some open questions, research gaps, and recent industry experiences are also explored. This material sets the premise and foundations for the discussions on synchronized waveform applications in the following chapter.

To summarize, this chapter discusses methods in the following classes:

1. Data transport: Continuous vs. trigger-based streaming
2. Data storage and handling: Data compression and compressed sensing
3. Data analysis:
    a. Continuous applications: Frequency and ROCOF estimation
    b. Disturbance analysis and characterization: Event detection, classification, and localization

Table 4. Summary of methods discussed in this chapter

Class	Category	Potential Applications	Existing Approaches	Open questions
Data Streaming	Continuous	High-frequency oscillation monitoring, continuous monitoring and evaluation of IBR performance	Transport through ethernet available in most devices.	• Large bandwidth and data storage requirements, • Need for additional communication infrastructure to support continuous streaming
	Trigger-based	Post-mortem analysis of disturbance events	Cloud streaming available in devices like Power Monitors Seeker	• Determining optimal thresholds for triggering, • Triggering needs to be agnostic to the nature of the disturbance/event.
Data Compression	Trigger-based	Post-mortem analysis of disturbance events	Curve-fitting based 'Goodness of fit' metric to determine if system conditions deviate from sinusoidal model	• Determining optimal thresholds for triggering • Triggering needs to be agnostic to the nature of the disturbance/event • Strategies for combining compression algorithms that assume a sinusoidal model with general purpose compression techniques when a deviation from the sinusoidal model is expected, to optimize compression ratio, information loss, and computation burden
			THD as a metric for determining deviations from fundamental-frequency phasor model	
	Lossless Lossy		Triggering if an event is detected	
			Phasor estimation	
			Dynamic phasor estimation, e.g. Functional Basis Analysis (FBA)	
Data analysis	Lossless		Cyclical High Order Delta Modulation (CHDM)	
		Signal distortion calculation	STTP Time Series Special Compression	

	Disturbance analysis and characterization Steady-state Disturbance analysis and characterization	Event detection	General purpose compression schemes (e.g., LZMA, Gzip, etc.)	
		Frequency estimation	Dynamic phasor estimation (e.g. FBA)	
		Signal distortion calculation	Curve-fitting residuals, signal-to-noise ratio (SNR), THD, etc.	
		Event detection	Differential waveforms	

4.1. Data Streaming: Continuous vs. Trigger-based

As mentioned in Section 2.1, WMUs may report synchro-waveforms as a continuous (gapless) stream of measurement samples, or they may operate on an event-triggered basis, where waveform data are discarded (i.e., not reported) unless specific event detection criteria/logic are met [10].

Gapless streaming of synchro-waveforms can cause a huge big data challenge, as we discuss next.

4.1.1. Handling Large Volumes of Synchro-Waveform Data

As waveform data reporting rates (~kHz) are much higher than those of synchro-phasor rates (30/60 or 50/100 frames per second), continuous streaming of waveform measurements is a significant challenge considering the current communication infrastructure deployed by utilities. A survey shows that communication infrastructure limitations prevent several waveform applications from being deployed in the field in the near-term [53]. At the same time, commercial devices offer the ability to continuously stream waveform measurements. For example, SEL Axion offers streaming over Ethernet, while Power Monitors Seeker offers streaming to cloud platforms.

The size and volume of streaming synchro-waveform measurements necessitates that applications aimed at utilizing them have certain features, including:

1. *Bandwidth:* Any application that requires continuous streaming of synchro-waveform data will require robust communications networks capable of handling the sheer volume of data transfer required.
2. *Storage:* Storage requirements increase with waveform sampling rates. A signal segment sampled at 1 kHz over 1 second and quantized to 24 bits will take up roughly 3 kB without any extra information added for things such as communication packets. Similarly, that same signal sampled at 1 MHz over 1 second and quantized to 24 bits will require 3 MB.
3. *Computational burden:* Any signal processing or other computational processes that need to be performed on the data will be lengthened as the size of the data increases. For example, a low-pass FIR filter to smooth out noise with N taps requires 2N operations to produce a single output sample. For a signal sampled at 100 Hz, this would require 200N operations per second, whereas for a signal sampled at 15,360 Hz (a common synchro-waveform sampling frequency that equates to 256 samples per cycle at 60 Hz operating frequency), 30,720N operations per second are necessary. Naturally as the filter size N increases, so does the number of required operations.

A pilot study at Dominion Energy in the US showed that the continuous streaming of waveform data from 66 substations at 16 samples/cycle generated 3.9 TB of data each day. Even with high-speed (1 Gbps) communication, there were several hours of time delay in the data transport [54]. Instead of costly communication bandwidth upgrades, the use of distributed learning and edge computing approaches has been proposed to stream only critical actionable information to control centers, as also discussed in Chapter 2.

Trigger-based streaming, i.e. streaming snippets of waveform data corresponding to suspected abnormal conditions, has also been proposed as an alternate method to aggregate waveform measurements from different grid locations for centralized analysis. A common way for triggering could be based on the activation of protection elements like overcurrent relays. In Figure 22, an example multi-phase fault from the Grid Event Signature Library [55] is shown. This data record has instances of both event and non-event (i.e. "normal"). The portions boxed in red are what are considered the "event", and thus are what the relay or other measurement device would store/stream for further evaluation.

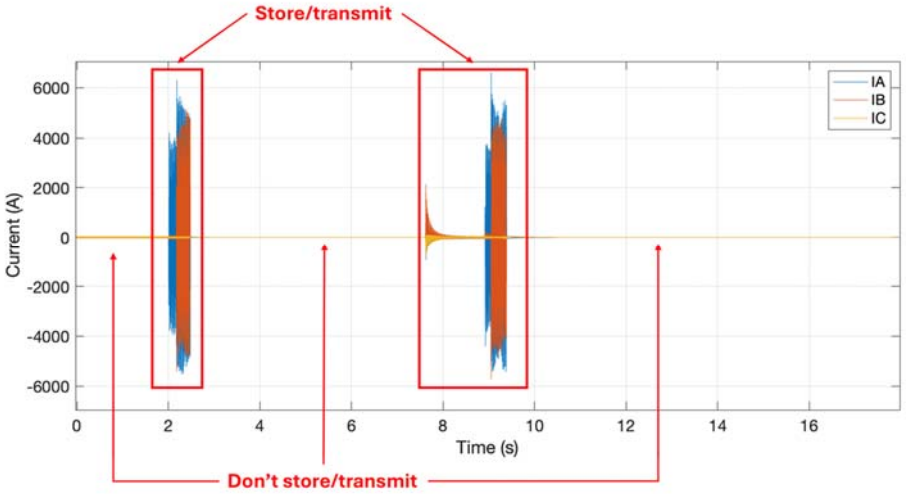

Figure 22 : Event vs. "normal" regions. Event ID 679 from the Grid Event Signature Library [55]**.**

Determining optimal thresholds for event-agnostic triggering remains an open question and an alternate method for determining triggers is described next.

4.1.2. When Synchro-waveforms are Needed Instead of Synchro-phasors

If phasor representations fail to accurately represent system conditions during a disturbance, triggering the streaming of waveform measurements will be valuable for end-use analysis.

Phasor estimation assumes that the preprocessed input signal is sinusoidal. With this assumption, the signal parameters, i.e.,phasor amplitude, phase angle, frequency, and ROCOF, are estimated from the data. Under ambient conditions, this assumption on the signal model is reasonably valid. However, during disturbance events, the waveform data deviates from the sinusoidal signal model. The phasors estimated during events are prone to error and may mislead monitoring applications. Misinterpretation of grid measurements can have severe impacts on power grid operation, posing safety risks to operators, and can even trigger cascading effects on generation across the grid. For

example, poor quality estimations of frequency and ROCOF can lead to false triggering of Loss of Mains (LOM) protection, as seen in a study on the Bornholm Island grid in the Baltic Sea [56], which found that PMUs reported ROCOF estimates of several hundred Hz/s when phase shifts were present in the waveform [56]. Similarly, in 2017, erroneous frequency estimates during a fault in California undesirably tripped inverters connecting a number of solar power plants, resulting in the loss of nearly 1200 MW of generation [44].

This limitation on the sinusoidal model, imposed by phasor representation, motivates the need to formulate a trust metric on the reliability of the estimates. Using the curve fitting-based phasor estimation approaches, the least-squares error (LSE) between the data and the fitted model can be a measure of this trustworthiness [57]. A large value of LSE indicates that the measurement window contains non-sinusoidal waveform data, and the phasors estimated in that window should, therefore, be used with caution. Similar approaches, like [58], also define the trust metric of estimation as goodness-of-fit (GOF) of the normalized fitting error expressed in the logarithmic scale. A low GOF is equivalent to high LSE and low trust on the PMU data.

The use of an LSE-based metric for detecting non-sinusoidal waveforms and assessment of trust on phasor estimates is demonstrated using the example below. A snippet of three-phase field-measured waveform data from the Grid Event Signature Library [55], is shown in Figure 23. The data contains the recording of a 1-cycle disturbance event at t = 2.05 s due to a line-to-line fault which self-cleared. With the exception of this short data window, the voltage waveforms as seen in Figure 23 are nearly sinusoidal. The estimated phase amplitudes and the LSE values are also shown in Figure 23. The LSE values are low before the occurrence of the fault and sharply rise to a high value in the event window. This, as mentioned, is indicative of two things: (a) the window contains non-sinusoidal data, and (b) the estimated phasors in this window are less reliable.

For data windows with non-sinusoidal data where PMU estimates are not very reliable, the direct use of waveform data may be needed. Short bursts of time-synchronized WMU data, recorded only for the event windows, offer deeper and more accurate insights into disturbance analysis.

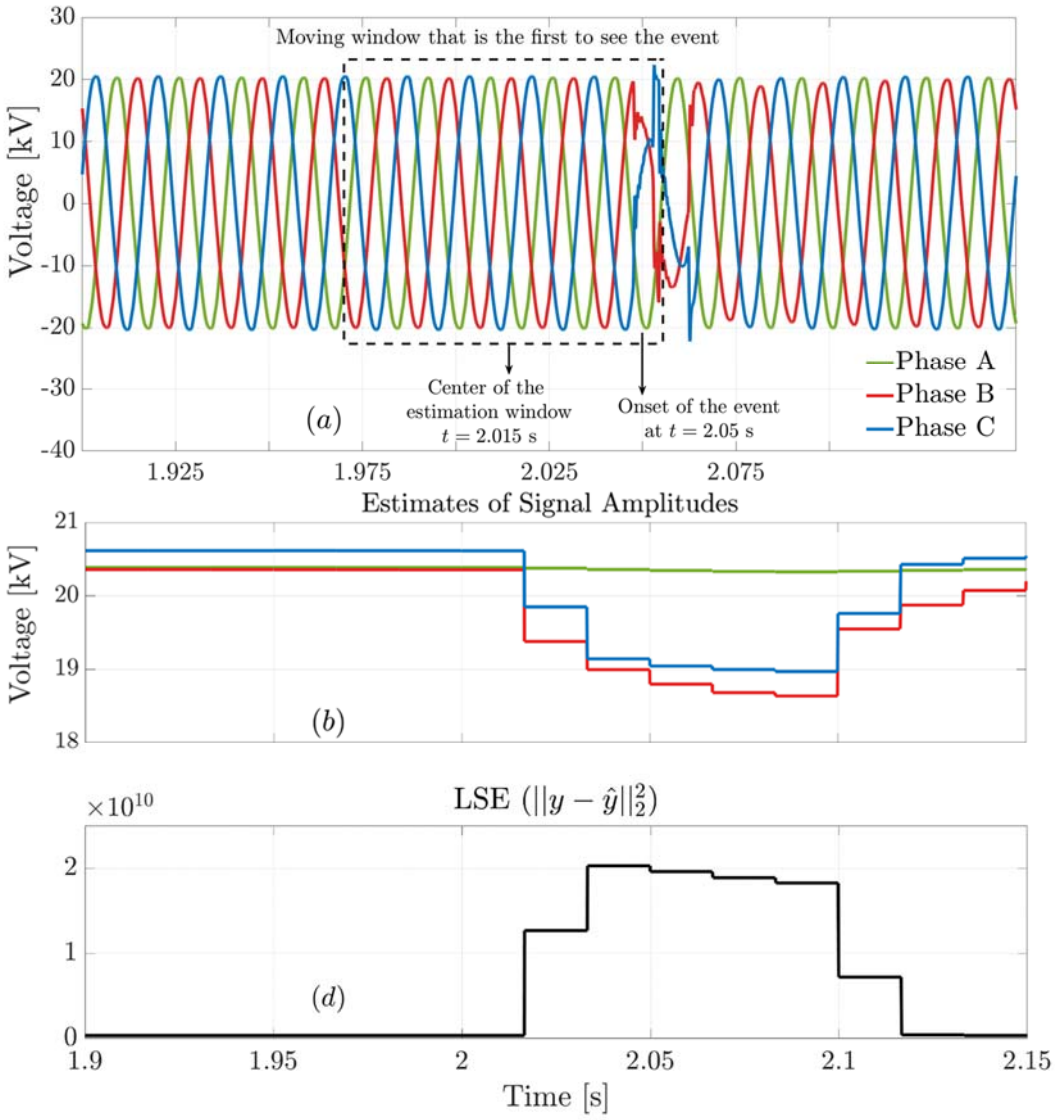

Figure 23. (a) Field-measured voltage waveforms capturing a line-to-line fault, (b) estimated voltage phasor magnitudes, and (c) LSE values indicating trust on phasor estimates.

4.2. Data Storage and Handling: Data Compression and Compressed Sensing

Data compression refers to the encoding processes of reducing the size of data for storage or transmission over a telecommunication link. The large volume of waveform measurements necessitates exploring efficient compression techniques that reduce data volume while preserving the essential information. Employing data compression techniques is key to the seamless transfer of synchro waveform data for many applications, facilitating its integration with other relevant data sets and supporting valuable insights for operational and analytical purposes.

Data compression methods are classified as lossy and lossless compression. The former discards low-importance or redundant information, rendering the original data not fully recoverable, while lossless compression is reversible such that the original signal can be exactly reconstructed.

4.2.1. Lossy Compression Techniques

Lossy compression techniques aim to achieve a higher Compression Ratio (CR) by sacrificing acceptable some less important data. Typical lossy compression methods include Fourier Transform, Discrete Cosine Transform (DCT), and Wavelet Transform (WT). In the lossy compression approach, a combination of templates can be generated from previous time nodes or transformations. However, the lossy compression method suffers from information loss due to the sensitivity of the frequency calculation, which may result in missed or falsely triggered events.

While data compression commonly refers to data bit reduction and encoding, signal model extraction (e.g., phasor estimation or the identification of other parametric models) can be considered a lossy compression of a time-domain waveform to a simpler representation requiring a reduced set of parameters. While the original data may not be fully recoverable, the model and corresponding parameters can capture the essential characteristics of the waveform, much like feature extraction in Principal Component Analysis (PCA) and sparse coding techniques [59].

The amount of data loss involved in signal model representation depends on how closely the model matches the analyzed waveform and the accuracy of the extracted parameters. Most commercial PMUs rely on the classical static phasor model where the parameters are identified by means of various implementations of the Discrete Fourier transform (DFT). The use of the DFT is preferred due to its simplicity of implementation and short latency and window length. However, while static phasor estimation may be an appropriate data compression approach for AC voltage and current waveforms during steady-state operation, it involves significant loss of critical information when analyzing signal dynamics. During electromechanical and electromagnetic signal dynamics (e.g., frequency ramps, modulations or steps in the amplitude or phase), waveforms exhibit broadband frequency spectra[1], as thoroughly explored in recent literature [60] [61] [62] [63]. Consequently, these signals are poorly captured by the static phasor model, which, by definition, is a narrowband representation with a single fundamental tone.

Alternatively, the dynamic phasor model permits some variation of the amplitude and phase within the observation window [64] and, therefore, results in a more accurate representation with lower loss of information during the compression. Common algorithms in this class use the Taylor series expansion or the Taylor-Fourier (TF) transform, in combination with Weighted Least Squares or Compressed Sensing theory, to approximate higher order derivatives of the phasor and improve the estimation of the underlying fundamental tone [65] [66] [67] [68]. However, dynamic phasor models are unable to represent faster variations or discontinuities (e.g., amplitude or phase steps present during faults or switching actions) in the waveform which could lead to inaccurate frequency estimations, erroneous power flow calculations, and inappropriate control actions [60] [61] [69]. Contributing to this field, the Functional Basis Analysis (FBA), developed in [60] [70] [71], is a broadband signal estimation technique which expands the signal model to include several of the most common signal dynamics expected in power grids: modulations in the amplitude and/or phase, linear frequency ramps, phase and/or amplitude steps and various combinations of these dynamics. FBA method identifies the relevant signal dynamics and estimates the corresponding

[1] A broadband spectrum is continuous with a generic bandwidth (i.e., the continuous signal spectrum and energy content cannot be reconstructed by a finite set of sinusoidal components). In contrast, a narrowband spectrum is one where the energy is concentrated around a single or few sinusoidal components.

parameters. Thanks to the more flexible and richer signal model, the FBA can achieve less lossy data compression as the extracted model is more representative of the measurement waveforms in modern power grids. Much like a PMU, an FBA-enabled measurement device can convert time-domain data into a finite set of parameters (e.g., modulation frequency, step location, frequency ramp rate) which are streamed to a central data concentrator for post-processing.

4.2.2. Lossless Compression

Lossless compression methods have been developed to address the issue of information loss. These encompass a range of successful techniques such as dictionary-based and variable-length compression algorithms. Prominent examples like Gzip, LZ77, Lempel-Ziv-Markov chain algorithm (LZMA or 7Zip), and Lempel–Ziv–Welch encoding have demonstrated their ability to attain a high CR when applied to files with extensive archived data. Despite their effectiveness, the computational latency associated with these methods poses considerable challenges for real-time embedded system operations. The applicability of compression algorithms designed for phasor data (e.g. STTP-compatible Time Series Special Compression) shows that these algorithms may have poor performance if the sampling rate of waveforms is too low. Strategies for utilizing phasor-domain strategies in conjunction with general purpose compression can be explored to find optimal approaches balancing compression ratio, information loss, and computation latency.

To efficiently compress high-rate electrical-grid time series, [22] proposes Cyclical High-order Delta Modulation, which utilizes delta and delta-of-delta encoding methods for processing waveform data. To increase the compression ratio, a multi-stage hybrid coding framework [23] is proposed based on variable frame compression and lossless compression, as depicted in Figure 24.

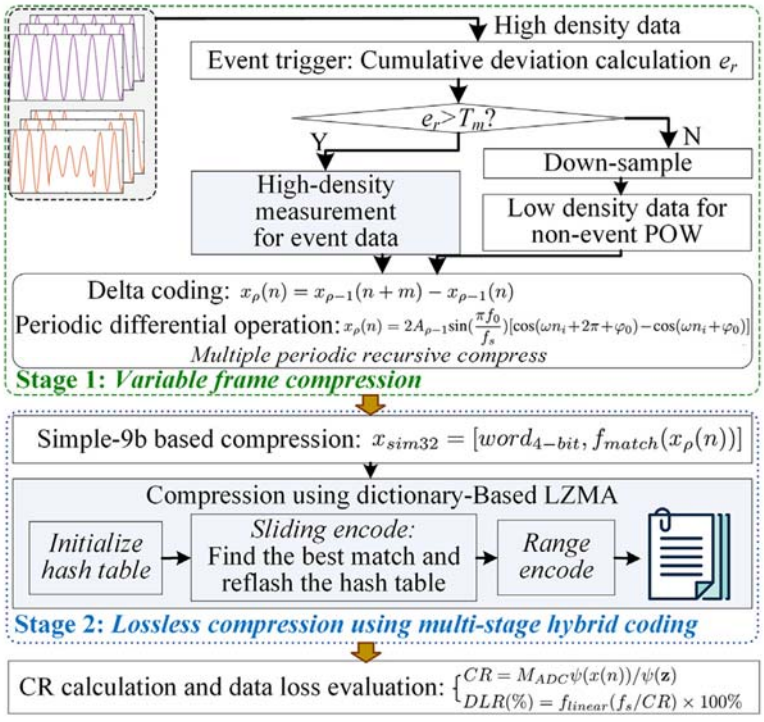

Figure 24. A multi-stage hybrid coding framework, based on variable frame compression and lossless compression, to increase synchro-waveform data compression [23].

Delta encoders are widely used for data transmission and storage. The basic principle behind delta encoding is to quantize and encode the difference or delta between consecutive samples of a signal, rather than encoding the absolute amplitude of each sample. This approach can be particularly useful for synchro-waveforms in power systems because these waveforms are dominated by the fundamental frequency (60 Hz or 50 Hz) component that is periodic and superimposed by the high-frequency transients that are typically noisy in the real world.

In a delta encoder, the input signal elements are compared with previous values, and the pair-wise difference is quantized and encoded. The encoded delta signal is then transmitted or stored digitally. The following equation defines the standard delta encoder, where k is the distance to the previous sample and α is a scalar applied to the previous sample.

$$f(x_n) = x_n - \alpha x_{n-k}, \qquad \text{where } k > 0 \text{ and } n > k \tag{1}$$

In a traditional delta encoder k = 1, so the algorithm subtracts the previous sample from the current sample. As an example, a five-sample series of (5,5,5,5,5) may represent a brief current interruption which can be encoded by the delta signal of (5,0,0,0,0). The zeros theoretically require only 1 bit to represent as opposed to 3 bits for the 5s. This process can be repeated or chained multiple times to gain a higher compression ratio until the saturation point where the resulting difference signal becomes less compressible. Figure 25 shows the delta signals applying the half-cycle and full-cycle encoding to a DC-biased fault waveform. As seen, the full cycle encoding results in a comparatively higher compression ratio by shrinking the transient signal amplitudes.

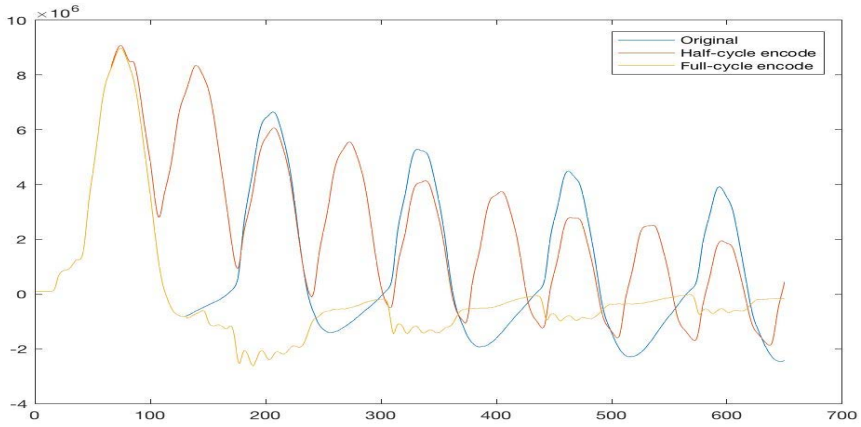

Figure 25. Half-cycle and full cycle delta encoding of a fault waveform.

Overall, delta encoders and other advanced compression techniques provide an effective means to mitigate the data volume challenge in handling synchro-waveforms. Many device manufacturers implement standard or proprietary techniques to compress device data with minimum loss and enable advanced power system analytics at scale.

4.3. Data Analysis

4.3.1. Steady State: Frequency and ROCOF Estimation

Measurements of power system frequency and ROCOF are valuable indicators of the current and anticipated state of the grid [72] [73] [74]. As is well known, the system frequency measures the balance between electricity generation and consumption and a drop in frequency typically indicates excess load that puts the stability of the grid at risk. ROCOF, as the first time-derivative of the frequency, can be considered a predictive filter which is highly sensitive to frequency variation [73]. Monitoring frequency deviations helps identify and respond to rapid load or generation changes, preserve grid stability, and prevent cascading failures. These metrics are critical to reliable grid operation and are deployed in power balancing, protection, and system inertia calculations.

While frequency and ROCOF are typically evaluated using PMUs, these phasor-based estimations are notoriously sensitive to variations in the analyzed waveforms and require further study of advanced signal processing techniques to ensure their quality and validity [72] [74] [56] . As previously discussed in Section 4.2.1., the static phasor model fails to capture broadband signal dynamics, such as phase modulations or amplitude steps. Consequently, phasor analysis of such waveforms may result in significant frequency and ROCOF deviations that do not accurately represent the true underlying dynamics. In particular, abrupt step changes in the phase or amplitude of the waveforms, caused by network reconfiguration, circuit breaker operations or faults, can be falsely reported as large deviations in the frequency, inducing temporary unrealistic ROCOF estimations [72]. Limitations of Fourier analysis on non-stationary waveforms, compounded by the ambiguity of the signal frequency during step changes [74], leads to unreliable parameter estimates that are not reflective of the true grid dynamics.

Literature on frequency and ROCOF estimation involves step detection, adaptations of the static phasor model, and predictive strategies for fault ride-through. For example, in [75], wavelet analysis is used to first identify the location of discontinuities in the waveform, followed by an adaptive windowing technique to fit a quadratic polynomial signal model to pre- and post-event data. In [56], the output of a least-squares trajectory estimator is compared to the measured signal to detect divergence from the expected trajectory and the presence of phase steps. The FBA approach, mentioned in Section 4.2.1, exploits properties of the Hilbert transform-derived complex analytic signal to identify and fit phase/amplitude modulations, frequency ramps and phase/amplitude steps in measured waveforms [71]. These strategies provide a more nuanced and accurate interpretation of the grid state which enhances the overall resilience and operational efficiency of the power system.

Existing frequency estimation algorithms use non-parametric and parametric techniques. Non-parametric techniques use the signal's spectrum, commonly described in terms of known function coefficients such as Fast Fourier Transform (FFT), Interpolated DFT, PLL and Wavelet transform. Among these, the FFT is fast, robust to noise, easy to implement for estimation of frequencies owing to its low processing time, and improved elimination of harmonics. FFT has some drawbacks, such as disappointing results when the fundamental frequency diverges from its fundamental value. The fixed frequency bins of the FFT may not capture the intricacies of such signals, resulting in inferior frequency estimates. In FFT-based frequency estimation, spectral leakage effects are common, especially for signals that do not align perfectly with integer multiples of the analysis window length. Therefore, in emerging smart grid scenario these methods are not sufficient to meet the desired requirement as per the IEEE/IEC standard 60255-118-1a [37].

To meet the requirements of IEEE standard 60255-118-1a [37], parametric techniques may be utilized to appropriately capture the signal and estimate model parameters using the given data. These approaches include Kalman filter, Prony, Adaptive Linear Elements (ADALINE), and the estimation of signal parameter via rotational invariance technique (ESPRIT). Model inconsistencies, inappropriate model layout, and noise reduce the precision of parametric approaches. The challenges are further resolved by implementing variable center maximal correntropy-based l1-norm constraint (zero attractive) recursive Gauss Newton filter (VCMC-ZARGN) for dynamic phasor and frequency estimation. This method estimates the dynamic phasor and frequency of power signals in Gaussian and impulsive noise environments using only one fundamental cycle data. The cost function includes l1-norm restriction (zero attractor term) to utilize sparseness in Gauss Newton filters, resulting in a novel technique with increased accuracy and responsiveness.

4.3.2. Disturbance Analysis: Event Detection and Classification/Cluster

Events are defined broadly as any change in any component in the power system that can affect the voltage or current waveforms at one or multiple measurement locations. Events may include major faults and equipment failures that can affect the stability and reliability of the system. There are several methods to detect and capture events in voltage and current waveform measurements.

A popular approach is to compare the measured waveform with a reference waveform representing normal system behavior. If there is a considerable difference between the measured waveform and the reference waveform, abnormal behavior is inferred, which in turn can trigger an event capture. For example, we may simply compare two consecutive cycles, i.e., to take the waveform in the previous cycle as the reference to detect an event in the waveform in the present cycle. There are different ways to compare two cycles of measured waveforms. For example, we can use the concept of *differential waveform* [5]:

$$\mathrm{D}x(t) = x(t) - x(t - NT), \tag{2}$$

where x(t) is the measured current waveform or voltage waveform; T is the waveform interval, i.e., T = 1/60 second for a 60 Hz waveform; and N is a small integer number, such as 1, 2, 3, 4, or 5. Basically, the differential waveform is the difference between the original waveform measurement and a *delayed* version of the same waveform measurement, where the delay is equal to N cycles. An example is shown in Figure 26. Here, there is an event in the second cycle, as marked on the figure. A delayed version of the current waveform measurement is shown in Figure 26(b). The delay is at N = 1 cycle. The corresponding differential waveform is shown in Figure 26(c). It is obtained by subtracting the delayed waveform in Figure 26(b) from the original waveform in Figure 26(a). We can see that the event has created two distinct blips in the differential waveform, which are denoted by 1 and 2. Note that both of them are associated with the same event. The first blip is due to comparing the event cycle with the previous normal cycle, where the normal cycle serves as the reference. The second blip is due to comparing the next normal cycle with the event cycle, where the event cycle serves as the reference.

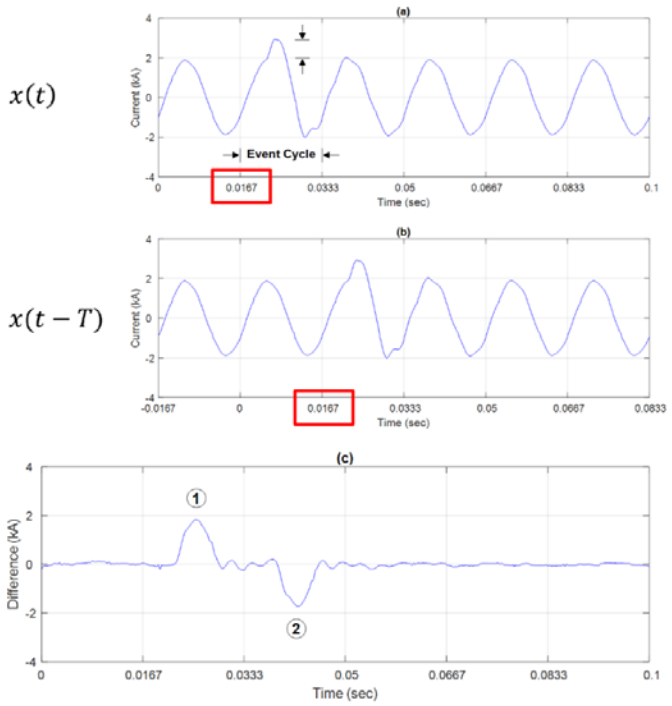

Figure 26. Event detection based on the analysis of differential waveforms [5].

Another option is to use the concept of per-cycle THD that we previously defined in Section 3.5. In fact, the analysis of the per-cycle THD in Figure 19 already resulted in detecting two sub-cycle events, as we previously saw in form of the two spikes in the per-cycle THD profile in Figure 19.

Per-cycle THD can also be used to identify local versus non-local events. A non-local event is an event that is simultaneously detected by multiple WMUs at *multiple* sensor locations. An example is shown in Figure 27. The two sub-graphs in this figure show the value of |ΔTHD|, which is the difference between the THD in the present cycle and the THD in the previous cycle [5]. The measurements in the two figures are time-synchronized, since they are derived from synchro-waveforms at two different WMUs in two different locations on the same power network. A non-local event is clearly detected in this figure, where both WMUs observe a spike in |ΔTHD|.

Other examples of methods to detect an event in synchro-waveform data are available in [42].

4.3.3. Disturbance Analysis: Event Location Identification

Synchro-waveforms can also identify event location both at transmission and distribution levels.

At the distribution level, event location identification seeks to answer the following question [76]: for those events with root causes in distribution network, what is the location of such root cause, i.e., at what exact distribution bus does the load switching, capacitor bank switching, DER connection / disconnection, or device malfunction occur? Figure 28 shows the general layout for

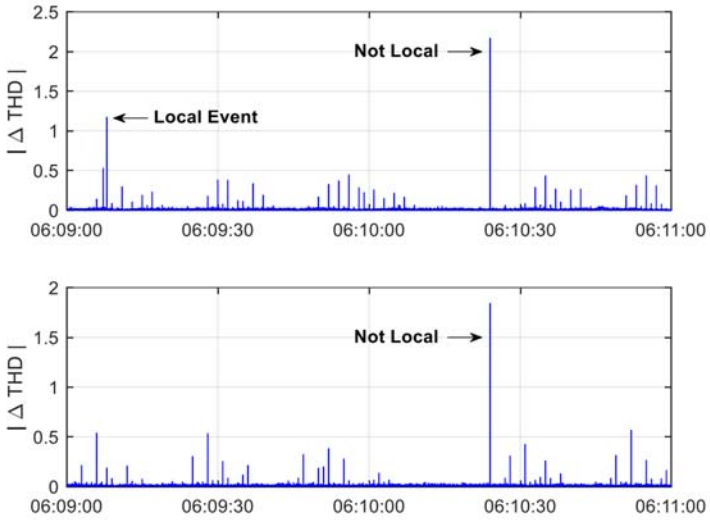

Figure 27. Distinguishing local events from non-local (system-wide) events by comparing the ΔTHD profiles of the synchro-waveforms from multiple WMUs. The event at 06:10:24 is system-wide [42].

the event location identification on a power distribution feeder. The figure on the left shows the network layout. Only the main is shown here; however, laterals can also be considered with additional sensors. The two sensors provide synchronized measurements, while the location of the event is unknown. The figure on the right shows the waveform measurements (at one sensor) during an event. The research question we seek to answer is how we can use the measurements from the two synchronized sensors to identify the source location of the event.

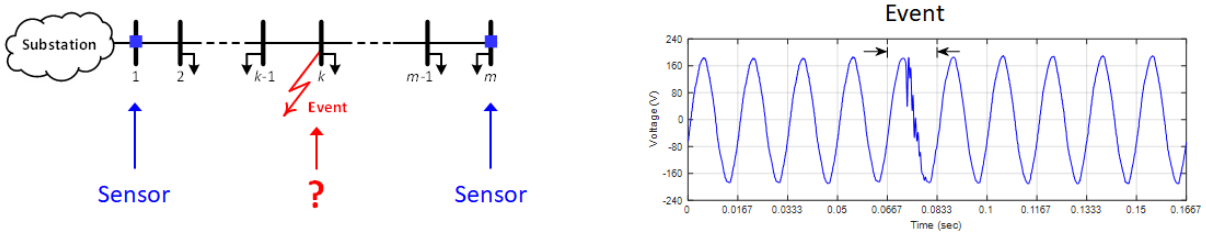

Figure 28. Event location identification problem in a power distribution system with synchronized measurements: (left) network layout, location of sensors, and unknown location of the event; (right) an example event that causes both transient and steady-state changes in waveforms.

One class of algorithms, in the context of this problem, uses a combination of forward sweep and backward sweep to solve the circuit based on synchronized measurements from two sensors, where the location of the event is identified by minimizing the difference between the results from forward sweep and backward sweep. Depending on the type of synchronized measurements, the analysis of the circuit can be done in different modes, i.e., fundamental mode, harmonic mode, or damping oscillatory mode. These three approaches are shown in Figure 29. All the methods seek to identify the location of the same event, as shown on the right-hand side. While the method in the top and the middle figure focus on using sinusoidal modes (whether fundamental or harmonic) that are captured before and after the event, the method in the bottom figure focuses on using the

damping sinusoidal mode during the event. All three methods can be applied to synchro-waveforms, given the fact that synchro-waveforms can provide all various data representations.

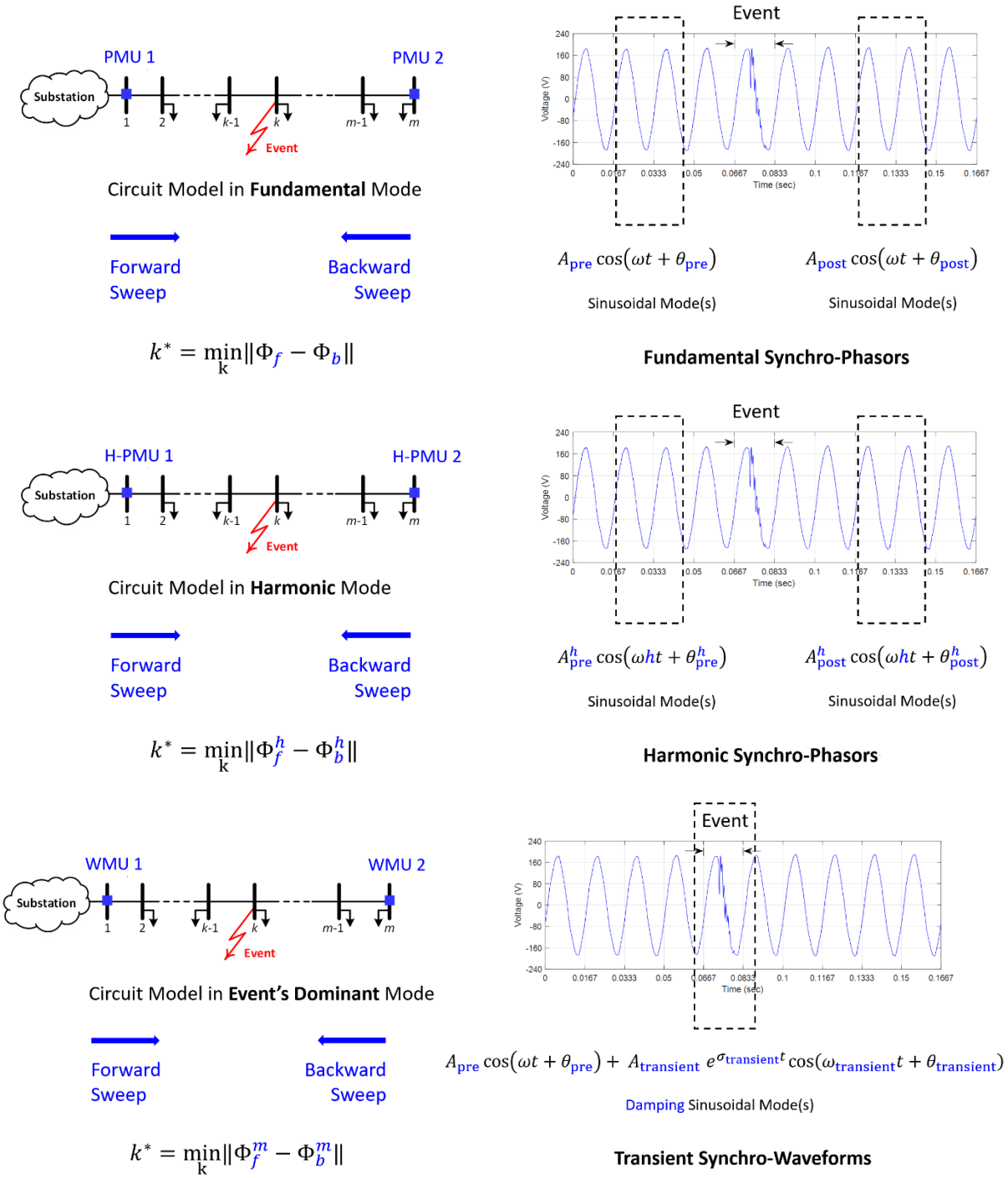

Figure 29. Event location identification using the same forward-sweep/backward-sweep method but by using different types of synchronized measurements and different types of data representation. (top) using fundamental synchro-phasors that are captured before and after the event [76]; (middle) using harmonic synchro-phasors that are captured before and after the event [30]; (bottom) using synchro-waveforms that are captured during the event [77].

5. Case Studies and Future Applications

This section discusses case studies with industry relevance in the short- to long-term, highlighting both current applications and potential future use cases of synchro-waveforms. Synchro-waveforms have become integral across various segments of the power system, including transmission, distribution, and grid edge. While the primary focus will be on major examples, it is important to note that numerous other use cases exist, showcasing the versatility and broad applicability of this technology.

Included use cases discuss the role and impact of IBRs in protection mechanisms and dynamic response studies, detection of incipient faults, localization of partial discharge and arcing, wildfire monitoring, and estimation and validation of network parameters. Additional applications include cyber security, ensuring microgrid stability and control, and detection of geomagnetic disturbances. These diverse use cases intend to underscore the possibilities and importance of synchro-waveforms in modern power systems.

5.1. IBRs (Dynamics and Protection)

WMUs can particularly help in monitoring IBRs and other power electronics apparatus. In this section, we discuss both current technology use cases and potential future applications in this area.

5.1.1. Current Technology Use Cases

Traditionally, the dynamic behavior of power systems has been determined by the dynamic performance of synchronous generators and loads. With the large-scale integration of power electronics-based systems, such as IBRs for utility-scale solar and wind power generation, the dynamic response of power systems has become faster and more complex, due to the fast response of the power electronic devices. The time scales related to IBR controls and dynamics may encompass from microseconds to a few milliseconds, and they may not be observed accurately by phasor measurements. Furthermore, the dynamic behavior in voltage and current waveforms is no longer dominated by the fundamental frequency component of the power system. Consider the example in Figure 30. This figure shows the voltage and current waveforms at an IBR point of interconnection, before, during, and after a minor disturbance in the power system. The disturbance in this example was caused by a switching event at a nearby capacitor bank. This disturbance by itself is a benign phenomenon. It only resulted in a minor and momentary high-frequency agitation in voltage. However, this disturbance triggered an unusual subsequent dynamic sub-synchronous oscillatory behavior by the IBR.

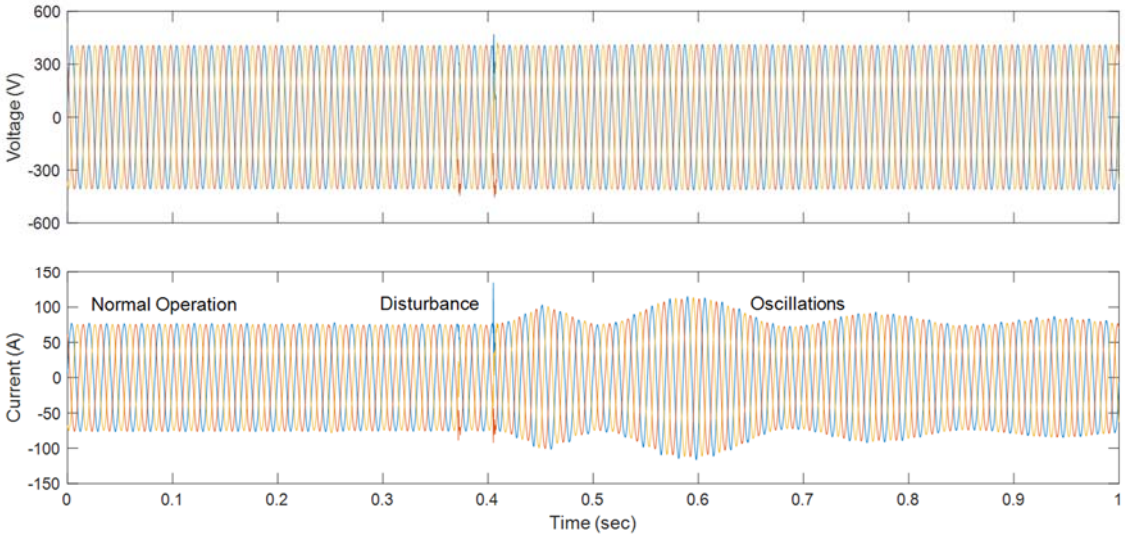

Figure 30. Sub-synchronous oscillations caused at an IBR shortly after a minor disturbance [10].

Two other examples are shown in Figure 31. Both examples involve the same pair of PV Inverters. PV 1 and PV 2 are on the same sub-transmission system, but on two different distribution feeders. They have the same model of three-phase inverters, but with different sizes, i.e., different solar power generation capacities. Figure 31(a) and 30(b) show the IBR's responses to the same sub-cycle disturbance. The disturbance causes momentary distortions in voltage waveforms across the sub-transmission system, which is visible in the voltage waveforms in both Figure 31(a) and Figure 31(b). This results in a dynamic response by each of the two IBRs, in the form of momentary agitations in current waveforms. The dynamic responses of the two IBRs are generally similar, with two back-to-back high-frequency oscillations. However, a precise modal analysis reveals that each IBR has its own unique dynamic response. Next, consider Figure 31(c) and 30(d), which show the IBR's responses to a fault. The fault causes a severe unbalanced voltage sag on all phases. In response, both IBRs trip and cease production, which is evidenced by the severe drop in current in both PV 1 and PV 2, reaching zero current after a few cycles. Notice that, even though the fault itself was cleared after three to four cycles, neither of the two IBRs could ride through the fault. It took several minutes for these two IBRs to restart and resume production after they tripped (not shown here). Importantly, if several IBRs cease production in response to the same fault, it can suddenly cause a major loss of generation capacity across the power system, which can result in ripple effects, such as excursion in frequency. Such system-wide impacts of faults on IBRs and subsequent frequency excursions have been reported recently in California and Texas. For example, see the report from NERC on "900 MW Fault Induced Solar Photovoltaic Resource Interruption Disturbance" which happened in Southern California on October 9, 2017.

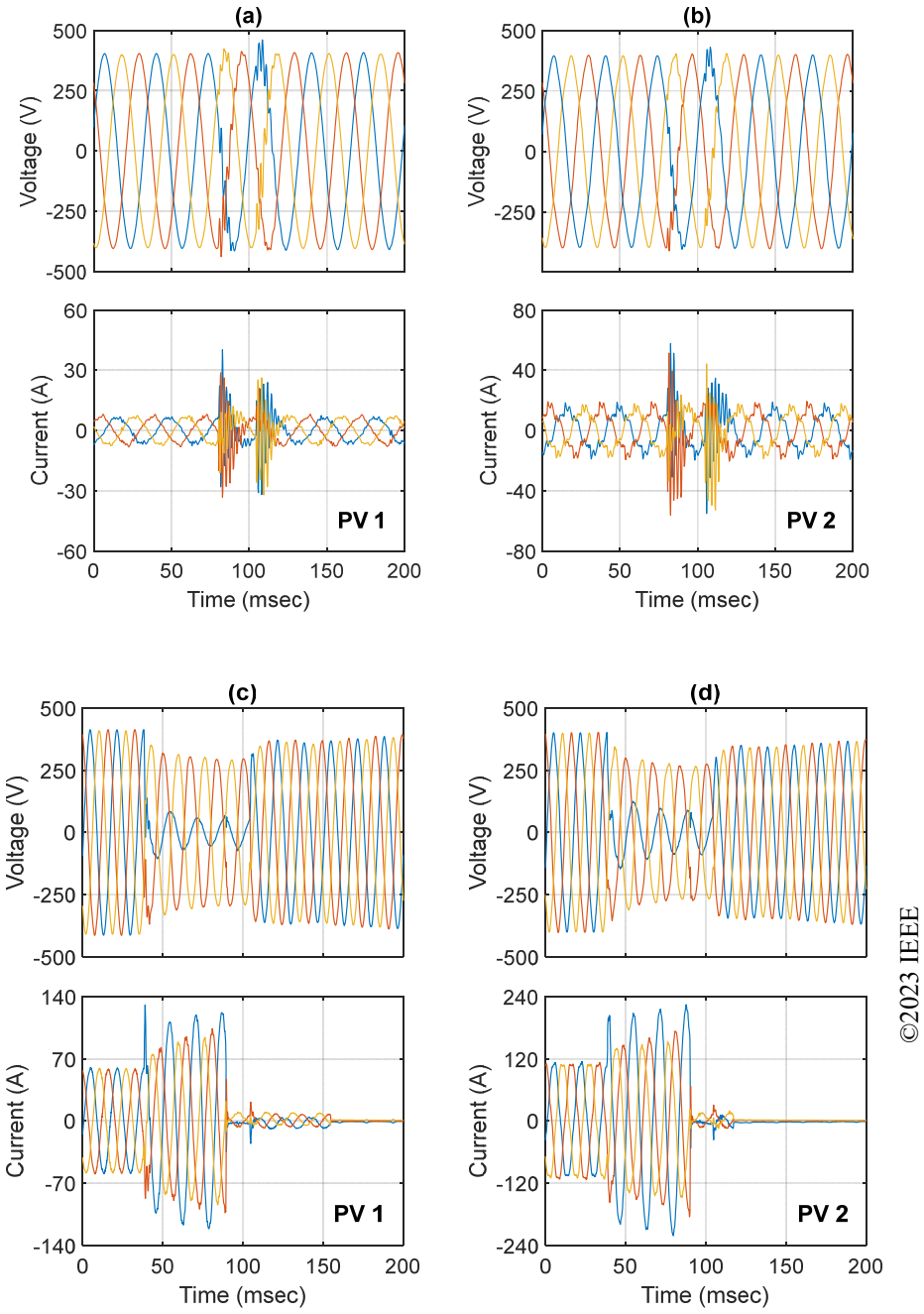

Figure 31. Using synchro-waveforms to monitor IBRs: (a)(b) Simultaneous dynamic waveform response of two PV units during a system-wide sub-cycle disturbance; (c)(d) Simultaneous waveform response of two PV units that cease production when a system-wide fault occurs fault occurs [1] [28].

5.1.2. Emerging Applications (IBRs)

In this section, we discuss some emerging applications of synchro-waveforms in monitoring IBRs.

5.1.2.1. Sub-synchronous Oscillations (SSOs)

One of the potential applications for synchro-waveforms is addressing SSOs in transmission systems with high penetrations of IBRs. As demonstrated with many real-world examples, [78] shows that these SSOs are typically related to type-3 wind power plants interconnected with series compensated networks or to various types of IBRs in weak grid conditions. If SSO risks are identified during interconnection studies, they can be addressed with specialized protection systems. As suggested in [3], synchro-waveforms could be used to support these protection systems while also serving other functions, improving the return on investment. However, it is unlikely that interconnection studies will identify all SSO risks, so widely deployed WMUs can play an important role in monitoring, mitigation, and post-event analysis. For example, [79] discusses how measurements were used to associate an oscillation with a solar plant's mode of control. In particular, synchro-waveforms were used to correctly identify the oscillation's frequency as 22 Hz after it was first observed at the aliased frequency of 8 Hz in PMU measurements. This use case serves as an example of the important role continuous synchro-waveform measurements can play in addressing SSOs.

5.1.2.2. New Methods and Tools Integration

As the power grid evolves with the integration of IBRs, the role of Data-Driven Dynamic State Estimation (D-DSE) becomes increasingly critical in managing the complexities introduced by these renewable energy sources [80]. A review of these common methods is detailed in [81], highlighting their significance in the context of conventional synchronous generators (SGs).

However, as IBRs replace SGs, there is a compelling need to adapt and extend DSE techniques to include waveform measurements, such as by extending D-DSE and Control-Physics DSE [82] methods, where the latter leverages both control theory and physics-based models to enhance accuracy and robustness in state estimation in the presence of high penetration of IBRs [83] [84].

5.2. Incipient Faults

Monitoring the transient behavior that are caused by equipment operation can inform us about the state of the health of the equipment and the possible signs of *incipient faults* (i.e., early-stage faults) that could become problematic in the future, as well as the overall response of the system under potential contingencies. WMUs and synchro-waveforms can directly help in this application area.

5.2.1. Current Technology Use Cases

5.2.1.1. Analysing Incipient Faults in Distribution Systems

Incipient faults in electrical distribution systems represent the initial stages of failures that may lead to significant disruptions if undetected. Factors such as aging infrastructure, harsh environmental conditions, and inadequate maintenance practices often contribute to these faults, with common issues including insulation degradation in underground cables, connectors, and transformers.

5.2.1.1.1. Field Experiment Setup

To capture and analyze the incipient faults, an extensive field experiment was set up using high-resolution Low Voltage (LV) waveform measurement sensors and Medium Voltage (MV) line sensors distributed across a live distribution feeder. LV sensors continuously capture data, globally synchronized, and send captured data when triggered by MV sensors. These LV sensors have a sampling rate of 16 kHz, allowing the detection of subtle discrepancies in waveform that indicate the onset of faults. Furthermore, MV sensors placed at the feeder's starting point monitor the currents of all three phases and can activate the LV sensors to stream data upon detecting faults.

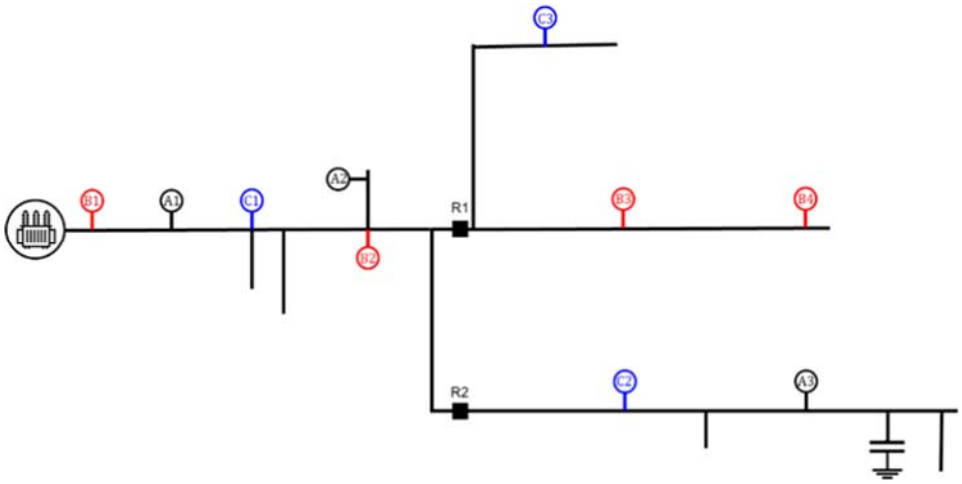

Figure 32. Placement of LV synchro-waveform sensors across the distribution feeder.

5.2.1.1.2 Waveforms from Multiple Sensor Locations

Figure 34 displays three events recorded by LV sensors installed on the A phase. The first event occurred on 4/07/23, followed by the second event on 4/27/23, and the last event on 4/29/23. The first two events were identified as incipient faults, while the last event was classified as a permanent fault. These faults took place near an underground cable in proximity to sensor A3 in Figure 33. Notably, the LV sensors detected the incipient faults well in advance of the permanent fault, and slight variations in waveform patterns were observed at different locations. These events were verified by the utility, and the underground cable was subsequently repaired.

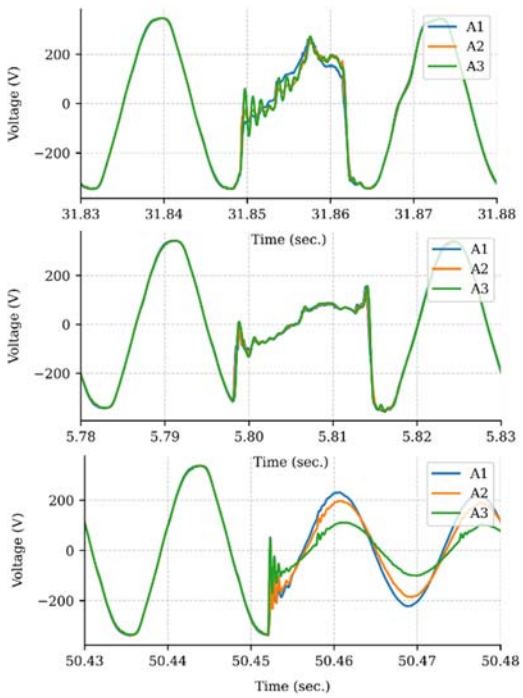

Figure 34. LV sensor captures: Incipient and permanent faults near underground cable.

5.2.1.1.3. Waveform Analysis Using Short-Time Voltage Harmonic Distortion

Data-driven algorithms can be developed to extract Short-time Total Harmonic Distortion (STHD) using waveform data reported by sensors at various locations along a feeder. By analyzing this data, one can obtain comprehensive insights into the voltage distortions during various fault conditions. Since the onset of data collection, the deployed sensors have identified three incipient faults as well as several temporary faults that led to recloser operations.

Table 5 summarizes the incipient fault data, including the fault duration and the maximum feeder current flowing into the circuit.

Table 5. Some properties of captured incipient faults for the test feeder

Fault #	Faulty Phase	Fault Duration (ms)	Maximum Fault Current (p.u.)
I	C	32	32.4
II	A	15	33.7
III	A	12	36.3

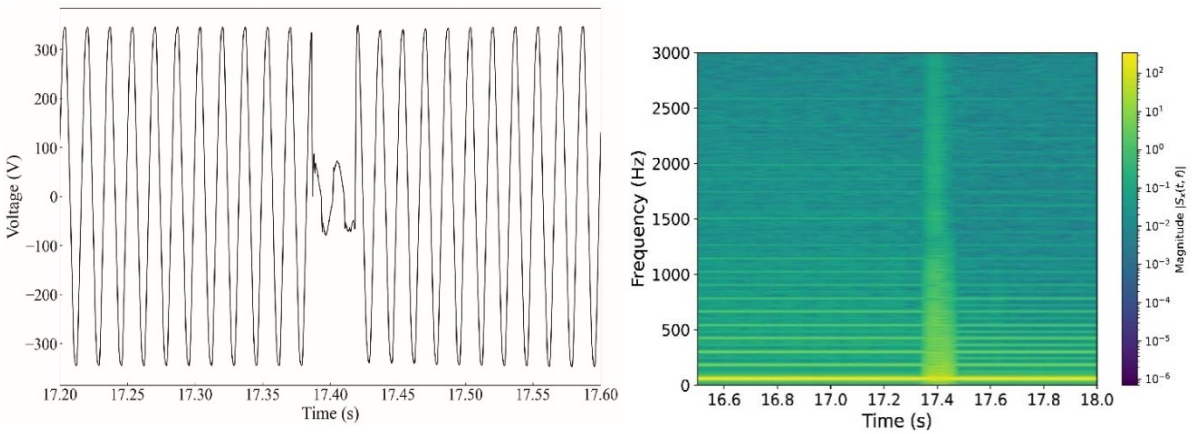

(a) (b)

Figure 35. (a) Voltage waveform measured by sensor C3 during transient fault I; (b) time-frequency spectrogram of the voltage waveform.

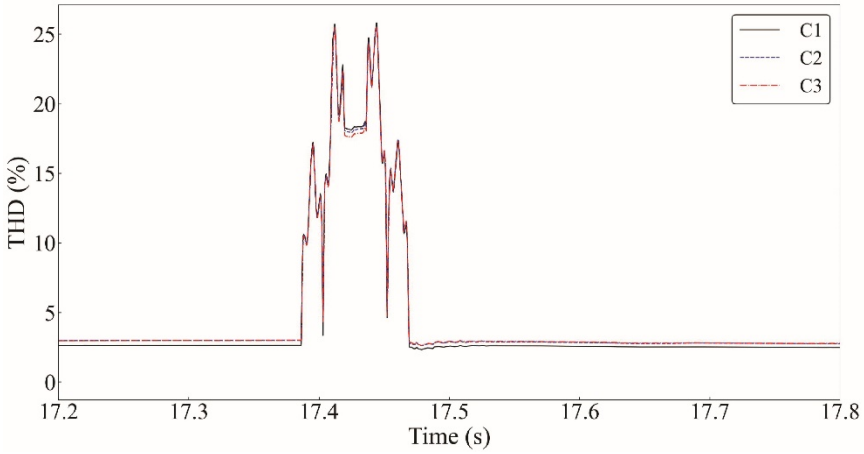

Figure 36. STHD as a function of time for the fault I

Figure 35(a) shows the instantaneous voltage recorded by sensor C3 during fault I, and Figure 35 (b) displays the magnitude of frequencies in the voltage signal recorded by the sensor as it varies with time. The STHDs calculated for different locations under this incipient fault are shown in Figure 36. Table 6 summarizes the STHD data for all the incipient faults.

Table 6. STHD statistics data for different incipient faults

Fault #	Average STHD Under Steady State (%)	Maximum STHD During Fault (%)	Maximum STHD at Clearance Time (%)
I	3	25	22.6
II	3.4	18.2	12.9
III	3.1	18	16.8

The results indicate that the voltage distortions during fault intervals can differ depending on the sensor location; thus, STHD values can be utilized to detect and localize incipient faults [43]. This analysis highlights the effectiveness of using advanced diagnostic tools to discern variations in waveforms, which are often precursors to more severe faults. These differences in LV synchronous waveform patterns are vital for accurate fault localization and can greatly aid in targeted maintenance and repair efforts. The findings from this study not only demonstrate the capability of modern sensor technology in fault detection but also pave the way for future research into more integrated and automated fault management systems.

5.2.1.2. Case Study: Distribution Fault Location

Automated fault location is critical for the field crews to be dispatched to the site of a fault directly, thus avoiding line patrols and to be proactive in case of incipient faults. Several primary methods are traditionally used in distribution management systems to estimate the reactance (or distance) to a fault; however, it does not pinpoint the exact location on the circuit. Utilities commonly use various techniques such as customer outage calls and breaker status reports to narrow down the fault to a unique location. This approach has severe limitations directly traceable to lack of grid observability and interoperability of sensing systems. Increased observability of the distribution grid results in massive amounts of raw data that can be used to assist the fault management process, but automated analytics are required to handle this new data. The main challenges are:

- Anomaly detection and characterization of fault data from the WMUs or similar waveform measurements are challenging tasks, as the profile of a fault voltage and current can vary across different fault types and grid layouts.
- Currently available grid edge measurements are imperfect.
- As incipient faults self-clear within a brief time, it is particularly challenging to identify and locate them using a sole source.
- Waveform measurements with high resolutions increase the challenges of working with the data due to technological constraints.
- The performance of the methods that rely only on the accuracy of the grid impedance parameters are not consistent due to the high sensitivities and imperfect data management.

The following example of an incipient underground failure demonstrates utilizing imperfect but real-time grid edge measurements as one of the opportunities in the context of these challenges. Figure 37 compares two methods of fault location estimation: 1) fault current modeling based on the waveforms recorded at the substation, and 2) AMI-based spatiotemporal modeling combining the waveform signatures from the same synchro-wave recording device. The first method resulted in a potential area to be patrolled, but the second method estimated the fault location to be beyond a branch line fuse as one of the three unique locations. The eventual failure after 46 days (about 1 and a half months) proved to be a primary underground component. There were no reported customer calls prior to the final failure. Underground failures like this incident may remain unknown for longer periods of time and present problems for safety, equipment damage, and power quality.

The short duration of the disturbance resulting from the failure, as shown in Figure 38, which can be in addition to the low magnitude in some cases, makes it challenging to use traditional methods.

However, grid edge data sources as shown in Figure 39 and signature detection algorithms were leveraged to detect the failure and its location.

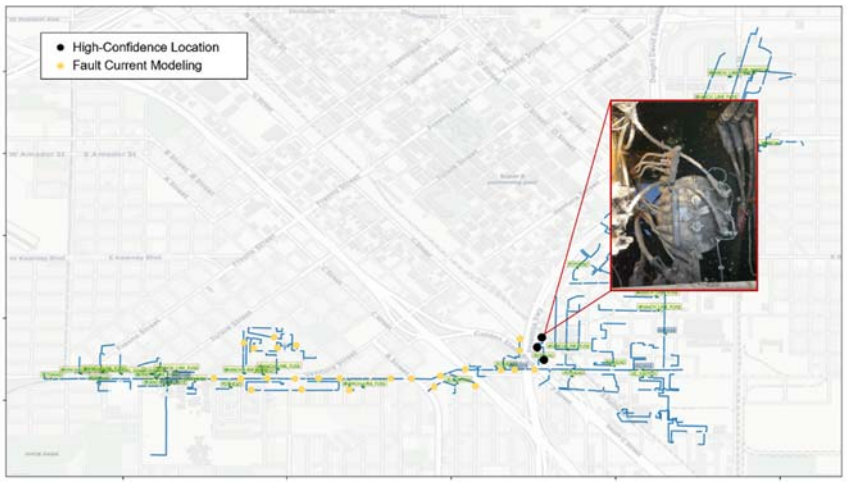

Figure 37. An example of a data-driven high-confidence location estimation for an incipient underground fault versus a more traditional method.

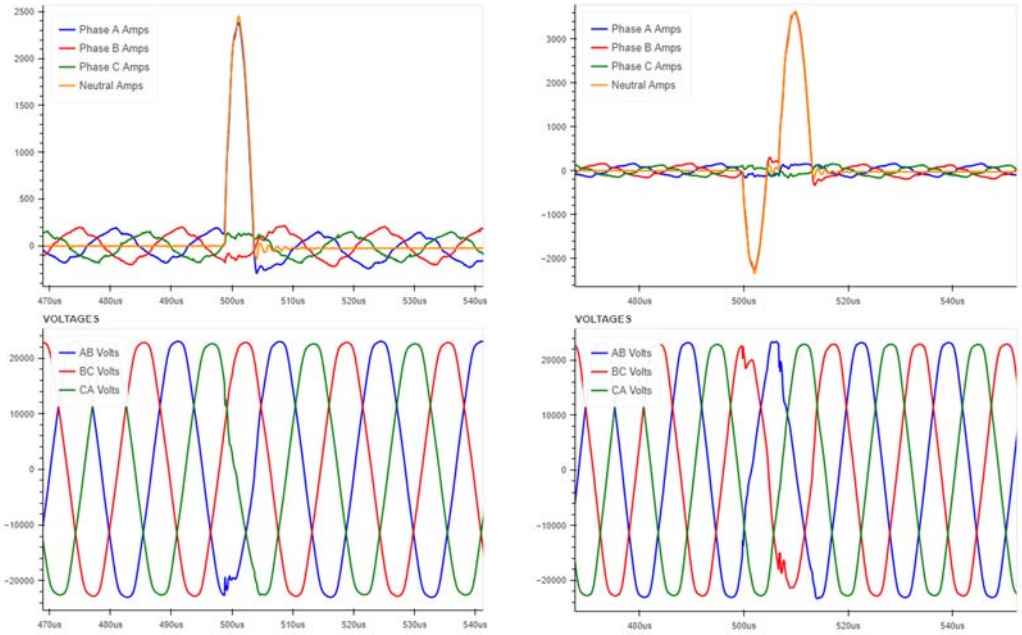

Figure 38. Two sets of three-phase voltage and current signatures detected before the eventual underground failure of Figure 37.

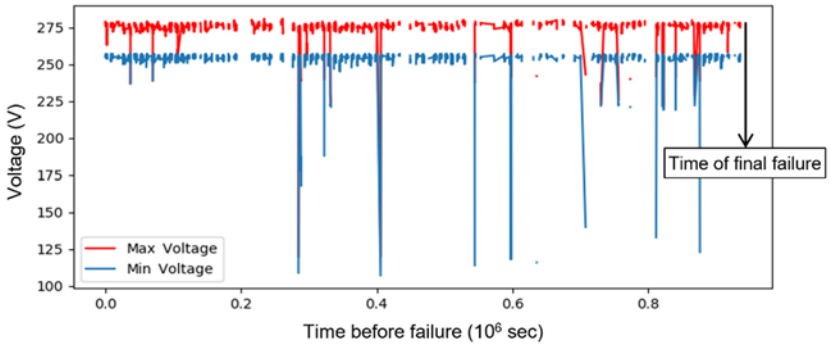

Figure 39. AMI-based abnormal voltage recordings during the incipient underground failure of Figure 37. In order to pinpoint fault location, spatiotemporal modeling of imperfect and sporadic edge measurements is required that utilizes characteristic waveform recordings at the substation.

5.2.1.3. Wildfire Monitoring

Monitoring grid-caused wildfires is a critical and challenging task in the utility industry. There is a growing literature aimed at predicting, detecting, and mitigating the impact of such wildfires. Here, any source of data can be valuable, including data from power systems sensors. However, so far, the focus has been mainly on the analysis of fault data, such as the data from protection relays and fault indicators. Synchro-waveform measurements from power quality meters capture not only all the faults but also a wide range of additional power quality events. Hence, they often provide a more comprehensive dataset of signatures compared to fault sensors. Furthermore, it is common for several power quality meters at different locations in the power system to capture the same event. As a result, the synchro-waveform measurements from power quality meters can allow us to validate our analysis by using multiple independent datasets.

Figure 40 shows the total number of power quality events that were recorded in the utility's service territory between October 14, 2007, and October 28, 2007. Nine wildfires were reported in this period. The first fire started early in the morning on October 21. The last fire started late afternoon on October 24. The fires were mostly contained by October 25. While the number of power quality events was on average 34 events per day before the start of the fires, it suddenly increased to close to 1000 events per day after the fires started [85]. Accordingly, the wildfires in this real-world example created a large footprint on power quality data.

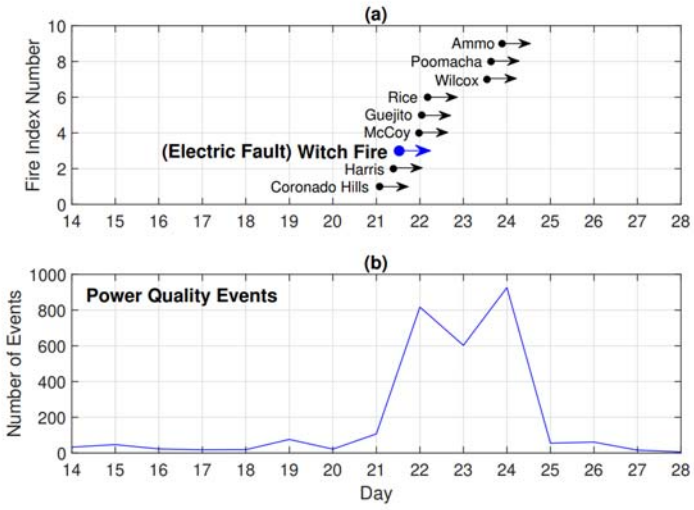

Figure 40. The impact of wildfires on the number of power quality events across a utility's service territory over a period of two weeks, from October 14 till October 28. Nine wildfires were reported in this period. The most destructive wildfire (Witch Fire) was caused by electric fault [86]**: (a) the start date and time for each wildfire; (b) the total number of power quality events per day** [85]

Of high interest in this study is the Witch Fire, see the blue arrow in Figure **41**(a). This fire was caused by a fault in a Transmission Line (TL), between two substations [86]. The fault that caused the fire occurred at 12:23 PM on October 21. Two other faults had already occurred on the same TL on the same day, at 8:53 AM and 11:22 AM. Also, a fault happened three hours after the start of the fire, at 3:25 PM. These four faults were automatically cleared by circuit breakers. The line was automatically reclosed ten seconds after each fault, in all four cases. The line was manually de-energized after the fourth fault. The timing of these four faults, denoted by Faults 1, 2, 3, and 4, is shown in Figure **41**(a). Next, consider the timing of the power quality events that were recorded on the same day at one of the two substations; see Figure **41**(b). This substation is connected to the faulted TL. All four faults that we saw in Figure **41**(a) are also visible in Figure **41**(b). In addition, two other power quality events were recorded around the time of Fault 3. One power quality event happened seven minutes before Fault 3 and one power quality event happened 10 seconds after Fault 3. By comparing Figure **41**(a) and Figure **41**(b), it is clear that the waveform measurements from power quality meters are more comprehensive than the fault data [85].

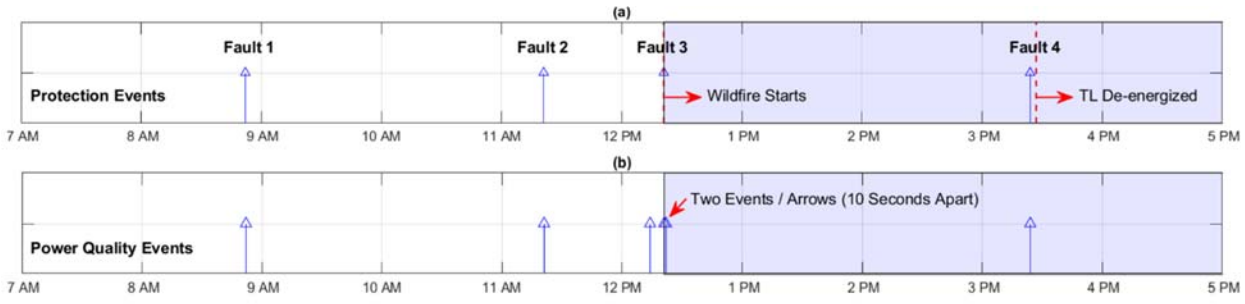

Figure 41. Comparing the events captured by the fault recorder (protection relay) versus the events captured by the power quality meter on the day when Witch Fire started. The power quality meter captured all the faults that the fault recorder captured, plus some additional events [85]**.**

Since our analysis is based on power quality data, as opposed to protection data, we can conduct a similarity analysis based on power quality data from multiple substations. In essence, the waveforms from these various power quality meters can serve as synchro-waveforms to characterize the abnormality based on how its impact is captured by power quality meters at various locations in the system. First, consider the results in Figure 42(a). This figure is based on the differential voltage and differential current signatures of 92 power quality events that were captured between October 14 and October 28 at Creelman substation [86]. This substation is close to the fault location. In Figure 42(a), Faults 2, 3, and 4 are distinctly separated from every other event at this substation, in terms of their similarity to Fault 1. It is evident that Faults 2, 3, and 4 were repetitions of Fault 1. Thus, Fault 2 and 3 could have served as precursors to Fault 3 that caused the fire. Next, consider the results in Figure 42(b), which are based on the differential voltage and differential current signatures of 73 power quality events that were captured between October 14 and October 28 at Loveland substation [85] [86]. This substation is far from the fault location. Nonetheless, the power quality meter at this substation captured the occurrences of Faults 1, 2, 3, and 4 as power quality events. The event signatures corresponding to Faults 2, 3, and 4 are distinctly separated, in terms of similarity to the event signature of Fault 1, compared to every other event that at this substation. This is another evidence that Faults 2, 3, and 4 were repetitions of Fault 1. The result from Figure 42(b) is an independent verification of the similar conclusion from Figure 42(a). This is a key outcome of using power quality data from multiple locations.

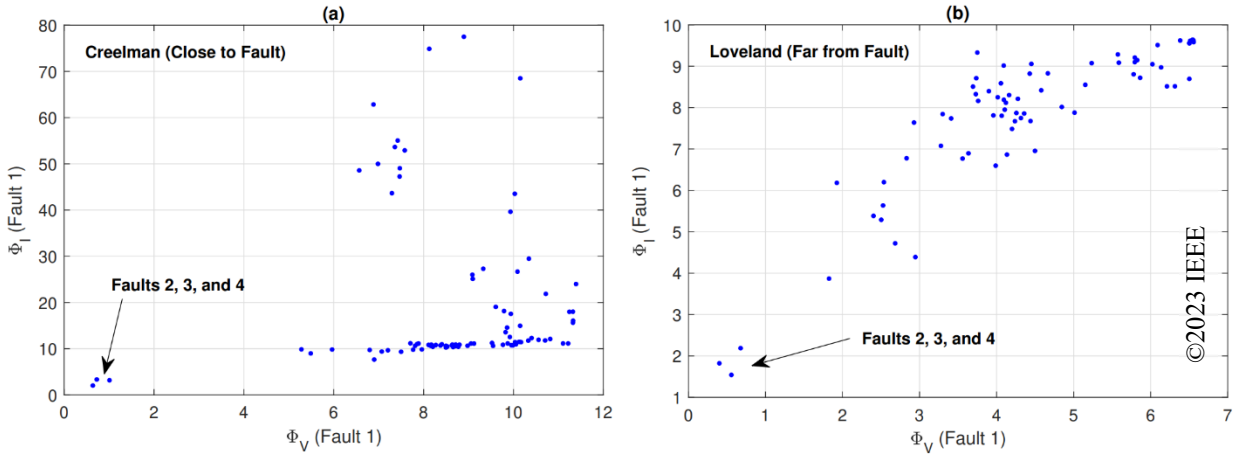

Figure 42. The similarity indexes between the differential waveforms of Fault 1 and those of every other power quality event that happened from Oct 14 to Oct 28, including Faults 2, 3, and 4: (a) events at Creelman substation (close to fault); (b) events at Loveland substation (far from fault) [85]. Lower index means higher similarity.

5.2.2. Emerging Applications

5.2.2.1. Partial discharge localization

Distribution and transmission power networks are subject to a range of electromagnetic disturbances caused by both natural and man-made sources, such as high circulating currents, thermal runaway/overheating, insulation degradation and partial discharge (PD) events,

harmonics, and overvoltage. These disturbances badly affect the power quality, produce supply interruptions and outages, and accelerate cable insulation deterioration and failure [87]. In particular, cable insulation deterioration is often caused by PDs that are localized electrical discharges, starting in defects of the cable insulation. The PDs are regarded as one of the best 'early warning' indicators of cable failure [88]. Because statistics indicate that more than 85% of equipment failures are linked to insulation failure, the adoption of on-line PD location methods is the most suitable for equipment health monitoring, and diagnosing types of insulation degradation, and is thus a desired feature in the protection schemes of modern power grids.

The most adopted on-line PD location methods are reflectometry or traveling wave-based techniques [89] [90] [91] [92] [93] based on the fact that PD events produce electromagnetic waves that travel in either direction towards the cable ends. Most of the methods are based on multi-end synchronized measurement techniques of the incident wave and the reflected waves from the cable ends, produced by a PD. The PD source is located using the knowledge of the times of arrival of the measured signals, (time of arrival, ToA, methods). The practical implementation of multi-end ToA methods is difficult due to the synchronization and the accuracy is influenced by the distortion phenomenon that characterize the propagation of PD signals on power cables and by the presence of noise on power lines. Electromagnetic Time Reversal (EMTR) theory [94] has been recently used to locate sources of electromagnetic disturbances in power systems and a method to locate PDs has been developed [95]. The advantages of the EMTR-based method, with respect to traditional PD location techniques, are the applicability to inhomogeneous and complex network topologies, and the robustness against the presence of noise.

The basic steps of the EMTR-based method are: **1)** Measuring the PD signal at one observation point (OP) along the line. **2)** Simulating using a lossless 1D Transmission Line Matrix (TLM) model the time-reversed injection of the PD signal for different guessed PD locations (GPDLs). **3)** Locating PD source by identifying the GPDL characterized by the highest energy concentration. Details on the design of the EMTR-based method for PDs localization and its performance can be found in [95] [96] [97] [98].

Figure 43 shows the effectiveness of the EMTR method in localizing the PD source in the power line 1, in service, with the characteristic reported in Table 7 [96]. As the figure shows, the EMTR method localizes PD at 478.8 m from the OP and the source is 475m far from OP, so with a relative error, with respect to the line total length, of about 0.14%. To localize the source, an initial step of 10 m between each GPDL has been used, and a maximum of the energy has been identified at 479 m from the OP. Then, the research has been refined repeating it in a section of the line around the 479 m location reducing the step to 1.8m. A total computational time of 2 minutes and 15 seconds was necessary to localise the PD source, using a 64-bit pc with an Intel® Core™ i7-8700K CPU at 3.70GHz, 32GB RAM and 1TB disk.

Table 7. LINE CHARACTERISTICS AND PD SOURCE LOCATIONS [96]

Line	Characteristic	Value	PD Source
1	Length, l Propagation speed, u	1882 m $0.18 \cdot 10^{+9}$ m/s	475 m
2	Length, l Propagation speed, u	1900 m $0.18 \cdot 10^{+9}$ m/s	796 m

Figure 44 shows the results obtained using the EMTR method on the power line 2 of Table 7. As the figure shows, the measured PD signal at the OP is noise. Using the classical TDR methods it is difficult to evaluate the time of arrival of the direct and reflected signals to evaluate the PD source location and the measurement must be denoised. Using time reversal, the PD source is located with an error of 0.31% in about 2 minutes, directly using the measurement with the noise.

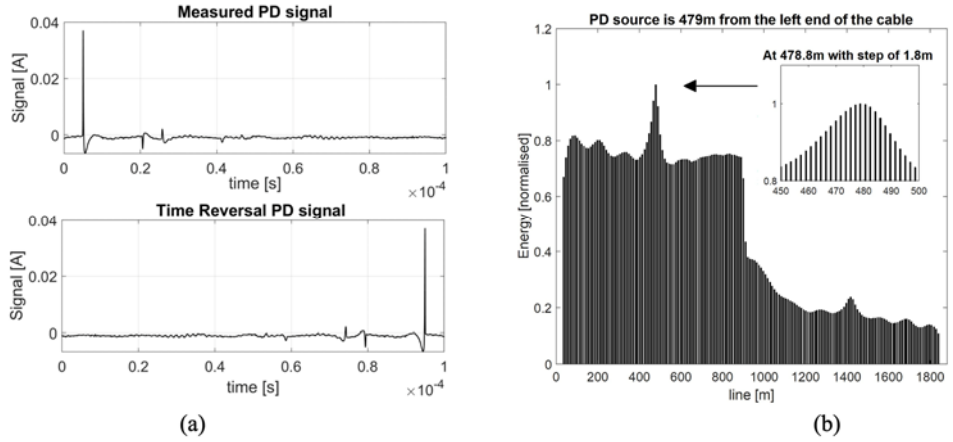

Figure 43 Measured (top) and time reversed (bottom) PD signal measured in line 1 (a); the normalized energy at the GPDLs (b) [96].

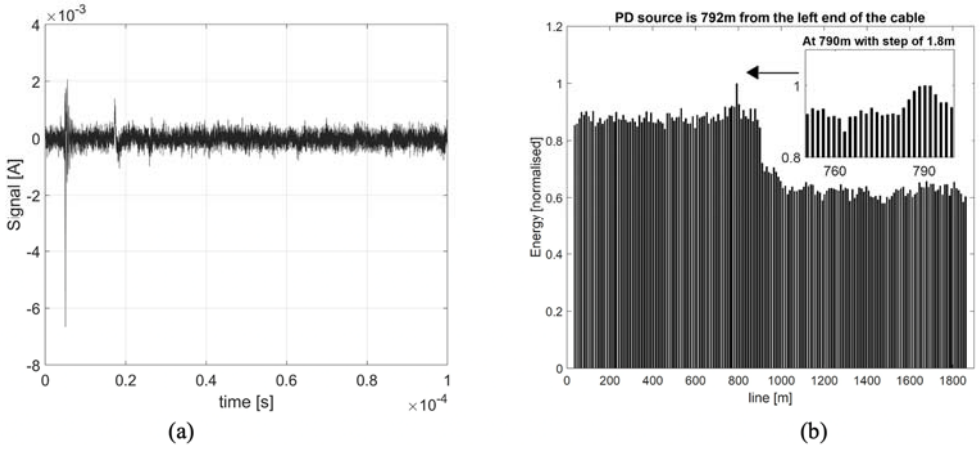

Figure 44 Time reversed PD signal measured in line 2 (a) and the normalized energy at the GPDLs during the EMTR simulations (b) [96].

The method was also numerically tested in a line with Ring Main Units (RMUs) [97] [98]. In Figure 45, a line with an OP located in an RMU monitors a XLPE cable section [98]. As the Figure 45 shows, a second 75 m PILC cable is connected to the RMU, and a second 100 m PILC cable is connected to the second end of the XLPE cable. In this case, when a PD occurs in the monitored XLPE section, at the OP, the direct signal coming from the PD source is measured together with the signal reflections coming from the end of 100m PILC section and with the interfering signals coming from the 75m PILC cable section. The recorded (simulated) PD signal at the OP, when the PD source is 240 m away from the OP, as shown in Figure 46(a), is affected by the interfering signals and several reflections from the PILC cables and the interpretation of the individual peaks, necessary to localize the source with classical reflectometry methods, can become hard and tend to fail since the waveform is affected by several reflections and the overlapping peaks coming from the PILC cables. As shown in Figure 46(b), the EMTR-based method can localize the PD source even with the presence of this interfering signals using the recorded signal in Figure 46(a) to perform the time reversal procedure [98].

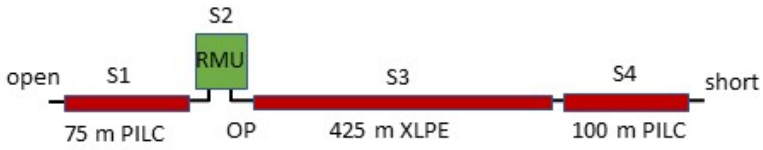

Figure 45 Configuration of the investigated line including an RMU [98].

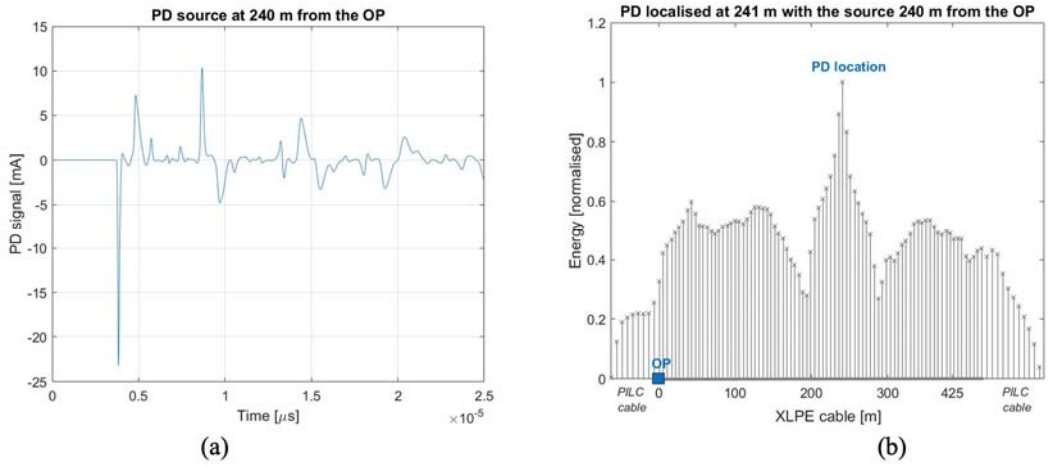

Figure 46. PD signals recorded (simulated) at the OP (a) and the EMTR localisation of the PD source in the monitored XLPE cables section (b) when the PD source is 240 m away from the OP [98].

The experimental and numerical investigations developed so far, shown that a PD localization method based on time reversal can overcome the shortcoming of the classical reflectometry methods caused by noise and distortion phenomena.

Follow-up investigations of the EMTR-based method are to apply it in localizing PD sources in more complex network topologies, i.e. radial lines with several branches and ring lines, with longer

cable sections. In these cases, when the line topology is too complex and the cable sections too long, a single OP may not be enough to localize the PD source and synchronized measurement, so more than one OP will be necessary.

5.2.2.2. Predictive Maintenance

Analysis of synchro-waveforms for detection and identification of incipient faults can also contribute to predictive maintenance. Predictive maintenance uses a combination of condition-based monitoring, sensor devices, and advanced analytics, including machine learning, to predict equipment failures before they occur [99]. By analyzing data from various sensors and equipment, including WMUs, predictive maintenance can *prevent equipment failure*, *optimize maintenance schedules*, *increase asset uptime*, *reduce costs on labor and parts*, and *enhance safety*. Real-time synchro-waveform data analysis can minimize unplanned downtime and ensuring a safer work environment. However, challenges such as data collection, organization, and quality must be addressed, as we discussed in Chapter 2. Investing in data integration tools and regularly cleaning data can help overcome these obstacles, ensuring accurate and reliable predictions.

5.3. Model Estimation

Synchro-waveforms can help with estimating various parameters in power systems.

5.3.1. Current Technology Use Cases

5.3.1.1. Network Parameter Estimation and Model Validation

The operation and planning of power system studies rely on the accuracy of the power system component models. Validation of these models under steady state and dynamic conditions is crucial for analyzing the network's reliability. The performance validation process starts during the initial commissioning of any new facility to the system, but many utilities require a periodic re-validation of the existing models due to aging, replacement, or refurbishment of the equipment [100]. In case of a disturbance event, the post-event performance validation is used to analyze and understand the event and minimize any reliability risks in the future. Model validation is done by using measurement devices and recording the field data. Then, the actual data is played back in the offline software and compared with the responses of the simulated model.

For the conventional synchronous generators, using synchro-phasor data in the performance model validation might be enough to capture the dynamic response of the units. NERC Reliability Guideline recommends a rate of 60 samples/second, as lower resolutions may not capture the full dynamic behavior of the units [100]. Recently, many grids have started to integrate high-penetration levels of inverter-based renewable resources, i.e., fast-power electronic-based resources. During disturbances, PLL of the inverters may experience an instantaneous and large distortion in the phase measurement due to the voltage waveform distortion, causing miscalculation of the frequency [101]. For example, during phase-to-phase line faults, the phase jumps in the affected phases are equal but opposite, and this results in a minimal change in the phasor. In real incidents, the inverters tripped because of such sub-cycle transients in their terminal voltage [102], [45]. Therefore, NERC identifies this gap in their reliability standards and

recommends including high-resolution measurement devices, e.g., 16 samples/cycle or 960 samples/second [46]. Figure 47 shows the voltage waveforms at the IBR terminal sub-cycle distortion that led to inverter tripping.

Similar to the model validation of the resources, network parameter validation is necessary to model the steady-state and dynamics behavior of a power system accurately. Power system studies, from market to system stability, have relied on accurate network parameters and considered them to be known and fixed over time [103]. These parameters have been calculated based on theoretical calculations and measurements during the initial commissioning of the network components [104]. System operators need positive-sequence network parameters to perform RMS studies. The mismatch between the actual values and the obtained parameters can reach 25-30% [105]. Such values will get more crucial and errors can get magnified if and when system operators utilize old values of impedances to determine dynamic line ratings to alleviate problems with large system loading [129]. To minimize this error, the real-time synchro-phasors data are utilized to accurately estimate the network parameters [130] [131] [132]. Although the synchrophasor-based approaches provide promising results, there are some limitations to estimating the mutually coupled and not fully transposed sections of the network. The use of synchro-waveform measurements should overcome these shortcomings as the full three-phase parameters can be estimated.

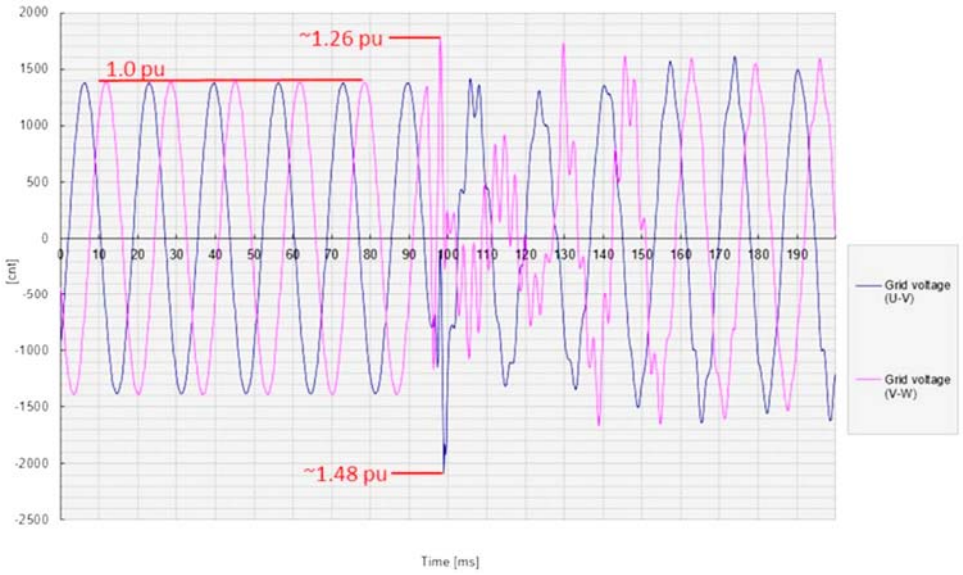

Figure 47. Inverter terminal voltage waveforms during a fault [102]. Notations U, V, and W denote the three phases; where U-V and V-W denote the phase-to-phase voltages.

5.3.2. Emerging Applications

5.3.2.1. Network Parameter Estimation / Model Validation

The integration and utilization of Synchro-Waveforms within Static State Estimation (SSE) as well as D-DSE can represent transformative elements in addressing the challenges posed by the

evolving electricity network [106]; see Figure 48. The massive incorporation of IBRs and the ensuing digital transformation of the grid herald a new paradigm characterized by decentralization, decarbonization, digitalization, and democratization (4D) [107]. This shift towards a more dynamic electricity network brings forth significant scientific challenges related to the stability and reliability of the entire electrical system, especially the transmission network [108].

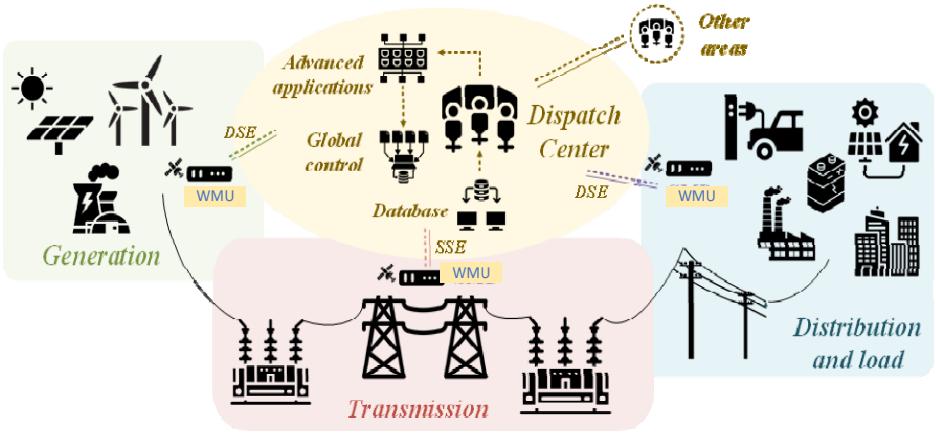

Figure 48. Schematic of DSE and SSE in Power System Layers Incorporating WMU.

Synchro-Waveforms are at the forefront of enabling this paradigm shift. They provide real-time, synchronized measurements across the electrical network, which is critical for achieving extended Dynamic Wide-area Situational Awareness (D-WASA) [107] [109]. This capability is vital for understanding the current state of the electrical network in real-time, enabling the rapid detection and response to any anomalies or instabilities that might arise due to the intermittent nature of DERs or other factors. The real-time data gathered from Synchro-Waveforms facilitate the development of intelligent, resilient decision-making frameworks that can operate on fast algorithms to respond to dynamic changes within the network in less than a second.

Moreover, the application of D-DSEs (see Section 5.1.2.2), powered by Synchro-Waveforms or WMUs data, can offer a new approach to protection and control within the electricity network. D-DSE with synchro-waveform capabilities can also potentially help with detecting cyber-attacks [110] and make the power system more resilient and more reliable [111].

This can be achieved for example by using synchro-waveforms in developing digital twins to a) simplify the protection and control processes by negating the need for coordination among protection functions; b) enhance functionality in conditions of low short circuit current and low inertia; c) provid means to validate and auto-calibrate relay inputs/measurements; and d) enhance the ability to pinpoint the origins of anomalies—ranging from defects and hidden failures to cyber-attacks—through statistical hypothesis testing. Such capabilities yield actionable insights for determining parameters and fine-tuning models for transportation equipment and DERs [112].

5.4. Cyber-security Applications

Synchro-waveforms may also help in cyber-security, especially in physics-based cyber-security.

5.4.1. Emerging Applications

5.4.1.1. Anomaly Detection and Synchro-Waveforms

Synchro-waveforms capture the inherent physical characteristics of power systems, offering a level of temporal detail beyond conventional sensing technologies. This high-resolution data serves as a foundational element for artificial intelligence (AI) in detecting anomalies. By emulating standard operational patterns—such as voltage, current, and frequency values and their variations as part of the system operations—AI models leverage synchro-waveforms. These models refine agents, enabling early detection and systematic categorization of anomalies within power systems.

The detailed insights provided by synchro-waveforms empower the identification of subtle deviations from normal behavior. Swift localization of sudden disturbances or inconsistent measurements - deviating from other agents' readings - becomes possible. The system's physical properties, combined with input from the IT infrastructure, assist in identifying and classifying anomalous system behavior. Anomalies can be mapped to normal disturbances or more interestingly to cyber intrusions. Agents, collecting these measurements, leverage the dispersed nature of synchro-waveforms to enable distributed intrusion detection systems. Decentralized agents at wind turbines, solar panels, substations, and meters collaboratively analyze waveforms to promptly identify and localize compromised components and strengthening overall system security and resiliency to cyber threats.

Real-time synchro-waveforms empower distributed anomaly detection, providing granular data and fostering a robust network of monitoring agents. As power systems face evolving threats, leveraging these waveforms can help with better securing the critical infrastructure.

It is also worth mentioning that in recent years, several machine learning or data-driven approaches for anomaly detection have been proposed but the performance of a multitude of such methods rely on the availability of sufficiently large amount of "labelled" training data. Here "labelled" data means that the data should be properly marked with the true target or label, absent which its usage in training of data-driven methods is limited. One way by which the absence of labels can be overcome is the use of pseudo labels by relying on similarly of unlabelled and labelled training samples [133], that arises due to similar location and event type. In this context, the richer data collected by WMUs offers the benefit of more accurate computation fo similar scores that can lead to better anomaly or event detection, not just for current events but also applicable for older events.

5.5. Stability and Control in Micro-grids

Microgrid stability is defined as the ability, once subjected to a disturbance, to recover "all state variables to (possibly new) steady-state values which satisfy the operational constraint, and without the occurrence of involuntary load shedding" [113]. Stability in grid-connected microgrids is generally limited to the stability of individual devices, given that the voltage and frequency are mainly governed by the upper grid. On the other hand, stability in islanded microgrids is considerably different from bulk power systems, exhibiting a range of under-studied dynamic phenomena, including voltage and frequency coupling, PLL synchronization issues, harmonic resonance of parallel inverters, etc. These are due to the unique characteristics of microgrids as

compared to bulk power systems, including lower system inertia, resistive feeders, low short-circuit capacities, unbalanced operations, and higher penetration of DERs [113].

Considering the above-mentioned characteristics, classical modeling and analysis tools and techniques developed and used for the stability of conventional power systems are not adequate for microgrid studies. For example, stability analysis techniques based on linearized balanced power systems are not applicable to unbalanced IBR-penetrated microgrids [113]. In another example, average inverter models for microgrid simulation may result in considerably inaccurate stability margins in unbalanced and/or highly loaded islanded microgrids [114]. In this context, novel methods based on synchro-waveforms can capture the inherent unique dynamic phenomena of microgrids, leading to more accurate and reliable stability monitoring, analysis and mitigation.

Consider the modified version of the CIGRE benchmark for microgrids, shown in Figure 49 and discussed in [114]. A case of instability for this system is shown in Figure 50. The instability is triggered by a sudden 200 kVAR increase in the reactive power demand and manifests itself as unsustained oscillations. Note that the system is highly unbalanced. A zoomed-in plot of the instantaneous three-phase voltages is provided in Figure 51. A visual study of the instantaneous three-phase voltage demonstrates a significant change in the pattern pre- and post-disturbance. Such a pattern, for example, the flatter peak of the voltage at phase A post-disturbance, may have valuable information about the stability margin of the system, enabling the control system to perform proactive measures to mitigate instabilities in the system.

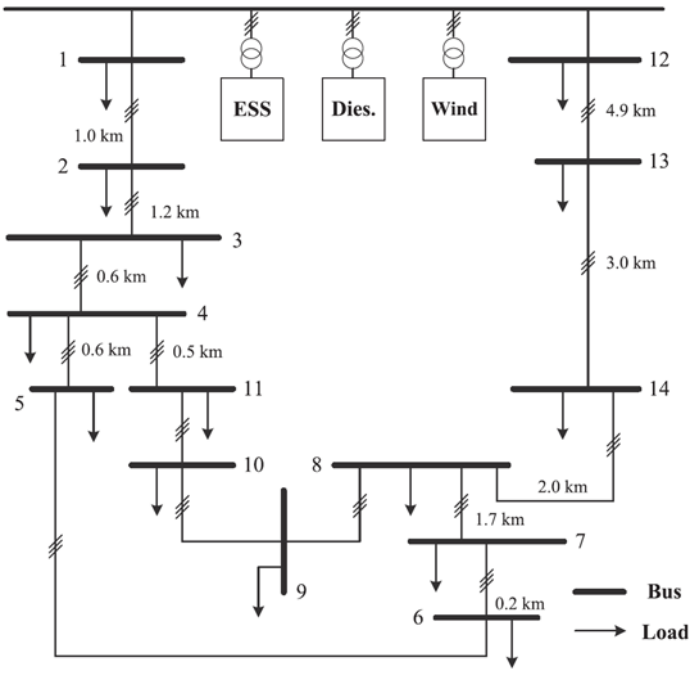

Figure 49. The modified version of the CIGRE benchmark for microgrids [114].

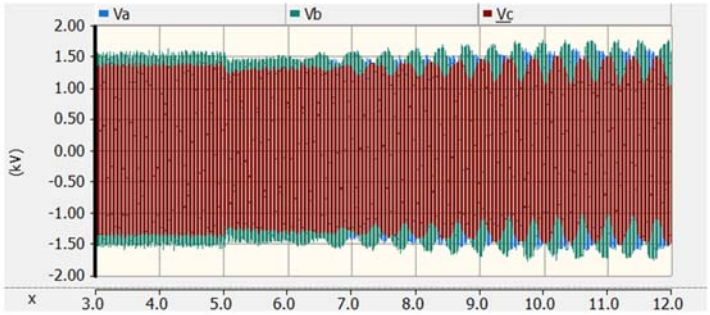

(a)

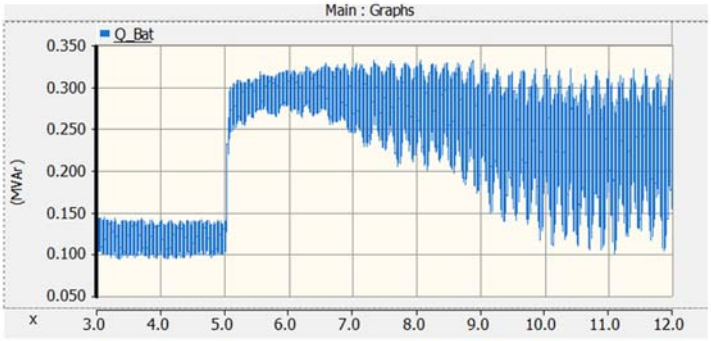

(b)

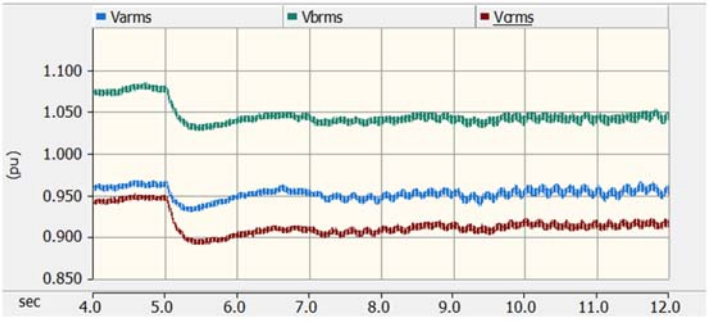

(c)

Figure 50. Instability case: (a) instantaneous three-phase voltage at the battery terminal; (b) battery injected reactive power; (c) three-phase RMS voltage at the battery terminal.

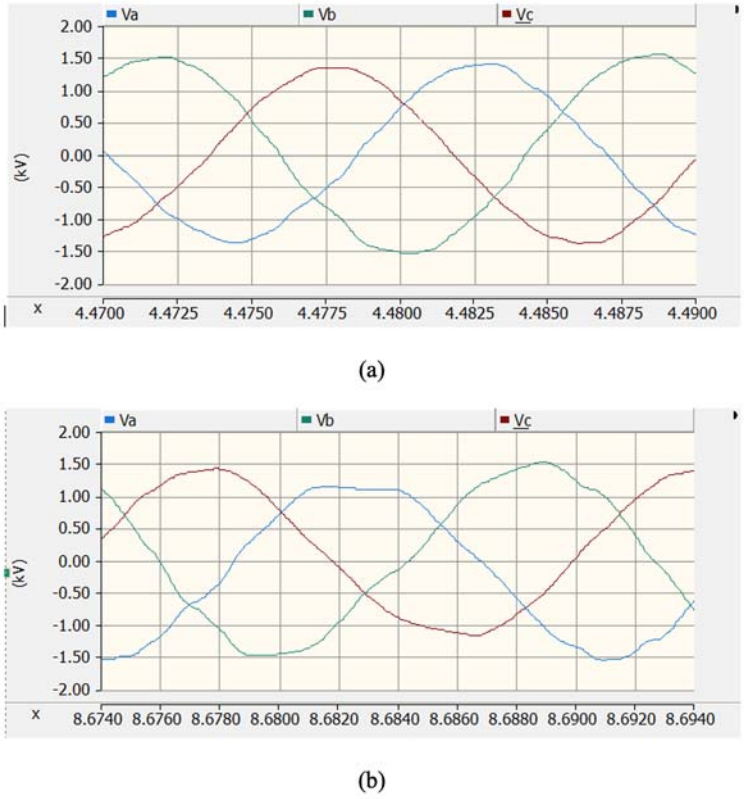

Figure 51. Instantaneous three-phase voltage of the battery: (a) pre-fault; (b) post fault.

5.6. Geomagnetic Disturbances

5.6.1. Current Technology Use Cases

The Sun constantly emits a solar wind of charged particles that typically take several days to reach Earth. Following a coronal mass ejection, these particles can reach Earth much faster and with greater intensity, resulting in a geomagnetic disturbance (GMD). The fluctuations of Earth's geomagnetic field during a GMD produce geomagnetically induced currents (GICs) that appear as DC in bulk power systems due to their very low frequency. This DC current drives transformer cores into saturation, resulting in overheating, suppressed voltages, and harmonic distortion. The consequences for bulk power system operation can be significant, as demonstrated by the March 13, 1989 GMD that impacted grids across North America and caused a blackout of the Hydro-Québec system [115].

To address the risks posed by GMDs, the U.S. DOE released a report in 2019 outlining a suggested monitoring approach [116]. The report suggests the use of both synchro-phasor and waveform measurement systems. Though the phasors of the fundamental 60 Hz waveform are deemed useful, [116] focuses on using PMUs to report the phasors of harmonics. This approach reflects the system developed by Hydro-Québec following the 1989 GMD, which uses customized PMUs to obtain harmonic information [117]. As an alternative to this customization, a synchro-waveform

measurement system would provide the raw measurements needed to monitor harmonic information, as suggested in [3]. The system could also meet two additional needs identified in [116].

The first use of synchro-waveforms identified by [116] is to validate the SCADA and synchro-phasor measurements that also support the system. This is particularly important for the GMD application because these measurement systems are not well vetted for the unusual grid conditions a GMD creates. Second, [116] emphasizes data gathering to better understand the impacts that GMDs have on equipment. Synchro-waveform measurements are essential to develop and validate models that can predict equipment and system impacts.

The use of synchro-waveforms for GMD monitoring is timely. Solar storms follow a fairly regular cycle of about 11 years with large storms in 1989, 2003, and 2012 [116]. Effective use of measurement systems can help grid operators be well prepared for the next GMD.

5.7. Interaction with Existing Decision Tools

Waveform capture devices and data have been utilized within utilities for decades and the benefits and uses of the information still hold a tremendous value to the various engineering and operations organizations. As waveform capture device technology improves, the higher fidelity recordings combined with the ability to produce large quantities of data dictate the need for improved systems to handle the data from these devices at both speed and scale.

Speed of the data may be dependent on the use cases that the waveform data would feed into. For example, engineers and analysts evaluating post-fault incidents may not have a dire need for real-time or near real-time waveform data. A timeframe of hours may be sufficient as these studies may not be time sensitive, compared to an operator who requires information about the circuits or system they are operating in real-time. For operations, the speed requirement may have to be within seconds or faster.

Furthermore, depending on what type of personnel is responsible for utilizing the waveform data, different levels of abstraction may be required. This means that engineers (as an example) may want to work directly with the raw waveform data to be able to perform various studies on it, to system operators who would desire the waveform data distilled into an immediately actionable signal (e.g., opening a circuit breaker).

While the above descriptions are more human-in-the-loop specific, meaning there is still a person involved in the interaction with the waveform data, the increasing speed and scale in which waveform data is generated is facilitating the push for increasing automation to handle ingestion, storage, analysis, and action on the waveform data. This automation will have a heavy integration into the various tools, systems, and software that utilities use to analyze and operate the grid.

Essentially, waveform data integrated into a Grid Management System (GMS) platform would ideally be processed by the system and have the information distilled immediately into something an operator can glean insight from with minimal cognitive load or the system itself would take immediate actions based on pre-defined logic. Information from these waveforms can identify hazards such as energized wires on the ground, uncharacteristic harmonic content on a circuit, confirmation of switching operations besides just through SCADA, identifying fault location, etc.

For a wide-area monitoring system, this may entail abstraction, sub-sampling or even feature extraction in-situ at the WMU location itself, with the reduced signal sent int to the control center. Such an abstraction may be more amenable with current signaling infrastructure to minimize impact on communication bandwidth, while ensuring that the abstraction is informative enough for centralized decisions.

Other tools and systems that can benefit from integration with waveform data could be more robust testing of relay settings using previously captured high fidelity waveforms to be replayed through the relay to check if the relay would operate as intended. Having a large library of events to test along with improving testing automation may increase the confidence and the operational performance of the relay and settings as potential issues may be identified before making operational in the field.

Lastly, integration into systems and software that can further extract various insights from the waveform such as load characteristics, harmonic content, fault characteristics on circuits can provide system planners, engineers, power quality advisors with improved insight that can inform better circuit construction and identify latent issues that if mitigated earlier could avoid certain circuit issues in the future.

6. Synchro-waveform Standardization Needs

6.1. Background and historical insight into Synchro-phasor standardization

The U.S. Department of Energy (DOE) partnered with the Bonneville Power Administration (BPA) and the Western Area Power Administration (WAPA) to launch the Wide Area Measurement Systems (WAMS) project in 1995 [118]. Moving beyond the relatively slow telemetry associated with Supervisory Control and Data Acquisition (SCADA), WAMS provided a means to measure the dynamic behavior of the interconnected power system. Also enabled by low cost and precise (microsecond-class uncertainty) time synchronization, the PMU is included within this realm of advanced measurements. These were first postulated in the 1980s and have subsequently become more common in the intervening years [119].

The first IEEE Standard for power system synchro-phasor measurements was IEEE 1344-1995 [120]. This was replaced with Standard IEEE C37.118-2005 which was much more comprehensive, including measurement error requirements that could be tested for compliance and a communications protocol. This was split into two standards in 2011, the measurement standard IEEE C37.118.1 and the communications standard C37.118.2. The newest standard describing the measurement requirements is IEC/IEEE 60255-118-1 published in 2018. And various standards for the streaming of synchro-phasor data are being developed under IEC 61850 [121] and IEEE, for example the Standard for Streaming Telemetry Transport Protocol (IEEE 2664-2024) [122]. This protocol incorporates security features and lossless data compression to efficiently transmit streaming power system data over Internet Protocol (IP) communication systems. It defines both data and control channels and employs a publish-subscribe model to manage signal-level data access. STTP allows the transfer of real-time and historical time-series data at either full or down-sampled resolutions.

These standardization efforts were nurtured by DOE through various forums. In addition to the WAMS activities, primarily in the western interconnection, DOE formed the Eastern

Interconnection Phasor Demonstration Project in 2002 [123]. In 2006 DOE brought these efforts together by forming the North American Synchro-Phasor Initiative (NASPI) [124]. These forums were comprised of professionals from utilities, academia, manufacturers and government with the goal of helping to nurture the adoption of phasor measurement technology through standardization. Through work group meetings to discuss and develop the requirements prior to being taken up by the standards setting organization, the standards development effort could benefit from the sharing of best practices and innovative concepts. Additionally, NASPI published technical reports and guidelines that also later became the basis for codified standards by the IEEE and the IEC. NASPI continues to provide a liaison role with these organizations for the collective benefit of all stakeholders working in this technical arena.

From the work in synchro-phasors some standard guidelines for their measurement capabilities were derived. Below is some of that information as many of the items listed may still be applicable for Synchro-waveforms.

Table 8. Standards for Synchro-Phasor Measurements [37]**.**

Steady-state Synchro-Phasor Requirements						
Influence quantity	**Minimum range of influence quantity over which PMU shall be within given limits**					
	Performance- P class			**Performance- M class**		
	Range	Max. FE	Max. RFE	Range	Max. FE	Max. RFE
Freq. Deviation	±2 Hz	5mHz	0.4Hz/s	±5 Hz	5mHz	0.1Hz/s
Harmonic Distortion	1% each harmonic upto 50th	5mHz	0.4Hz/s	10% each harmonic upto 50th	5mHz	No Required
Out-of-band Interference	-	-	-	10% of input signal	10mHz	No Required
Dynamic Synchro-Phasor Requirements						
Amplitude/ Phase Modulation	10%, f_m varies 0.1 to 5 Hz	60mHz	0.6Hz/s	10%, f_m varies 0.1 to 5 Hz	30mHz	0.1Hz/s

Frequency Ramp	±2 Hz	10mHz	0.4Hz/s	±5 Hz	10mHz	0.2Hz/s
Amplitude/Phase Step change	±0.1/±10˚	90ms	120ms	±0.1/±10˚	280ms	280ms

Performance Metrics:

The performance of the most efficient parametric-based methods (VCMC-ZARGN and EKF), compliant with the IEC/IEEE 60255-118-1a standard, is shown in the figures. Frequency Deviation (Static, Steady-state): Figure 52 reveals that the variation in frequency hardly disturbs the FE and RFE of the proposed approach and it is well within compliance level of the standards. Modulation Tests (Dynamic): Figure 53 shows VCMC-ZARGN shows higher performance in terms of lower FE and RFE range. The performance of the parametric-based methods for frequency and ROCOF estimation of power signals are compared as shown in Table 9 for different tests cases.

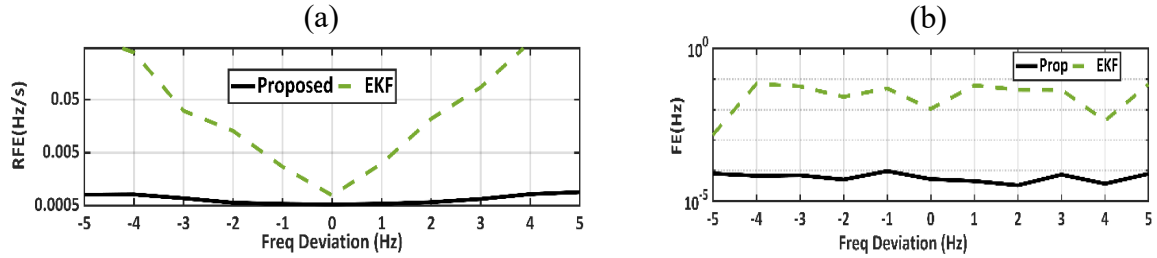

Figure 52. (a) RFE (b) FE for the frequency test complying IEC/IEEE 60255-118-1a under static case.

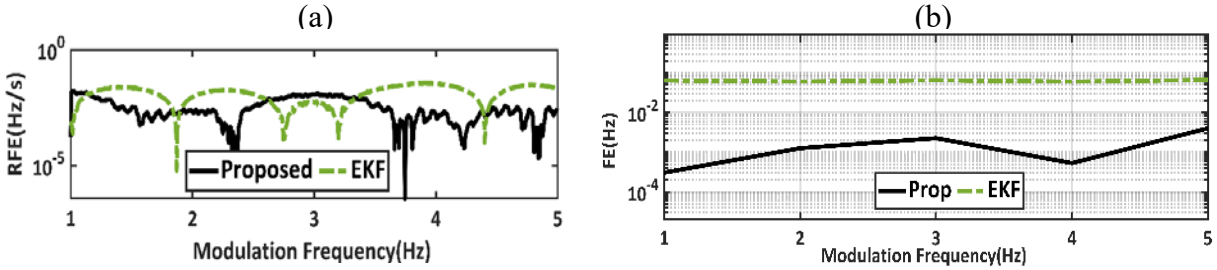

Figure 53. (a) RFE (b) FE with different modulation frequency complying IEC/IEEE 60255-118-1a under dynamic case.

Table 9. Performance Analysis as per IEC/IEEE 60255-118-1:2018 (A:FE_{mean}Hz), (B:RFE_{mean}Hz/s)] IEEE Standard (FE (mHz)/RFE(Hz/s)): F_{Range}: $(5/0.4)$; F_{Ramp}: $(10/0.4)$;

Test	EKF		Proposed	
	A	B	A	B
F_{Range}	0.008	0.008	0.002	0.020
F_{Ramp}	0.002	0.002	0.005	0.0025
AM/PM	0.002	0.002	0.01	0.004

6.2. Device and Sensor Standards

When comparing synchro-waveform measurements across systems, it is important to understand the inherent errors of each of the various sensors in the comparison. The MV Smart Grid Sensor and Sensor Systems within IEEE have released a technical report IEEE PES-TR102 that covers some of the information that goes into determining conditional accuracy of a measurement system which included the sensors, wiring, and the actual measurement device itself. These factors are crucial for accurately capturing harmonic frequencies across systems. This work is still an ongoing area of investigation, but the need for it has been proven. Also, there have been recent working groups formed to look at the accuracy of sensors themselves across broad frequency ranges (through 3kHz). As electrical systems move more toward higher inverter-based generation and inverter-based load penetration across the grid, accurate measurement of higher frequency will become crucial.

IEC standards around measurement capability of power quality devices (IEC 61000-4-30) is also a good source of information to consider when evaluating measurement instruments. This standard defines the requirements for a Class A and a Class S instrument. Although this technical report is focused on synchro-waveforms, the information minimum standardization on measurement instruments can play an important function when evaluating data and trying to discern insight. Comparison of features such as samples/cycle, triggering capability, harmonic limitations within the instrument measurement capability, time precision, as well as other intricacies of the device can come into play depending on what granularity of event/ data one is trying to compare.

6.3. Waveform and Data Sharing Formats

A key issue to address when discussing synchro-waveform standardization is the format in which data files will be shared in. This is an important point since in practicality many of the devices that will be used to accomplish the data capture will come from a variety of manufacturers, device models, and even metadata sources all, potentially, with their own proprietary software or file types. There are two well-known IEEE standards that relate to waveform file types.

Traditionally, the most common format for waveform file type has been the COMTRADE (Common Format for Transient Data Exchange) file format. This format is standardized in IEEE C57.111-2013 (latest standard version) and was made popular over the years due to its importance

when reviewing protection relay waveform files. It can contain both channel analog quantities as well as channel digital quantities for a captured event. Comtrade files can be stored as ASCII or Binary files and typically come in pairs of three files for each observation/event; header file, configuration file, and data file (.HDR, .CFG, and .DAT). Also, the data contained within a COMTRADE file is related to one single observation/event capture.

The PQDIF (Power Quality Data Interchange Format) file type is standardized in IEEE 1159.3. This robust file format has been used extensively in the transfer of Power Quality data and is capable of handling multiple observation/event records within a single file, varying sample rates, and varying types of quantities. It can be stored in XML or binary files. All data is stored in one self-contained (.pqdif) file and separate header and configuration files are not needed. The most recent draft (IEEE 1159.3) [122] also includes additional metadata tags specifically for synchronized-waveform data.

In addition to file formats for storing data, various real time streaming standards include capabilities for streaming synchronized-waveform data. IEEE 2664-2024 includes features, such as, high resolution timestamps, specifically designed to allow streaming of synchronized-waveform data.

The new draft of IEEE C37.118.2-2024 also mentions the importance of supporting synchronized-wave form data. While the standard does not go as far as including synchronized waveform-data in the most recent scope, several publications are available discussing the use of the standard for this data [125].

It is also important to establish a standard naming convention for synchro-waveforms, to ensure consistency and facilitate developing a standard naming convention for synchro-phasor measurements is crucial to ensure consistency and facilitate searchability. Adopting a standard naming convention makes it easier to determine data usage and availability for future analyses. Notably, naming conventions may vary across different companies, so it is recommended to adhere to existing naming standards as much as possible. The convention should also be concise yet provide all necessary information, as it will be displayed on dashboards or other interfaces where screen space is limited.

It is advisable to develop and adopt a naming convention as early as possible and avoid assuming that it can be easily fixed later. Leveraging existing naming conventions is also recommended. To ensure the convention meets the needs of all stakeholders, it is important to involve engineers, operators, and IT professionals in its development.

Although a naming convention is not technically a data archive or networking issue, it can significantly improve data usage. The basic framework hierarchy should include assets, measurement devices, and control systems organized in a way conducive to each use case’s specific analyses. This approach allows for intuitive data organization, enabling both overview and drill-down capabilities for KPI displays and dashboards.

Naming conventions developed for synchrophasor technology is directly usable for synchro-waveforms naming [126], [127]. In a brief, for device naming, it is recommended that device names are unique and should include the following information:

- Substation Name

- Internal Location
- Nominal Voltage
- Asset Identifier
- Primary Secondary Identifier

A period (.) is a good choice for a separator since it is not typically used as a wild card character.

Signal names do not have to be unique and in most cases will not be. However, the full name of the measurement and the combination of the PMU name and the signal name will be unique.

It is recommended that once the naming convention is finalized, the names are used in the hardware configuration of the device. Although it is possible to use a concentrator to rename the device and signals as it is concentrating the data, it is not advisable.

References

[1] H. Mohsenian-Rad and W. Xu, "Synchro-Waveforms: A Window to the Future of Power Systems Data Analytics," *IEEE Power and Energy Magazine,* vol. 21, no. 5, pp. 68-77, September 2023.

[2] W. Xu, Z. Huang, X. Xie and C. Li, "Synchronized waveforms–A frontier of data-based power system and apparatus monitoring, protection, and control," *in IEEE Trans. Power Delivery,* vol. 37, no. 1, pp. 3-17, Feb 2022, doi: 10.1109/TPWRD.2021.3072889.

[3] A. Silverstein and J. Follum, "High-resolution, time-synchronized grid monitoring devices," North American Synchrophasor Initiative, Tech. Rep. PNNL-29770/NASPI2020-TR-004, 2020.

[4] A. F. Bastos, S. Santoso, W. Freitas and W. Xu, "Synchrowaveform measurement units and applications," in *Proc. IEEE PES General Meeting*, Atlanta, GA, USA, 2019.

[5] H. Mohsenian-Rad, *Smart Grid Sensors: Principles and Applications*, Cambridge University Press, UK, Apr., 2022.

[6] C. Halliday, "Visualisation of Real Time System Dynamics using Enhanced Monitoring (VISOR)," VISOR: Close Down Report, 2018.

[7] D. Laverty, M. Rusch, D. Saba and A. Von Meier, "Open Source Time Synchronised Sampled Value Logger for Power System Studies," in *Proc. of the 33rd Irish Signals and Systems Conference (ISSC)*, Cork, Ireland, 2022.

[8] Z. J. Ye and H. Mohsenian-Rad, "A Data-Driven Time-Synchronization Method to Convert Power Quality Waveform Measurements into Synchro-Waveforms," in *2024 International Conference on Smart Grid Synchronized Measurements and Analytics (SGSMA)*, 2024.

[9] Z. J. Ye and H. Mohsenian-Rad, "Transforming Conventional Waveform Measurements into Synchro-Waveforms: A Data-Driven Method for Event Signature Alignment and Synchronization Operator Estimation," *IEEE Transactions on Smart Grid,* 2024.

[10] H. Mohsenian-Rad, M. Kezunovic and F. Rahmatian, "Synchro-waveforms in Wide-Area Monitoring, Control, and Protection," *under review,* December 2023.

[11] J. M. Lim and M. Mousavi, "Synchronized Distributed Waveform Analytics: Requirements and Applications," Panel presentation, IEEE PEG General Meeting, 2020.

[12] S. G. Laughner, "Wideband Voltage Sensors For the Modern Substation," in *CIGRE US National Committee Grid of the Future Symposium*, US, 2018.

[13] T. Laughner and J. Wischkaemper, "PQ Monitoring Systems," in *IEEE PES Joint Technical Committee Meeting*, Jacksonville, FL, 2023.

[14] S. Sharma, A. Kathe, T. Joshi, and T. Kanagasabai, "Application of Ultra-High-Speed Protection and Traveling-Wave Fault Locating on a Hybrid Line," in *Proceedings of the 46th Annual Western Protective Relay Conference*, Spokane, WA, 2019.

[15] F. Shanyata, S. Sharma, D. Joubert, R. Kirby, and G. Smelich, "Evaluation of Ultra-High-Speed Line Protection, Traveling-Wave Fault Locating, and Circuit Breaker Reignition Detection on a 220 kV Line in the Kalahari Basin, Namibia," in *Proceedings of the 48th Annual Western Protective Relay Conference*, Spokane, WA, 2021.

[16] T. Laughner, "Framework For Automating PQ Data Resources," in *EPRI Electrification 2024*, Savannah, 2024.

[17] "IEEE Draft Guide for Centralized Protection and Control (CPC) Systems within a Substation," IEEE PC37.300/D6.4, June, 2023.

[18] M. P. Andersen and D. E. Culler, "BTrDB: Optimizing Storage System Design for Timeseries Processing," in *14th USENIX Conference on File and Storage Technologies (FAST 16)*, 2016.

[19] S. Blair and J. Costello, "Slipstream: High-Performance Lossless Compression for Streaming Synchronized Waveform Monitoring Data," in *2022 International Conference on Smart Grid Synchronized Measurements and Analytics (SGSMA)*, 2022.

[20] C. Presvôts and T. Prevost, "Compression of Sampled Current and Voltage Signals Via a Multi-Model Coding Scheme," presented at the NASPI Webinar, 2023.

[21] J. R. Carroll and F. R. Robertson, "A Comparison of Phasor Communications Protocols," Pacific Northwest National Lab. (PNNL), Richland, WA (United States), 2019.

[22] C. Chen, W. Wang, H. Yin, L. Zhan and Y. Liu, "Real-time lossless compression for ultrahigh-density synchrophasor and point-on-wave data," *IEEE Transactions on Industrial Electronics,* vol. 69, no. 2, pp. 2012-2021, 2021.

[23] W. Qiu, H. Yin, Y. Wu, C. Chen, L. Zhan, C. Zeng and Y. Liu, " Synchro-waveform data compression using multi-stage hybrid coding algorithm," *ELSEVIER, Measurement,* vol. 232, p. 114709, 2024.

[24] Y. Wu, H. Yin, W. Qiu and Y. Liu, " Enhancing Data Transmission and Storage Efficiency in Power Grids Through Compression of Point-on-Wave Data. I," in *in 2023 IEEE Industry Applications Society Annual Meeting (IAS)* , Nashville, TN, 2023.

[25] R. Brown, S. Caruso and S. Glennon, "Realizing Infrastructure Convergence For Rapid Grid Modernization," CableLabs, 2024.

[26] "CableLabs," [Online]. Available: https://www.cablelabs.com/.

[27] A. McEachern, "Waveform apparatus disturbance detection and method," U.S. Patent 4,694,402, filed 1985, expired 2009.

[28] F. Ahmadi-Gorjayi and H. Mohsenian-Rad, "Data-Driven Models for Sub-Cycle Dynamic Response of Inverter-Based Resources Using WMU Measurements," *IEEE Trans. on Smart Grid,* vol. 14, no. 5, pp. 4125-4128, September 2023.

[29] F. Ahmadi-Gorjayi, L. Lampe and H. Mohsenian-Rad, "Event Signatures in H-PMU Measurements: An Information-Theoretic Analysis of Real-World Data.," in *In 2024 IEEE Power & Energy Society Innovative Smart Grid Technologies Conference (ISGT)* , Washingtone, DC, USA, 2024.

[30] M. Farajollahi, A. Shahsavari and H. Mohsenian-Rad, "Location identification of high impedance faults using synchronized harmonic phasors," in *In 2017 IEEE Power & Energy Society Innovative Smart Grid Technologies Conference (ISGT)* , Washington, DC, USA, 2017.

[31] A. Aligholian and H. Mohsenian-Rad, "GraphPMU: Event Clustering via Graph Representation Learning Using Locationally-Scarce Distribution-Level Fundamental and Harmonic PMU Measurements," *IEEE Trans. on Smart Grid,* vol. 14, pp. 2960-2972, July 2023.

[32] S. K. Jain, P. Jain and S. N. Singh, "A fast harmonic phasor measurement method for smart grid applications," *IEEE Transactions on Smart Grid,* vol. 8, pp. 493--502, 2016.

[33] L. Chen, M. Farajollahi, M. Ghamkhari, W. zhao, S. Huang and H. Mohsenian-Rad, "Switch status identification in distribution networks using harmonic synchrophasor measurements," *IEEE Transactions on Smart Grid,* vol. 12, pp. 2413--2424, 2020.

[34] F. A. Gorjayi and H. Mohsenian-Rad, "A physics-aware MIQP approach to harmonic state estimation in low-observable power distribution systems using harmonic phasor measurement units," *IEEE Transactions on Smart Grid,* vol. 14, pp. 2111--2124, 2022.

[35] A. Aligholian, A. Shahsavari, E. M. Stewart, E. Cortez and H. Mohsenian-Rad, "Unsupervised event detection, clustering, and use case exposition in micro-pmu measurements," *IEEE Transactions on Smart Grid,* vol. 12, pp. 3624--3636, 2021.

[36] L. Chen, X. Xie, J. He, T. Xu, D. Xu and N. Ma, " Wideband oscillation monitoring in power systems with high-penetration of renewable energy sources and power electronics: A review," *Renewable and Sustainable Energy Reviews. 2023,* vol. 175:113148, 2023.

[37] "IEEE/IEC International Standard - Measuring relays and protection equipment - Part 118-1: Synchrophasor for power systems - Measurements.," *IEC/IEEE 60255-118-1,* p. 1–78, 2018.

[38] J. Man, L. Chen, V. Terzija and X. Xie, "Mitigating High-Frequency Resonance in MMC-HVDC Systems Using Adaptive Notch Filters," *IEEE Trans. Power Systems,* vol. 37, no. 3, pp. 2086-2096, 2022.

[39] X. Xie, Y. Zhan, J. Shair, Z. Ka and X. Chang, "Identifying the Source of Subsynchronous Control Interaction via Wide-Area Monitoring of Sub/Super-Synchronous Power Flows," *IEEE Transactions on Power Delivery,* vol. 35, no. 5, pp. 2177-2185, 2020.

[40] H. Tianqi and F. D. Leon, "Lissajous curve methods for the identification of nonlinear circuits: Calculation of a physical consistent reactive power.," *IEEE Transactions on Circuits and Systems I,* vol. 62, pp. 2874--2885, 2015.

[41] M. Izadi and H. Mohsenian-Rad, "A Synchronized Lissajous-based Method to Detect and Classify Events in Synchro-waveform Measurements in Power Distribution Networks,," *IEEE Trans. on Smart Grid,* vol. 13, no. 3, pp. 2170-2184, May 2022.

[42] N. Ehsani, F. Ahmadi-Gorjayi, Z.-J. Ye, A. McEachern and H. Mohsenian-Rad, "Sub-cycle Event Detection and Characterization in Continuous Streaming of Synchro-waveforms: An Experiment Based on GridSweep Measurements," in *Proc. of the IEEE NAPS*, Asheville, NC,, 2023.

[43] Y. Seyedi, L. Piyasinghe and R. Smith, "Field Study on Short-Time Voltage Harmonic Distortion in Incipient Faults Using Low Voltage Waveform Data," in *IEEE PES Grid Edge 2025*, San Diego, CA, 2025.

[44] NERC, "1,200 MW Fault Induced Solar Photovoltaic Resource Interruption Disturbance Report," 2017.

[45] NERC Report, "2022 Odessa Disturbance Texas Event," December, 2022.

[46] NERC Synchronized Measurements Subcommittee (SMS), White Paper, "Recommended Disturbance Monitoring for Inverter-Based Resources," February 2020.

[47] H. Mohsenzadeh-Yazdi, F. Ahmadi-Gorjayi and H. Mohsenian-Rad, "Sub-Cycle Dynamics Modeling of IBRs Using LSTM Methods and Synchro-waveform Measurements," in *2024 IEEE Power & Energy Society General Meeting (PESGM)*, Seattle, 2024.

[48] "IEEE Standard for Interconnection and Interoperability of Inverter-Based Resources (IBRs) Interconnecting with Associated Transmission Electric Power Systems," IEEE Std 2800-2022, 2022.

[49] C. Smith and B. Shultz, "NOGRR245 - Inverter-Based Resource (IBR) Ride-Through Requirements," Southern Power, 2023.

[50] NERC, "Odessa Disturbance Texas Events: May 9, 2021 and June 26, 2021 Joint NERC and Texas RE Staff Report," NERC, 2021.

[51] NERC, "Recommended Disturbance Monitoring for Inverter-Based," 2020.

[52] NERC, "PRC-028-1 – Disturbance Monitoring and Reporting Requirements for Inverter-Based Resources," 2024.

[53] J. Follum, R. Hovsapian, N.M. Stenvig, Y. Agalgaonkar, K. Chatterjee, K. Mahapatra, A. Riepnieks, et al., Advanced Measurements for Resilient Integration of Inverter-Based Resources: PROGRESS MATRIX Year-1 Report, Richland, WA: Pacific Northwest National Laboratory, 2023.

[54] Dominion Energy, "Continuous Oscillography Waveforms from the Substation to the Cloud," NASPI, 2024.

[55] "Grid Event Signature Library (GESL)," Oak Ridge National Laboratory, Lawrence Livermore National Laboratory, [Online]. Available: https://gesl.ornl.gov. [Accessed 16 July 2024].

[56] P. S. Wright, P. N. Davis, K. Johnstone, G. Rietveld and A. J. Roscoe, "Field Measurement of Frequency and ROCOF in the Presence of Phase Steps," *IEEE Transactions on Instrumentation and Measurement,* vol. 68, pp. 1688-1695, 2019.

[57] K. Chatterjee, D. Tarter, J. Follum, and A. Riepnieks, "A Nonlinear Least Squares Phasor Estimation Algorithm with a Trust Metric," in *Proc 2024 IEEE Power & Energy Society Innovative Smart Grid Technologies Conference (ISGT)*, Washington, DC, USA, 2024.

[58] A. Riepnieks and H. Kirkham, "An Introduction to Goodness of Fit for PMU Parameter Estimation," *IEEE Transactions on Power Delivery,* vol. 32, no. 5, pp. 2238-2245, October 2017.

[59] Yonina C. Eldar, G. Kutyniok, Compressed Sensing: Theory and Applications, Cambridge University Press, 2014.

[60] A.Derviškadić, G.Frigo, M.Paolone, "Beyond Phasors: Modeling of Power System Signals Using the Hilbert Transform," *IEEE Transactions on Power Systems,* vol. 35, p. 4, 2020.

[61] H. Kirkham and A. Riepnieks, "Dealing with non-stationary signals: Definitions, considerations and practical implications," in *Proc. of the IEEE PES General Meeting (PESGM)*, 2016.

[62] M. Vetterli, J. Kovačevic, V. K Goyal, *Foundations of Signal Processing*, Cambridge University Press, 2014.

[63] G. Barchi, D. Macii, D. Belega and D. Petri, "Performance of Synchrophasor Estimators in Transient Conditions: A Comparative Analysis," *IEEE Transactions on Instrumentation and Measurement,* vol. 62, pp. 2410-2418, 2013.

[64] J. A. de la O Serna, "Dynamic Phasor Estimates for Power System Oscillations," *IEEE Transactions on Instrumentation and Measurement,* vol. 56, pp. 1648-1657, 2007.

[65] W. Premerlani, B. Kasztenny and M. Adamiak, "Development and Implementation of a Synchrophasor Estimator Capable of Measurements Under Dynamic Conditions," *IEEE Transactions on Power Delivery,* vol. 23, pp. 109-123, 2008.

[66] P. Castello, M. Lixia, C. Muscas and P. A. Pegoraro, "Adaptive Taylor-Fourier synchrophasor estimation for fast response to changing conditions," in *2012 IEEE International Instrumentation and Measurement Technology Conference Proceedings*, 2012.

[67] M. Bertocco, G. Frigo, C. Narduzzi, C. Muscas and P. A. Pegoraro, "Compressive Sensing of a Taylor-Fourier Multifrequency Model for Synchrophasor Estimation," *IEEE Trans. on Instr. and Meas.,* vol. 64, pp. 3274-3283, 2015.

[68] D. Belega, D. Fontanelli and D. Petri, "Dynamic Phasor and Frequency Measurements by an Improved Taylor Weighted Least Squares Algorithm," *IEEE Trans. on Instr. and Measurement,* vol. 64, pp. 2165-2178, 2015.

[69] M. Paolone and P. Romano, "DFT-based synchrophasor estimation processes for Phasor Measurement Units applications: algorithms definition and performance analysis," *Advanced Techniques for Power System Modelling, Control and Stability Analysis,* pp. 77--126, 2015.

[70] A. Karpilow, et al., "Characterization of Non-Stationary Signals in Electric Grids: a Functional Dictionary Approach," *IEEE Trans. on Power Systems,* 2021.

[71] A. Karpilow, "Functional-Basis Analysis of Non-Stationary Signals in Modern Power Grids: Theory and Implementation in Embedded Systems," EPFL, 2024.

[72] G. Rietveld, P. S. Wright and A. J. Roscoe, "Reliable Rate-of-Change-of-Frequency Measurements: Use Cases and Test Conditions," *IEEE Trans. on Instr. and Meas.,* vol. 69, pp. 6657-6666, 2020.

[73] A. Derviškadić, Y. Zuo, G. Frigo and M. Paolone, "Under Frequency Load Shedding based on PMU Estimates of Frequency and ROCOF," in *2018 IEEE PES innovative smart grid technologies conference Europe (ISGT-Europe)*, 2018.

[74] A. J. Roscoe, et al., "The Case for Redefinition of Frequency and ROCOF to Account for AC Power System Phase Steps," in *2017 IEEE International Workshop on Applied Measurements for Power Systems (AMPS)*, 2017.

[75] J. Ren and M. Kezunovic, "An Adaptive Phasor Estimator for Power System Waveforms Containing Transients," *IEEE Transactions on Power Delivery,* vol. 27, pp. 735-745, 2012.

[76] M. Farajollahi, A. Shahsavari, E. Stewart and H. Mohsenian-Rad, "Locating the Source of Events in Power Distribution Systems Using Micro-PMU Data," *IEEE Trans. on Power Systems,* vol. 33, no. 6, pp. 6343-6354, November 2018.

[77] M. Izadi and H. Mohsenian-Rad, "Synchronous Waveform Measurements to Locate Transient Events and Incipient Faults in Power Distribution Networks," *IEEE Trans. on Smart Grid,* vol. 12, no. 5, pp. 4295-4307,, September 2021.

[78] Y. Cheng, L. Fan, J. Rose, S. Huang, J. Schmall, X. Wang, X. Xie, J. Shair, J. Ramamurthy, N. Modi and C. Li, "Real-World Subsynchronous Oscillation Events in Power Grids With High

Penetrations of Inverter-Based Resources," *IEEE Transactions on Power Systems,* vol. 38, no. 1, pp. 316-330, January 2023, doi: 10.1109/TPWRS.2022.3161418.

[79] C. Wang, C. Mishra, K. D. Jones, G. R. M. and L. Vanfretti, "Identifying Oscillations Injected by Inverter-Based Solar Energy Sources," in *2022 IEEE Power & Energy Society General Meeting (PESGM)* , Denver, CO, USA, 2022, doi: 10.1109/PESGM48719.

[80] K. Jones, P. Pourbeik, G. Kobet, A. Berner, N. Fischer, F. Huang, J. Holbach, M. Jensen, J. O'Connor and M. Patel, "Impact of inverter based generation on bulk power system dynamics and short-circuit performance," Task Force on Short-Circuit and System Performance Impact of Inverter Based Generation, Tech. Rep. PES-TR68, 2018.

[81] C. Wang, Z. Qin, Y. Hou and J. and Yan, "Multi-area dynamic state estimation with PMU measurements by an equality constrained extended Kalman filter," *IEEE Transactions on Smart Grid,* vol. 9, no. 2, pp. 900-910, 2016.

[82] H. Huang, Y. Lin, X. Lu, Y. Zhao and A. Kumar, "Dynamic State Estimation for Inverter-Based Resources: A Control-Physics Dual Estimation Framework," *IEEE Transactions on Power Systems,* vol. 2024.

[83] M. G. Dozein, B. C. Pal and P. Mancarella, "Dynamics of inverter-based resources in weak distribution grids," *IEEE Transactions on Power Systems,* vol. 37, no. 5, pp. 3682-369, 2022.

[84] B. Tan and J. Zhao, "Data-driven time-varying inertia estimation of inverter-based resources," *IEEE Transactions on Power Systems,* vol. 38, no. 2, pp. 1795-1798, 2022.

[85] H. Mohsenian-Rad, A. Shahsavari and M. Majidi, "Analysis of Power Quality Events for Wildfire Monitoring: Lessons Learned from a California Wildfire,," in *Proc. of the IEEE PES Innovative Smart Grid Technologies Conference*, San Juan, Puerto Rico, 2023.

[86] Public Utilities Commission of State of Californi, "Application of San Diego Gas Electric Company for Authorization to Recover Costs Related to the 2007 Southern California Wildfires Recorded in the Wildfire Expense Memorandum Account," Application 15-09-010, 2017.

[87] F. Auzanneau, "Wire Troubleshooting and diagnosis: Review and perspectives"," *Progress in Electromagnetics Research B,* vol. 49, 2013.

[88] Z. Du, P. K. Willett and M. S. Mashikian, "Performance Limits of PD Location Based on Time-domain Reflectometry," *IEEE Trans. on Diel. and El. Ins.,* vol. 4, no. 2, 1997.

[89] M. S. Mashikian, R. Bansal and R. B. Northrop, "Location and Characterization of Partial Discharge sites in Shielded Power cables," *IEEE Trans. on Power Delivery,* vol. 5, no. 2, 1990.

[90] F. P. Mohamed, W. H. Siew, J. J. Soraghan and S. M. Strachan, "Partial Discharge Location in Power Cables using a Double Ended Method Based on Time Triggering with GPS"," *IEEE Trans. on Diel. and El. Ins.,* vol. 20, no. 6, 2013.

[91] W. He, Q. Wang, C. Huang, H. Li and D. Liang, "A cost-effective technique for PD testing of MV cables under combined AC and damped AC voltage," *IEEE Trans. Power Delivery,* vol. 33, no. 4, 2018.

[92] G. Robles, M. Shafiq and J. M. Martínez-Tarifa, "Multiple Partial Discharge Source Localization in Power Cables Through Power Spectral Separation and Time-Domain Reflectometry," *IEEE Trans, on Instrumentation and Measurement,* vol. 68, no. 12, 2019.

[93] C. C. Yii, M. N. K. H. Rohani, M. Isa and S. I. S. Hassan, "Multi-end PD Location Algorithm using Segmented Correlation and Trimmed Mean Data Filtering Techniques for MV Underground Cables" - IEEE Trans. on Diel. and El, Ins. Vol. 24, No. 1; Feb. 2017," *IEEE Trans. on Diel. and El, Ins.,* vol. 24, no. 1, 2027.

[94] F. Rachidi, M. Rubinstein and M. Paolone, "Electromagnetic Time Reversal – Application to Electromagnetic Compatibility and Power System," *John Wiley & Sons Ltd,* pp. 95-97, 2017.

[95] A. Ragusa, H. Sasse, A. Duffy, F. Rachidi and M. Rubinstein, "Electromagnetic Time Reversal Method to Locate Partial Discharges in Power Networks using 1D TLM modelling," *IEEE Letters on EMC Practice and Applications,* vol. 3, no. 1, 2021.

[96] A. Ragusa, H. Sasse, A. Duffy and M. Rubinstein, "Application to real power networks of a method to locate partial discharges based on electromagnetic time reversal," *IEEE Trans. on Power Delivery,* vol. 37, no. 4, 2022.

[97] A. Ragusa, P. A. A. F. Wouters, H. Sasse and A. Duffy, "The effect of the ring mains units for on-line partial discharge location with time reversal in medium voltage networks," *IEEE Access,* 2022.

[98] A. Ragusa, P. A. A. F. Wouters, H. Sasse, A. Duffy, F. Rachidi and M. Rubinstein, "Electromagnetic Time Reversal for Online Partial Discharge Location in Power Cables: Influence of Signal Disturbance and Interfering Reflections from Grid Components," *IET Sci. Meas. Technol.,* 2024.

[99] CodeWave, "Big Data Analytics: Predictive Maintenance Strategies & Role," [Online]. Available: https://codewave.com/insights/big-data-analytics-predictive-maintenance-strategies-role/. [Accessed 2024].

[100] NERC Reliability Guideline, "Power Plant Model Verification and Testing for Synchronous Machines," July, 2018.

[101] B. Enayati, et al., "Impact of IEEE 1547 Standard on Smart Inverters and the Applications in Power Systems," IEEE PES Technical Report (PES-TR67), August, 2020.

[102] NERC Report, "April and May 2018 Fault Induced Solar Photovoltaic Resource Interruption Disturbances Report," January, 2019.

[103] K. R. Davis, S. Dutta, T. J. Overbye and J. Gronquist, "Estimation of Transmission Line Parameters from Historical Data," in *Proc. 46th Hawaii International Conference on System Sciences*, Wailea, HI, USA, 2013, doi: 10.1109/HICSS.2013.206.

[104] P. A. Pegoraro, K. Brady, P. Castello, C. Muscas and A. von Meier, "Line Impedance Estimation Based on Synchrophasor Measurements for Power Distribution Systems," *IEEE Transactions on Instrumentation and Measurement,* vol. 68, no. 4, pp. 1002-1013, 2019.

[105] G. L. Kusic and D. L. Garrison, " Measurement of transmission line parameters from SCADA data," in *Proc. IEEE PES Power Systems Conference and Exposition*, New York, NY, USA, 2004, doi: 10.1109/PSCE.2004.1397479..

[106] J. Zhao, A. Gómez-Expósito, M. Netto, L. Mili, A. Abur, V. Terzija, I. Kamwa, B. Pal, A. Singh, J. Qi and Z. Huang, "Power system dynamic state estimation: Motivations, definitions, methodologies, and future work," *IEEE Transactions on Power Systems,* vol. 34, no. 4, pp. 3188-3198, 2019.

[107] I. Kamwa, "Dynamic Wide Area Situational Awareness: Propelling Future Decentralized, Decarbonized, Digitized, and Democratized Electricity Grids," *IEEE Power and Energy Magazine,* vol. 21, no. 1, pp. 44-58, 2023.

[108] N. Hatziargyriou, J. Milanovic, C. Rahmann, V. Ajjarapu, C. Canizares, I. Erlich, D. Hill, I. Hiskens, I. Kamwa, B. Pal and P. Pourbeik, "Definition and classification of power system stability–revisited & extended," *IEEE Transactions on Power Systems,* vol. 36, no. 4, pp. 3271-3281, 2020.

[109] A. Alvi, T. Alford, M. Vaiman and M. Vaiman, "Pioneering Real-Time Control: The Deployment of a Distribution Linear State Estimator at Commonwealth Edison," *IEEE Power and Energy Magazine,* vol. 22, no. 2, pp. 67-77, 2024.

[110] S. Meliopoulos, G. Cokkinides, P. Myrda, E. Farantatos, R. Elmoudi, B. Fardanesh, G. Stefopoulos, C. Black and P. Panciatici, " Dynamic Estimation-Based Protection and Hidden Failure Detection and Identification: Inverter-Dominated Power Systems," *IEEE Power and Energy Magazine,* vol. 21, no. 1, pp. 59-72, 2023.

[111] I. Kamwa, L. Geoffroy, S. R. Samantaray and A. Jain, "Synchrophasors data analytics framework for power grid control and dynamic stability monitoring," *IET Eng. Technol,* pp. 1-22, 2016.

[112] X. Song, H. Cai, T. Jiang, S. Schlegel and D. Westermann, "Parameter Tuning for dynamic Digital Twin of Generation Unit in Power Grid," in *Proc 2021 IEEE PES Innovative Smart Grid Technologies Europe (ISGT Europe)*, 2021.

[113] M. Farrokhabadi, C. A. Canizares, J. W. Simpson-Porco, E. Nasr, L. Fan, P. A. Mendoza-Araya, R. Tonkoski, U. Tamrakar, N. Hatziargyriou, D. Lagos, R. W. Wies, M. Paolone, M. Liserre, L. Meegahapola, M. Kabalan, A. H. Hajimiragha, D. Peralta, M. A. Elizondo, K. P. Schneider, F. K.

Tuffner and J. Reilly, "Microgrid Stability Definitions, Analysis, and Examples," *IEEE Transactions on Power Systems,* vol. 35, no. 1, pp. 13-29, 2020.

[114] M. Farrokhabadi, S. Konig, C. A. Canizares, K. Bhattacharya and T. Leibfried, "Battery Energy Storage System Models for Microgrid Stability Analysis and Dynamic Simulation," *IEEE Transactions on Power Systems,* vol. 33, no. 2, pp. 2301-2312, 2018.

[115] North American Electric Reliability Corporation, "March 13, 1989 Geomagnetic Disturbance," 1989, [Online]: https://www.nerc.com/pa/Stand/Geomagnetic%20Disturbance%20Resources%20DL/NERC_1989-Quebec-Disturbance_Report.pdf.

[116] U.S. Department of Energy, "Geomagnetic Disturbance Monitoring Approach and Implementation Strategies," 2019, Available online: https://www.energy.gov/ceser/articles/geomagnetic-disturbance-monitoring-approach-and-implementation-strategies. .

[117] I. Kamwa, J. Beland, G. Trudel, R. Grondin, C. Lafond and D. McNabb, "Wide-area monitoring and control at Hydro-Quebec: past, present and future,," in *Proc 2006 IEEE Power Engineering Society General Meeting*, Montreal, QC, Canada, 2006.

[118] W. A. Mittelstadt, P. E. Krause, P. N. Overholt, D. J. Sobajic, J. F. Hauer and D. T. Rizy, "The DOE Wide Area Measurement System (WMAS) Project – Demonstration of Dynamic Information Technology for the Future Power System," in *EPRI Conference on the Future*, Washington DC, 1996, 1996, Online: https://www.osti.gov/scitech/servlets/purl/254951.

[119] A. G. Phadke, "Synchronized phasor measurements – a historical overview," in *IEEE/PES Asia Pacific Transmission and Distribution Conference and Exhibition*, Yokohama, Japan, 2002.

[120] K. Martin, A. Goldstein, G. Antonova, G. Brunello, R. D. R. Chunmei, B. Dickerson, D. Dwyer, J. Gosalia, Y. Hu and B. Kirby, " Synchrophasor Measurements for Power Systems under the Standard IEC/IEEE 60255-118-1," IEEE, 2018.

[121] Communication Networks And Systems For Power Utility Automation - Part 90-5, " Use Of IEC 61850 To Transmit Synchrophasor Information According To IEEE C37.118," IEC Technical Report, Online: https://webstore.ansi.org/standards/iec/iectr6185090eden2012?gad_source=1&gclid=Cj0KCQiA84CvBhCaARIsAMkAvkIih9ymVskVMDI39lo9XOJW0AS6ImHfe5Uz0O_je-0U5LW3Bih80hkaAufnEALw_wcB.

[122] " IEEE Standard for Streaming Telemetry Transport Protocol (STTP)", IEEE 2664-2024," [Online]. Available: https://standards.ieee.org/ieee/2664/7397/.

[123] M. Donnelly, M. Ingram and J. Carroll, "Eastern interconnection phasor project," in *Proc of the 39th Annual Hawaii International Conference on System Sciences (HICSS'06)*, Piscataway, New Jersey, 2006.

[124] J. E. Dagle, "The North American SynchroPhasor Initiative (NASPI)," in *Proc. IEEE PES General Meeting*, Minneapolis, MN, USA, 2009.

[125] D. Nakafuji, et al., "Integrating synchrophasors and oscillography for wide-area power system analysis," in *2017 70th Annual Conference for Protective Relay Engineers (CPRE)*, 2017.

[126] PJM, "PJM Technical Guidelines for Installation of Synchrophasor Measurements at Generation Facilities," [Online]. Available: https://www.pjm.com/-/media/markets-ops/ops-analysis/synchrophasor-tech/synchrophasor-technical-guidelines-package-for-generation-interconnection.ashx.

[127] SPP, "SPP PMU Communications Handbook," 2021. [Online]. Available: https://www.spp.org/documents/55158/spp%20pmu%20communication%20handbook%20v1.2.pdf.

[128] J. Britton, et al., IEEE PES Technical Report: PES-TR-102. "MV Smart Grid Sensor and Sensor Systems: Measurement Accuracy and Uncertainty Considerations", Oct 2022.

[129] T. Lee, V. J. Nair, and A. Sun. "Impacts of dynamic line ratings on the ERCOT transmission system." in *Proc. of the IEEE North American Power Symposium* (NAPS), 2022.

[130] J. Yu, Y. Weng, and R. Rajagopal. "PaToPaEM: A data-driven parameter and topology joint estimation framework for time-varying system in distribution grids" in *IEEE Transactions on Power Systems*, vol. 34, no. 3, pp. 1682-1692, May 2019.

[131] D. Deka, V. Kekatos, and G. Cavraro. "Learning distribution grid topologies: A tutorial." *IEEE Transactions on Smart Grid*, vo. 15, no. 1, pp. 999-1013, 2023.

[132] S. Park, D. Deepjyoti, and M. Chcrtkov. "Exact topology and parameter estimation in distribution grids with minimal observability." in *Proc. of the IEEE Power Systems Computation Conference (PSCC)*, 2018.

[133] W. Li and D. Deka, "PPGN: Physics-Preserved Graph Networks for Real-Time Fault Location in Distribution Systems with Limited Observation and Labels", in *Proc. of the 56th Hawaii International Conference on System Sciences*, January 2023.

Appendix

Network and Communications Architecture

Security, redundancy, and scalability often drive the type of architecture that is deployed. The architecture can be quite simple if all the instrumentation, communications, and servers are on the same network as shown in Figure 54.

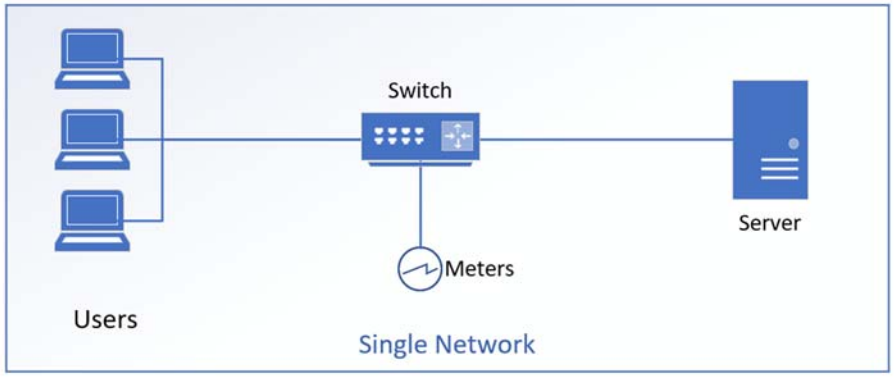

Figure 54. A simple data architecture with a single network

If redundancy is required, then any of the elements may be duplicated to ensure that the availability of the network system is high. For example, in the diagram in Figure 55, a second server is introduced. This could provide a backup if the primary server goes down. Alternatively, a second server could be used if the number of users or meters exceeds the capability of a single server. In this situation, the system loses the redundancy, and the number of servers needs to be increased so the system regains the redundant architecture.

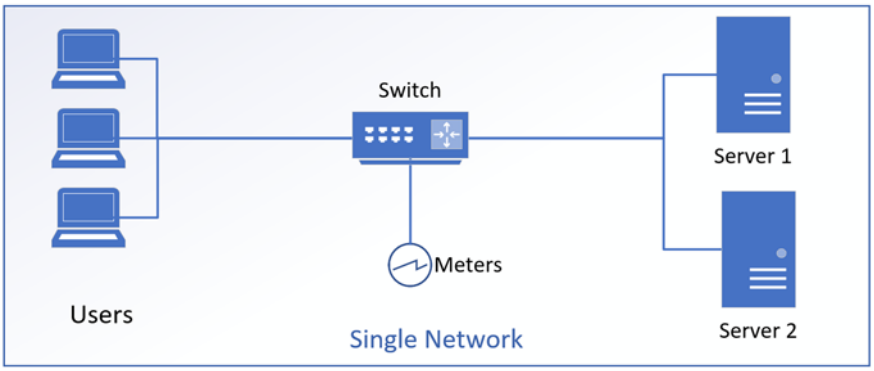

Figure 55. A data architecture with redundant servers

Generally, companies will choose to separate the operations network from the corporate network. This enables the operations network to continue to function even if there is a problem with the corporate network. Instrumentation and related data collection systems often live in the operations network sometimes referred to as the operations technology (OT) network. An example of this architecture is shown in Figure 56. Meanwhile the users of the data are often located in the

corporate or information technology (IT) network. This may require firewall rules to enable the users to access the data from the meters.

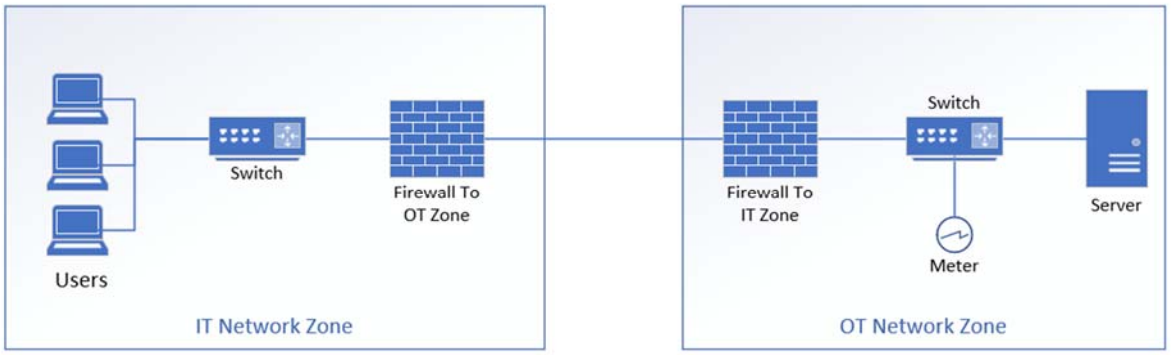

Figure 56. A data architecture with OT / IT Networks

Finally, in the most common architecture, the substation may have many devices in a substation zone. The data collection equipment may live in the OT network zone and the users may be in the IT network zone. This provides a secure environment for each of the separate zones and provides maximum insulation between the zones. An example of this architecture is shown in Figure 57.

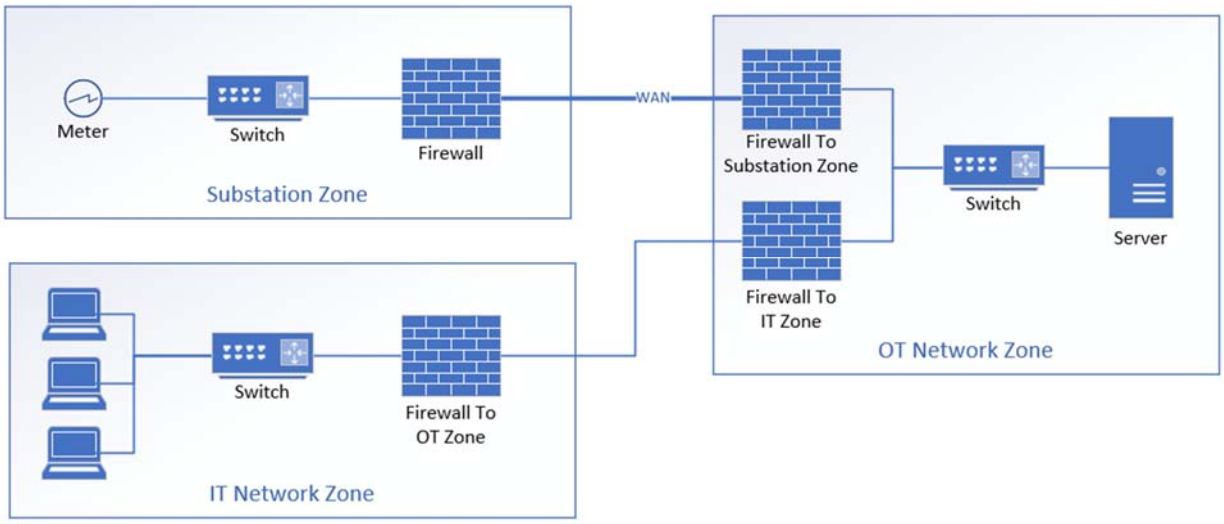

Figure 57. An architecture with Substation, IT, OT Networks